From Microporous to Mesoporous Molecular Sieve Materials and Their Use in Catalysis

Avelino Corma

Instituto de Tecnología Química, UPV-CSIC, Universidad Politécnica de Valencia, Avda. de los Naranjos s/n, 46022 Valencia, Spain

Received April 7, 1997 (Revised Manuscript Received June 16, 1997)

Contents

Avelino Corma Canos was born in Moncófar, Spain, in 1951. He studied chemistry at the Universidad de Valencia (1967–1973) and received his Ph.D. at the Universidad Complutense de Madrid in 1976. He became director of the Instituto de Tecnología Química (UPV-CSIC) at the Universidad Politécnica de Valencia in 1990. His current research field is zeolites as catalysts, covering aspects of synthesis, characterization and reactivity in acid–base and redox catalysis. A. Corma has written about 250 articles on these subjects in international journals, three books, and a number of reviews and book chapters. He is a member of the Editorial Board of *Zeolites*, *Catalysis Review Science and Engineering*, *Catalysis Letters*, *Applied Catalysis*, *Journal of Molecular Catalysis*, *Research Trends*, *CaTTech*, and *Journal of the Chemical Society, Chemical Communications*. A. Corma is coauthor of 20 patents, five of them being for commercial applications. He has been awarded with the Dupont Award on new materials (1995), and the Spanish National Award "Leonardo Torres Quevedo" on Technology Research (1996).

I. Introduction

It is possible to say that zeolites are the most widely used catalysts in industry. They are crystalline microporous materials which have become extremely successful as catalysts for oil refining, petrochemistry, and organic synthesis in the production of fine and speciality chemicals, particularly when dealing with molecules having kinetic diameters below 10 Å. The reason for their success in catalysis is related to the following specific features of these materials:[1] (1) They have very high surface area and adsorption capacity. (2) The adsorption properties of the zeolites can be controlled, and they can be varied from hydrophobic to hydrophilic type materials. (3) Active sites, such as acid sites for instance, can be generated in the framework and their strength and concentration can be tailored for a particular application. (4) The sizes of their channels and cavities are in the range typical for many molecules of interest (5−12 Å), and the strong electric fields[2] existing in those micropores together with an electronic confinement of the guest molecules[3] are responsible for a preactivation of the reactants. (5) Their intricate channel structure allows the zeolites to present different types of shape selectivity, i.e., product, reactant, and transition state, which can be used to direct a given catalytic reaction toward the desired product avoiding undesired side reactions. (6) All of these properties of zeolites, which are of paramount importance in catalysis and make them attractive choices for the types of processes listed above, are ultimately dependent on the thermal and hydrothermal stability of these materials. In the case of zeolites, they can be activated to produce very stable materials not just resistant to heat and steam but also to chemical attacks.

S0009-2665(96)00406-2 CCC: $28.00

Table 1. The Typical Larger Pore Zeolites/Zeotypes

material	ring size	year discovered	synthesis media	inorganic framework composition	channels/pores
cacoxenite	20-TO_4 ring		naturally occurring	Al, Fe, P	14.2 Å pore diameter
zeolites X/Y (FAU)	12-TO_4 ring	1950s		Al; Si	7 Å diameter pore 12 Å diameter cavity 3D channel system
$AlPO_4$-8 (AET)*	14-TO_4 ring	1982	*n*-dipropylamine template	Al, P	1D channel system
VPI-5 (VFI)*	18-TO_4 ring	1988	tetrabutylammonium/ *n*-dipropylamine templates	Al, P	13 Å channel diameter hexagonal arrangement of 1D channel system
cloverite (CLO)*	20-TO_4 ring	1991	(a) quiniclidinium template (b) F^- rather than OH as mineralizer	Ga, P	largest aperture of window is 13 Å 30 Å cavities 3-D channel system
JDF-20	20-TO_4 ring	1992	(a) triethylamine template (b) glycol solvent	Al, P	hydroxyl groups protruding into channel system
UTD-1	14-TO_4 ring	1996	$[(C_p^*)_2Co]OH$	Si, Al	1-D channel system 7.5 × 10 Å

Table 2. The Major Routes Employed by Zeolite Synthetic Chemists To Increase the Pore Size of Microporous Zeolites and Zeotypes

method employed to increase pore size	examples	structures
use specific spacing units to build the inorganic framework	addition of further four ring building units to six ring units in porous aluminophosphates	$AlPO_4$-5 framework further extended to VPI-5 (refs 182, 183, and 188)
use different oxide systems	use two sorts of tetrahedral atoms to yield diffrent T−O bond lengths	VPI-5 (aluminum and phosphorous) cloverite (gallium and phosphorous)
use specially designed templates	exploit the specific structure directing effect of an organic template	use of quinuclidine to form cloverite

Despite these catalytically desirable properties of zeolites they become inadequate when reactants with sizes above the dimensions of the pores have to be processed. In this case the rational approach to overcome such a limitation would be to maintain the porous structure, which is responsible for the benefits described above, but to increase their diameter to bring them into the mesoporous region. The strategy used by the scientist to do this was based on the fact that most of the organic templates used to synthesize zeolites affect the gel chemistry and act as void fillers in the growing porous solids. Consequently, attempts were made that employed larger organic templates which would not, as was hoped, hence result in larger voids in the synthesized material. This approach did not give positive results in the case of zeolites, but in contrast was quite successful when using Al and P or Ga and P as framework elements.[4−14] Only very recently a 14-member ring (MR) unidirectional zeolite (UTD-1) could be synthesized using a Co organometallic complex as the template[15,16] (Table 1). The template can be removed, and the thermal stability of the framework of the organometallic-free material is high, resisting calcination temperatures up to 1000 °C. The presence of framework tetrahedral Al generates Brønsted acidity which is strong enough to carry out the cracking of paraffins.

In a general way, we have summarized in Table 2 the different strategies directed toward the synthesize of ultralarge pore zeolites.

However, when the zeolite and zeotypes with the largest known diameters are considered in the context of their possible uses as catalysts the following can be said: cacoxenite,[17] which is a naturally occurring mineral with a 15 Å pore system, is thermally unstable and thus cannot be used as a catalyst. Cloverite, although this structure has potentially large pores, the diffusion of large molecules is restricted, owing to the unusual shape of the pore openings which are altered due to protruding hydroxyl groups. Likewise in VPI-5, stacking disorder or deformation of some of the 18-member rings during dehydration results in a decrease in the pore size from 12 to about 8 Å. In the case of the new zeolite UTD-1, the fact that it has to be synthesized with an organometallic Co complex, which has then to be destroyed, and the Co left has to be acid leached raises strong questions concerning its practical application, which remains in doubt unless a more suitable template and activation procedure can be found.

In conclusion, it can be said that despite the outstanding progress made in producing large pore molecular sieves, the materials so far synthesized are still not suitable to be used in the context of current catalytic processes. Largely for this reason alone another approach has been undertaken in order to increase the activity of the existing microporous materials for processing large molecules such as those existing, for instance, in vacuum gas oil and which need to be cracked and hydrocracked. This approach involves the generation of mesopores in the crystallites of the microporous zeolites.

II. Zeolites Containing Mesopores

Following the definition accepted by the International Union of Pure and Applied Chemistry, porous materials can be grouped into three classes based on their pore diameter (*d*): microporous, $d < 2.0$ nm;

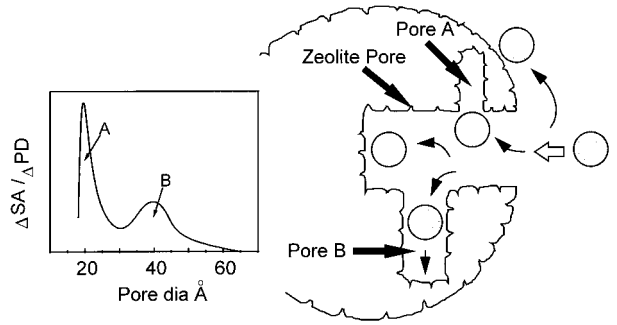

Figure 1. Schematic representation of mesopores formed in steamed zeolites.

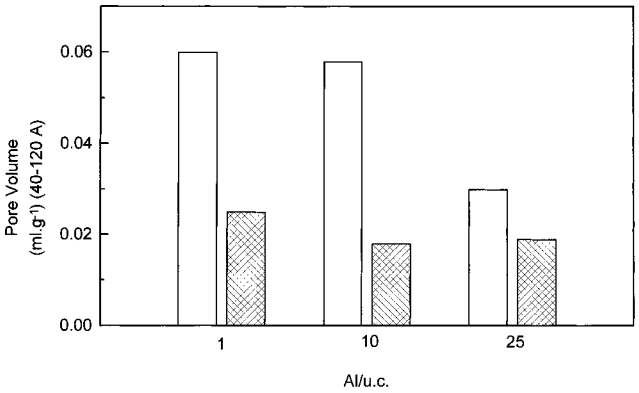

Figure 2. Pore volume in the mesoporous region for pores between 40 and 120 Å, of zeolites USY dealuminated by steam (□) and by $SiCl_4$ (■).

mesoporous, $2.0 \leq d \leq 50$ nm; macroporous, $d > 50$ nm. In the case of zeolites, for example zeolite Y and CSZ-1, it was shown[18,19] that during the dealumination of the zeolite by steam mesopores of mixed sizes in the range 10−20 nm were formed which could be characterized by different techniques including gas adsorption, high-resolution electron microscopy, and analytical electron microscopy.[19] When a large number of defects occur in a small area it can lead to coalescence of mesopores, with the formation of channels and cracks in the crystallite of the zeolite (Figure 1).

The presence of the mesopores in the crystallites of a given zeolite should basically increase the accessibility of large molecules to the external opening of the pores. In other words, and from the stand point of large reactant molecules, the presence of mesopores in the crystallites of the zeolite would be equivalent to increasing the external surface of the zeolite making a larger number of pore openings accessible to the reactant. The beneficial effect of the combination of micro and mesoporous region in the zeolite crystallites was shown by comparing the cracking activity of two series of Y zeolite dealuminated by $SiCl_4$ and steam.[20] The dealumination by $SiCl_4$ generated little mesoporosity and preserved most of the microporosity of the zeolite. On the other hand, the dealumination by steam produced many more mesoporous areas within the material while some of the microporosity was destroyed (Figure 2). When the catalytic activity of the two series of samples was compared for cracking a small reactant molecule (*n*-heptane) which can easily penetrate through the pores of the zeolite Y, it was found that the samples dealuminated by $SiCl_4$ treatment, and these, which have a greater microporosity, were more

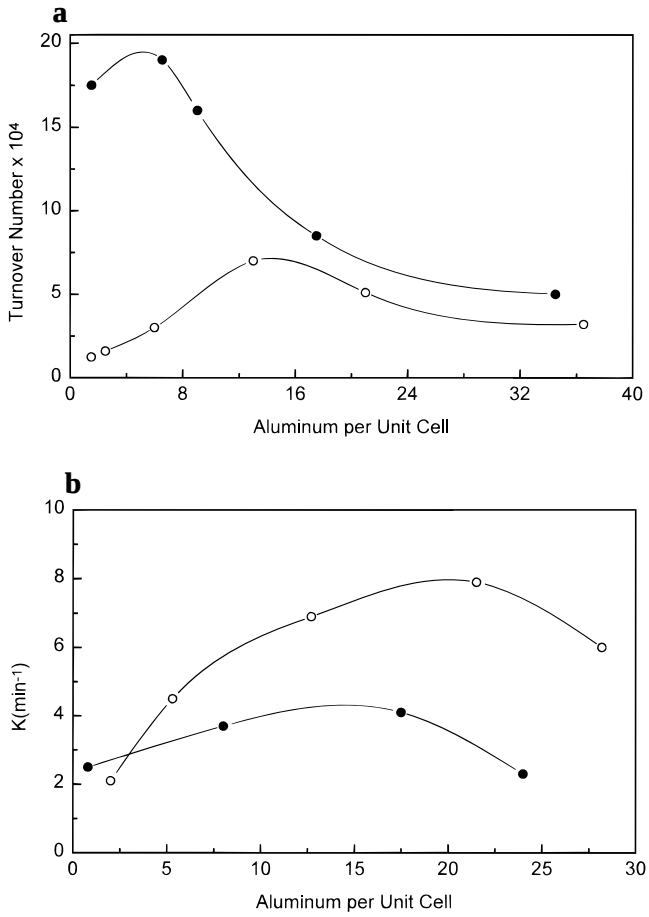

Figure 3. (a) Cracking of *n*-heptane on USY dealuminated by $SiCl_4$ (●), and by steam (○) and (b) cracking of gas oil on USY dealuminated by steam (○), and by $SiCl_4$ (●).

active than those dealuminated by steam. However, when the two series of dealuminated Y zeolites were used to crack a vacuum gas oil, containing molecules too large to penetrate deep into the microporous system, the steam-dealuminated samples, which contain a greater proportion of mesoporosity, gave a higher conversion (Figure 3a,b).

Increasing accessibility by producing mesopores during the activation of zeolites can have quite a profound impact in the case of fine and speciality chemical production, in which the performed catalyst will be working at low reaction temperatures and only moderate regeneration temperatures will be necessary. This is for instance the case for the esterification of fatty acids with alcohols.[21] Thus, because of the formation of mesopores by steam treating zeolite Y during the activation process, the modified catalyst gives good activity and selectivity, with a definitive optimum existing between the total number of acid sites and those accessible to the large molecules through the generated mesopores.

Unfortunately, in processes where the catalyst regeneration occurs at high temperatures the mesoporosity of the catalyst changes during the regeneration and in cases such as the FCC, this occurs in an uncontrollable way. It appears then that a procedure involving the formation of a secondary mesoporous system by steaming the microporous solid can only be adequate for some special cases and therefore, other more general solutions should be explored.

III. Pillared Layered Solids

Owing to the difficulties to synthesize zeolites having the required extra large channel and cavity sizes, a group of ultralarge pore materials consisting of layered structures with pillars in the interlamellar region, the so-called pillared-layered structures (PLS),[22−28] have been synthesized. The layered compounds typically used involve smectites, metal (Zr, Ti, etc.) phosphates, double hydroxides, silicas, and metal oxides. If the PLS is to be used for molecular sieve applications, the pillared material must have the following characteristics: uniform spacing between the pillars, suitable gallery heights, and layer rigidity. Among the different layered phases, smectites are probably the ones which best fulfill these requirements. The family of minerals known as smectites includes beidellite, hectorite, fluorhectorite, saponite, sauconite, montmorillonite, and nontronite. Smectites can be described simply on the basis of layers containing two sheets of silica sandwiching a layer of octahedral Al or Mg (2:1 layered clays). Substitution of some of the Al^{3+} for Mg^{2+} or Li^{+}, or the isomorphous replacement of tetrahedral Si^{4+} for Al^{3+} results in an amount of total negative charge on the layer, compensated in turn by the presence of hydrated cations in the interlayer region.

It was Barrer and McCleod[29] who first prepared pillared materials by exchanging alkali and alkaline-earth cations in a montmorillonite clay for quaternary ammonium compounds. However, the resulting material was thermally unstable and therefore, of no practical use for catalysis. An important qualitative advance was provided by the use of oxyhydroxyaluminum cations as the pillaring agent.[30,31] The general procedure for preparing these clays consists[32] of exchanging the cations in the interlamellar position, i.e., Na^{+}, K^{+}, and Ca^{2+}, with larger inorganic hydroxy cations. These hydroxy species are polymeric or oligomeric hydroxyl metal cations formed by the hydrolysis of metal salts of Al, Zr, Ga, Cr, Si, Ti, Fe, and mixtures of them. When the exchanged samples are subject to a careful thermal treatment, dehydration and dehydroxylation occur, forming stable metal oxide clusters which serve to separate the layers, creating a two dimensional gallery with an opening, which if properly prepared can be greater than 1.0 nm. The correct choice of the intercalated compound and the pillaring procedure and activation is essential not only for properly "cementing" the layers and therefore providing high mechanical and thermal stability, but also for generating active sites for their use in catalysis. Care should be taken to avoid overfilling the interlayer or in turn introducing too few pillars since then a nonporous intercalate or unstable structure is generated. The ideal situation is for the pillar height to be of the same order as the lateral separation between pillars, resulting in a product with a near uniform pore size distribution.[32] The resultant PLS materials have at least 50% of their surface in pores less than 3.0 nm (intralayer), and the rest is in pores larger than 3.0 nm, i.e., in mesopores (interlayer).[33] This situation arises from several different things: the nonparallel stacking of layers, the layers not being of uniform length, and also the presence of stacking disorder.[34]

Even though the most investigated substrates to be pillared include smectite clays,[35] phosphates and phosphonates of tetravalent metals,[36−40] and layered double hydroxides,[41−43] the ones showing most promising potential belong to the first group. In this case the main catalytic objective was directed to prepare cracking catalysts for FCC uses. Indeed, the openings of the interlayer spaces of PLS are of the molecular size of the feed stocks to FCC. By targeting this application, researchers have concentrated their attention on producing PLS with a high hydrothermal stability, while having adequate numbers of active sites able to convert the heavy molecules and able to produce liquid fuels with low selectivity to gases and coke.

To enhance stability, researchers have worked on both the nature of the pillars and the nature of the layered silicate. With regard to the pillars the first ones based on alumina were thermally stable, but their hydrothermal stability was limited. In these cases an aluminum tridecamer is thought to be the pillaring species in Al-pillared clays.[33] However, it was also possible to prepare a $GaAl_{12}$ structure in which the tetrahedral Al^{3+} of the Al_{13} cation is replaced with a Ga^{3+} ion, and the resulting structure can be described as the Baker−Figgs ϵ-isomer[44] of the Keggin structure. In this case the slightly larger ionic radius of the Ga^{3+} ion, makes the $GaAl_{12}$ structure more symmetric than its corresponding Al_{13} oligomer, and consequently, the former should be thermodynamically favored over the Al_{13} and Ga_{13} and also more thermally stable. Thus, montmorillonite has been pillared with GaAl pillars which were synthesized with different Ga/Al ratios.[45−48] The layer spacing varied from 1.8 to 2.0 nm at room temperature and between 1.7 and 1.8 nm after calcination at 500 °C. As expected, the thermal and hydrothermal stability of the GaAl PLS was higher than that of the clay pillared with Al alone.

Increasing thermal and hydrothermal stability of the original aluminum pillared smectites has also been attempted by intercalating them with Al and Ce precursors. In this way it was found that montmorillonite could be intercalated with an oligomer (Al/Ce = 25) prepared by copolymerizing soluble rare earth salts with a cationic metal complex of aluminum.[49] When the samples were calcined at 800 °C for 16 h the pillared with AlCe maintained surface areas above 220 $m^2\ g^{-1}$, while the areas of the corresponding pure Al counterpart were always smaller than 160 $m^2\ g^{-1}$. However, what is more important in this new sample is the fact that some of the AlCe-pillared samples maintained a surface area of 279 $m^2\ g^{-1}$ even after steaming at 760 °C for 5 h.

As alluded to above, it is possible to increase the stability of the resulting material not only by using different type of pillars (Al/Ga, Al/Ce), but also by changing the nature of the clay. For instance, Cuann et al.[50] indicated that when similar preparation techniques were used to pillar the clays, the final stability depended on the nature of the clay used. Among the different clays, rectorite was shown to be the most stable one. Rectorite is an interstratified layered silicate mineral formed by a regular stacking of mica and montmorillonite layers. Even though the

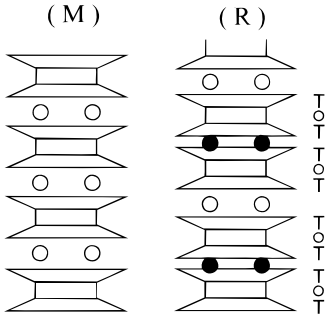

Figure 4. Schematic structures of montmorillonite (M) and rectorite (R). The T−O−T layer sequence (T = tetrahedral, O = octahedral) is represented by trapezoids and rectangles. Exchangeable and nonexchangeable charge compensating cations are represented by open and solid circles, respectively.

nature of the layers and their stacking sequence vary between and within samples, the most probable stacking sequence is shown in Figure 4. The mixed-layered rectorite clay consists of low charge density, montmorillonite-like layers and high charge density nonexpandable mica-like layers. Rectorites pillared with $[Al_{13}O_4(OH)_{24}(H_2O)_{12}]^{7+}$ have thermal and hydrothermal stability much superior to montmorillonites and hectorite catalysts prepared by similar means, probably due to the robust mica-like layers located between the expanded montmorillonite-like layers (see Figure 4).[51]

A natural evolution would then be to pillar rectorite with Al/Ce pillars, which were found to be highly stable. When this was done[52] it was found that highly stable materials retaining more than 75% of the surface area after a hydrothermal calcination at 760 °C for 4 h were produced. However, in addition and of more interest than just greater stability was the observation that different porosities were obtained with Al/Ce pillars in comparison to the pure Al pillars. Indeed, the Al/Ce rectorite has a *d* spacing of 3.49 nm corresponding to an interlayer distance of 1.57 nm which is larger than the interlayer distance (0.84 nm) of the Al rectorite.[52] When the samples were calcined, the pore diameter of the Al/Ce ranges from 0.5 to 1.6 nm with a sharp peak at 0.68 nm, while the Al rectorite showed a unimodal pore distribution centered at 0.73 nm. These results indicate that bulkier less uniformly distributed pillars were formed in the case of Al/Ce rectorite, which is clearly of importance when large molecules are reacting.

Besides the clays considered here, pillaring has also been recently accomplished in other clays such as kandites and metakaolin which do not have exchange capacity.[53,54]

In conclusion it can be said that pillared clays having the required stability have been developed into which acid and redox active sites can be introduced, generating potentially active catalysts whose main characteristics will be described below.

A. Pillar-Layered Silicates as Acid Catalysts

There are a large number of reactions which are catalyzed by acid sites, and their importance has surpassed the interest in the fundamental chemistry. It can be said that solid acids are the most important solid catalysts used today, when both the total amount used and the final economic impact are considered. The catalytic properties of a given acid catalyst will be determined by the number, type, and strength of the acid sites present. Then the questions one needs to answer are: what type of acid sites are needed, either Brønsted or Lewis, and what is the acid strength required to activate the reactant molecule. When these questions have been answered, it is then the role of the chemist to find ways to maximize the number of acid sites in a given solid acid.

1. Nature of the Acid Sites

a. Al-Pillared Clays. It was soon recognized that different Al-pillared clays such as montmorillonites, saponites, beidellites, etc., have both Brønsted and Lewis acid sites in varying relative proportion.[55−58] This has been shown by adsorbing pyridine and identifiying by IR spectroscopy the characteristic bands of pyridinium ions (1545 cm^{-1}) and pyridine coordinated to Lewis sites (1454 cm^{-1}) (Figure 5). However, in the case of solid acids, as important as the number and type of acid sites is their acid strength since this will be responsible for the extent to which a given bond in the reactant molecule will be polarized and, consequently, will determine the type of reaction that the solid acid will be able to catalyze.

Ming-Yuan et al.[59] have measured the total amount and strength of the acid sites present in montmorillonites pillared with Al polyhydroxy cations, using *n*-butylamine as a titrating base, and the results were compared with those obtained with amorphous silica-alumina and HY zeolite (Table 3). The results show that a strong increase in total acidity is observed when going from the starting Na montmorillonite to the Al-pillared material. Furthermore, the total

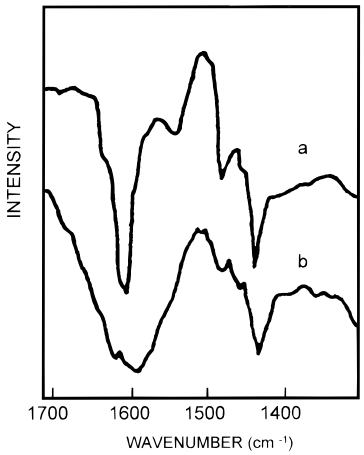

Figure 5. IR spectra of pyridine adsorbed on montmorillonite. The bands at 1545 and 1450 cm^{-1} correspond to pyridine adsorbed on Brønsted and Lewis acid sites, respectively.

Table 3. Amount and Strength of Acid Sites of an Al-Pillared Material and Its Comparison with Amorphous Silica-Alumina and Zeolite Y

acid strength distribution (mequiv g^{-1})	acidity (mequiv g^{-1})			
	0.2 (Na-Mont)	1.1 (Al-PLS)	1.3 (Si-Al)	1.65 (HY zeolite)
$-3.0 < H_o < 3.3$	0.2	1.1	0.9	0.3
$-5.6 < H_o < -3.0$	0	0	0.2	0
$-8.2 < H_o < -5.6$	0	0	0	0
$H_o < 8.2$	0	0	0.2	1.35

acidity of the PLS is close to that of the amorphous silica-alumina and lower than in a HY zeolite; the acid strength of the former, measured using Hammett indicators, being weaker than that of the other two aluminosilicates.[59] These results even if they appear reasonable should be considered with care, since the use of Hammett indicators is intrinsically inappropriate for measuring acid strength distribution in solid acids. Indeed, the use of the Hammett function (H_0) is adequate for homogeneous aqueous solutions of acids, but in the case of solid heterogeneous catalysts the reported H_0 values are meaningless.[60] On the other hand using a more reliable method for measuring acidity such as stepwise thermal desorption of ammonia, on a Wyoming montmorillonite pillared with hydroxy aluminium, resulted in a total number of acid sites equal to 0.35 mequiv g^{-1} with acid strengths comparable to that of HY zeolites.[61] Moreover this result has been confirmed from highly sensitive diffuse reflectance IR spectroscopy measurements, where Brønsted acid sites with an acid strength comparable to that of zeolites has been found.[61]

Since PLS are comprised of both the layers of the silicate and the pillars, it is of interest to determine which part of the composite material is responsible for the different types of acidity. This was elucidated from the correlation between the structural OH groups and the Brønsted acidity in PLS.[58,59] Interpretation of IR data concluded particularly in the calcined samples that the Brønsted acidity is related with the clay structure, while on the other hand the Brønsted acidity of the OH groups in the Al pillars can be disregarded. Moreover, it is noted that the pillars will strongly contribute to the Lewis acidity observed.

Since most of the Brønsted acidity of the Al-PLS is due to the clay, there is no doubt that one should be able to change the final acidity of the material by working with different clays. Indeed, Poncelet and Schulz[57] have considered this aspect by studying the acidity of montmorillonite and beidellite pillared with Al oligomers. In the case of the Al beidellite, and due to its larger proportion of Al^{IV} in the tetrahedral layers, the final material presents a higher amount of Brønsted sites.[62] In the case of Al-pillared saponites, a new OH stretching vibration at 3595 cm^{-1} which is absent in pillared montmorillonites, has been observed,[63] and the acid character of these OH groups was elucidated by pyridine adsorption. The higher acidity of the saponite with respect to Al-pillared montmorillonites is attributed, as in the case of beidellite, to the higher content and strength of the acid sites associated with Si—OH···Al groups produced upon proton attack of the tetrahedral Si—O—Al bonds.[57,58] If this was true, one should be able to increase the Brønsted acidity by performing an acid treatment of the clay prior to the pillaring. When this was done,[64−66] it was found that the pillared acid activated clays (PAACs) incorporated less Al than did the conventional PLS, with the former being more mesoporous and less microporous. The total pore volumes of the PAACs were higher and the surface areas increased consistently with acid/clay ratio to a maximum before decreasing. Furthermore, the surface acidity was increased. An increase in the number of both Brønsted and Lewis acid sites also occurs when the pillared clays are treated with sulfate or phosphate ions.[66]

Table 4. Acidity of Montmorillonites Pillared with Different Cations

sample	d_{001} (nm)	surface area ($m^2\ g^{-1}$)	acidity (μv)
Al-PM	1.73−1.89	190	425−442
Zr-PM	1.82	191	570
Ti-PM	1.50	−	620
Fe-PM	1.55	109	340
Ni-PM	1.48	58	228
Al-Zr-PM	1.56	−	390
Al-Fe-PM	1.58	−	340
NaM	1.28	51	86

b. Clays Pillared with Cations Other Than Al. It is logical to suppose that if silica-alumina pillars were prepared instead of the classical Al, one may combine the porosity of the pillared materials with the acid and catalytic properties of the amorphous silica-alumina.[67,68] The preparation of silica-alumina-pillared clays was carried out[67] by forming and aging hydroxy-alumina oligocations followed by reaction with $Si(OEt)_4$. In order to change the potential acid characteristics of the final material, different Si/Al ratios (0−2) and Al/clay ratios (7−22 m molAl (g of clay)$^{-1}$) were used, but unfortunately, the acidity of the hydroxy-silica-alumina-pillared clays is mainly of the Lewis type, a feature which appears to be independent of the Si/Al ratio.

The formation of pillars by using transition metals hydroxide oxides not only can introduce acidic properties to the material, but can also impart to the PLS other redox catalytic properties which are discussed later. Thus pillaring agents based on Zr, Cr, Fe, Ti, Sn, Tn, Ga, etc., have been prepared by forming polymeric cations of the corresponding ions,[69−91] and the acidity of the final material being observed to change significantly with the nature of the hydroxy-cation (Table 4).[59] As noted previously with Al pillars, most of the acidity of the intercalate pillars, regardless of the cation, is of the Lewis type. Lower acidities were produced when Fe pillars were used and in mixed Al-Zr and Al-Fe cases. It was described above that GaAl pillars led to highly thermally and hydrothermally stable PLS materials.[45−48] With regard to their acid properties, it has been found that the highest total acidity, measured by pyridine adsorption, occurs on PLS with large Al/Ga ratios. However, when the samples are heated at high temperatures only Lewis acid sites are present, indicating that the Brønsted sites of the solids have been dehydroxylated.

In conclusion, it appears that the introduction of transtion metal oxides as pillaring agents do not have any special advantage over the Al samples with respect to Brønsted acidity, confirming the observation that most of the Brønsted acidity comes from the clay, and very little, from the pillars. Then, the catalytic benefit of the transition metal oxides should be found in their Lewis acid character or redox characteristics.

2. Influence of Activation Conditions on Acidity

In the previous section, we discussed the relevance of the thermal and hydrothermal stability of pillared

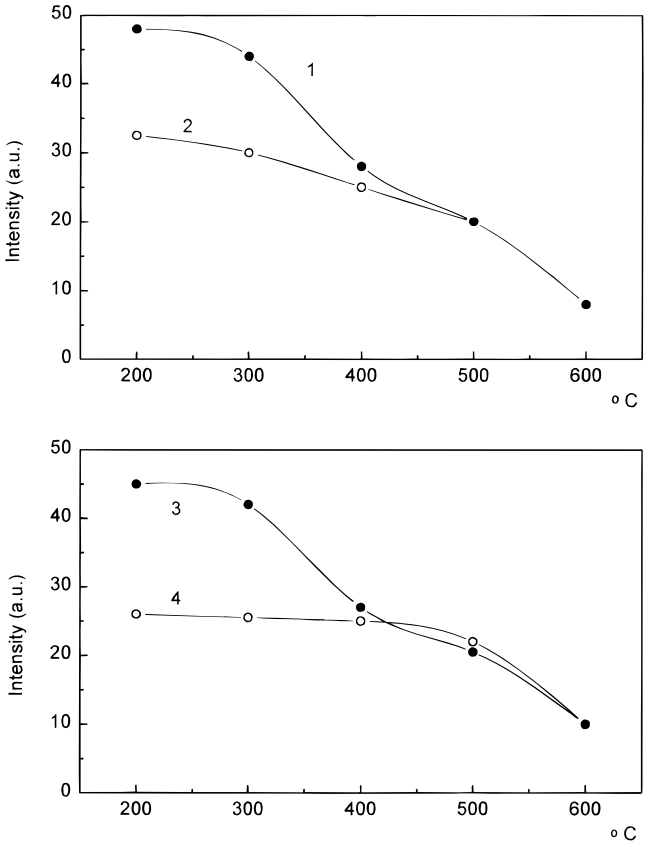

Figure 6. Variation of the intensity of the 3640−3620 cm^{-1} band as a function of the temperature of treatment: (1) Al-pillared montmorillonite; (2) NH_4-montmorillonite; (3) Al-pillared beidellite; and (4) NH_4-beidellite.

clays vis a vis their use in catalysis. Here we will show that in addition to the influence of calcination temperature on the textural and sieving properties of the PLS, it can also affect the total as well as the ratio of the Brønsted to Lewis acidity. This of course will have important implications on the activity and selectivity shown by PLS for acid-catalyzed reactions.

When samples are calcined either in vacuum or in air[56,57,59] a decrease in acid hydroxyls (dehydroxylation) and consequently on the number of Brønsted sites is observed (Figure 6). It can be said that Brønsted acid sites associated with the pillars strongly decrease with calcination, and at calcination temperatures approaching 500 °C, they have practically dissapeared. At this temperature, the only Brønsted acids sites remaining are those associated with the clay in cases such as beidellite, where there is some isomorphic substitution of silicon for Al in the tetrahedral layer (Figure 7).

The total amount of Lewis sites also decreases with calcination temperature, but however, there are still Lewis sites remaining at calcination temperatures above 500 °C.[57]

These observations are of paramount importance when PLS have to be used in a given catalytic process. Indeed, in order to stabilize the activity of the catalyst, one should calcine the solid before it is introduced into the reactor at a temperature above the reaction temperature. Then, we have to conclude that if PLS are to be used in reactions catalyzed by Brønsted sites they have to be limited to those reactions that do not require high calcination or regeneration temperatures of the catalyst. If higher

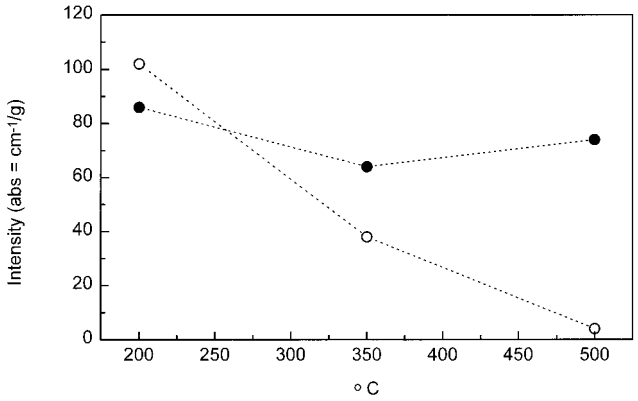

Figure 7. Intensity of the pyridinium band (1540 cm^{-1}) at different calcination temperatures: (●) Al-pillared beidellite and (○) Al-pillared montmorillonite.

calcination temperatures are to be used one should take into account that the PLS will only present Lewis acid sites except for the Brønsted acidity associated with the clay layers or that fraction which could be regenerated in the pillars by rehydroxylation of the Lewis sites.

3. Catalytic Activity of Acid PLS

There is no doubt that the primary interest in developing acid PLS was related with their use as cracking catalysts in FCC units. Indeed the possibility of preparing PLS where the large gas oil molecules could diffuse and encounter the active acid sites was a strong driving force for the development of such catalysts. However, and despite the importance of diffusion on catalytic cracking, it is remarkable that only a limited amount of diffusional studies of reactant molecules have been carried out on PLS. In one of the few experimental studies[92] the coupling of diffusion and reactivity was measured by carrying out the cracking of *n*-octane and 2,2,4-trimethylpentane (2,2,4-TMP) on an acid alumina-pillared montmorillonite. The sieving properties of the material were quantified by a time-dependent parameter analogous to the constrain index that the authors called the selectivity ratio and defined as log (fraction of *n*-C_8 remaining)/log (fraction of 2,2,4-TMP remaining). They showed that the branched alkane diffuses better in the case of the Al-PLS than in the case of faujasite zeolite. This result was in line with a mesitylene diffusion study which showed that this molecule diffuses twice as fast in a pillared Na-bentonite than in a Na Y faujasite.[93]

Theoretically, the diffusion in pillared clays has been studied by molecular dynamics simulation.[94,95] These authors have studied the diffusion of finite-size molecules in model pillared clays and found that the self diffusivity (*D*) is a monotonically increasing function of the temperature. Clustering of the pillars has a strong effect on the diffusivity of the molecules, and furthermore, *D* increases monotonically as the porosity increases.

It is evident that in the case of pillared materials, the preparation procedures are the determinant factor controlling the density and distribution of pillars, with clear implications on the diffusivity of the reactants in the galleries formed, and consequently on the adsorption and reactivity. In principle one could expect that only molecules with a diameter

Table 5. Adsorption Capacity of Al-PLS for Various Hydrocarbons

probe hydrocarbon	dimension (nm)	adsorption pressure (torr)	uptake [g/(100 g PLS)]
n-butane	0.46	600	8.0
cyclohexane	0.61	60	8.4
carbon tetrachloride	0.69	106	11.5
1,3,5-timethylbenzene	0.76	9.4	5.6
1,2,3,5-tetramethylbenzene	0.80	6.9	0
perfluorotributylamine	1.04	31.0	0

smaller than the interlayer distance could be adsorbed and consequently could react. This is not far from reality as seen from the adsorption capacity of an Al-PLS for various hydrocarbons (Table 5).[96]

However, it has been seen that the diffusion and adsorption are not only limited by the interlayer distance but also by the lateral distance between pillars, i.e. density of pillars. Indeed, in one study coronene (1.1 nm diameter) was successfully adsorbed on one Al-PLS with roughly the same interlayer distance than the material shown in Table 5. The adsorbent responsible had an Al content of 2.0 mmol/(g of clay)[97] instead of 2.41 mmol/(g of clay) of the sample in Table 5. Another piece of clear proof of the effect of pillar density on diffusion and adsorption is the observation[97] that a PLS with 2.0 mmol Al/(g of clay) was unable to adsorb porphyrin (1.9 nm diameter), while if the PLS was prepared with 1.25 mmol Al/(g of clay), adsorption of tetraphenylporphyrin was possible.

While in most cases the authors only consider as potential catalytic surfaces those contained within the galeries, these, however, are not the only ones we can make use of, particularly when dealing with large molecules. If one is able to produce an adequated aggregation between the PLS, meso-macropores could be formed which would permit for the adsorption of large molecules. In this sense, it has been presented[98] that air-dried pillared montmorillonites do not adsorb 1,3,5-triethylbenzene probably as a consequence of face to face aggregation resulting in the formation of zeolite-like structures. Meanwhile, freeze-dried samples adsorb appreciable amounts of the above molecule, which can be explained by assuming that freeze drying promotes edge to edge or edge to face aggregation and consequently macropores are formed. With these examples, we have tried to show the importance of the preparation procedures of PLS on their final textural characteristics and consequently on their diffusion, adsorption, and catalytic properties.

When the molecule has reached the surface of the catalyst it has to find the acid site whose characteristics have been described above. Even though one can measure the acidity of the sites using physicochemical techniques, many authors prefer to compare the acidity of different solids by means of chemical reactions in the hope that the results are more realistic from the catalysis point of view. In this respect cracking of pure compounds such as cumene,[99−102] *p*-isopropylnaphthalene, and alkanes, as well as dehydration of alcohols,[103−106] and isomerization and disproportionation of C_8 and alkylaromatics[107−110] has been widely used as a test reaction in order to compare the acidic properties of different PLS.

When gas oil was cracked, it was soon recognized[111−113] that layered silicates produced more coke than conventional FCC catalysts but their behavior was in fact still better than that of amorphous silica-alumina. Furthermore, it was found that different clays containing the same pillars gave different cracking results. For example[114] in hectorites and montmorillonite pillared with the same Al or Al Zr pillars, the former was less active but more selective toward gasoline production. Laponites[115] and saponites[116] have also been pillared with Al and tested for gas oil cracking. In all cases they give good activity and selectivity for LCO, but unfortunately they produce too much coke. Overall it can be said that the main practical limitation encountered by the PLS as FCC catalysts was the high coke production and their poor resistance to the high hydrothermal temperatures existing in the regenerator. Even though in the pursuit for stable pillars considerable progress has been made, the demands of FCC have arrived to the point where the structure of the clay itself was no longer stable enough. However, the use of the interest-ratified clay rectorite has opened up a real possibility of using them in FCC with or without addition of a zeolite copromoter. Then, the actual tendency is to produce rectorite pillared with highly stable Al-Ce pillars. Although there is still a high level of coke produced this may be overcome with the new ultrashort contact time risers, which when combined with new regeneration units (two stage regenerators) will decrease the hydrothermal stability requirements of the catalyst, and open up new possibilities for the use of PL rectorites as FCC catalysts.

It is fair to say that researchers, especially in academia, often forget that technical achievements are not enough if they are not accompanied by the economic viability of the process. It is clear that for the use of PLS as a commercial FCC catalyst it must be economically competitive with the actual FCC catalyst. In order to accomplish this, three criteria need to be met:[117] (1) Use the whole clay material and preferably a clay requiring the minimal pretreatment. (2) Pillar the Ca or Ca-Na forms, not the Na form in order to avoid the need for a pre-exchange. (3) Use a clay−polymer concentration >15% solids, that can be economically and effectively spray dried to give a good particle size distribution (40−200 μm).

Until all technical and economic requirements for the use of PLS in FCC catalysts can be achieved, one may think instead of using the pillared clay for another oil refining process which requires acidic PLS but is much less demanding than FCC from the viewpoint of hydrothermal stability, coke production, and catalyst conformation. The process in mind which fulfills this is hydrotreating of heavy and residual gas oils. Hydrotreating catalysts are bifunctional catalysts where hydrogenation−dehydrogenation reactions occur on metal centers such as those on Ni-Mo, Co-Mo, Pt, or Pd, whereas cracking reactions occur on acid centers usually provided by an amorphous aluminosilicate or a zeolite having the faujasite structure. It was clear that the role of the amorphous or crystalline aluminosilicate could be in this case carried out by the PLS.

Table 6. Hydrodesulfurization and Hydrocracking (HDS-HC) with Clays as Cracking component at 400 °C Reaction Temperature[a]

component	% NAP	% KER	% LFO	% TGO	% conv
HY zeolite	28.0	29.5	34.4	37.6	48.2
Al-CH bentonite	11.6	21.9	39.0	49.5	31.8
Zr-ACH bentonite	9.2	14.9	31.2	59.7	17.8

[a] NAP = naphtha (room temperature to 154 °C); KER = kerosene (190−271 °C); LFO = light furnace oil (190−360 °C); TGO = total gas oil (360 °C+).

The possibility of making bifunctional Pt/PLS catalysts has been illustrated by using test reactions such as the hydroisomerization and hydrocracking of *n*-alkanes.[118−124] These studies, in general, showed that there is a direct correlation between the Brønsted acidity of the PLS and the hydroisomerization/hydrocracking activity, and furthermore it is possible to achieve on these materials a good balance between hydrogenation−dehydrogenation and the cracking functions.

In the case of real refinery feeds, clays pillared with Al, Zr, or Ti have been used as the acid component of the hydrotreating catalyst formulation.[125−134] In these cases and since heavy and residual gas oils contain high levels of sulfur, the preferred hydrogenating−dehydrogenating functions (HDF) will be Ni-Co/Mo-W. A catalyst could then be prepared in which the metals are incorporated into the Al_2O_3 component of the catalyst, and this will be well mixed with the acid PLS component. There is no doubt that if this preparation procedure is selected, it is necessary to ensure that the distance between the HDF and the acid sites should be minimized, otherwise a fast deactivation of the catalyst by coking will occur. It is for this reason that the clay should be dispersed in a way such to produce clay layers that are completely surrounded by the inorganic oxide matrix.[135]

In Table 6 the hydrocracking activity for vacuum gas oil on Ni/Mo/Al_2O_3 with Al-pillared and Zr-pillared bentonite are compared with those of a catalyst formed by 70% of Al_2O_3 with Ni/Mo and 30% of HY zeolite.[134]

It can be seen overwhelmingly that there is a much lower activity for hydrocracking shown by the PLS with respect to the zeolitic catalyst. Since this difference is even larger than the one observed between them during direct cracking of vacuum gas oil feeds, one may think that the PLS were coked much faster than the zeolite when the metals are incorporated on the Al_2O_3. In order to probe this coking behavior further, the authors[134] have carried out the above reaction under identical conditions on the same materials, but in this case the Ni and Mo were incorporated directly on the PLS. It is evident from this second preparation that a better proximity between the acid and the metal sites should exist, and consequently hydrogen spillover should occur due to the smaller distances. The results given in Table 7, clearly reveal that in this case the PLS can give even better hydrocracking results.

In the light of the above results it is then apparent that PLS either by themselves or combined with large pore tridirectional zeolites (HY, HBEA) have real possibilities as hydrocracking catalysts.

Table 7. Hydrodenitrification and Hydrocracking (HDN-HC) with Clays as Hydrogenation Component Supports, at 400 °C Reaction Temperature

support	% NAP	% KER	% LFO	% TGO	% conv
HY zeolite	28.0	29.5	34.4	37.6	48.2
Zr-ACH bentonite	27.2	32.0	36.4	36.4	49.2
(Al,Si)-bentonite	34.5	30.5	35.8	39.6	59.2
Al-CH bentonite	49.6	35.7	37.7	21.7	70.1

The other field of acid-catalyzed reactions where the porosity of the PLS together with their acid properties can be of use, is in the preparation of chemicals and fine chemicals.[136−140] Indeed there is a strong driving force in this field to replace mineral acids such as H_2SO_4, H_3PO_4, $AlCl_3$, HF, etc. by solid acids. For instance, in the formation of phenol by decomposition of cumene hydroperoxide, diluted H_2SO_4 is used as the catalyst in the commercial process, but solid acids such as zeolites have also been claimed successful.[141] PLS can also decompose the cumene hydroperoxide in acetone and phenol,[142,143] but water has a negative effect on both its activity and selectivity and consequently the catalyst should be dried.

Acidic clays by themselves or pillared with Al, Zr, and Cr have been used to catalyze organic reactions requiring Lewis and Brønsted acids such as $AlCl_3$, HF, or H_2SO_4. In this respect, modified clays are good catalysts for carrying out acylations: propionylation of anisole, acylation of mesitylene with acetyl, and chloroacetyl chloride to produce 2,4,6-trimethylacetophenone and α-chloro-2,4,6-trimethylacetophenone as well as benzoylation reactions.[144] Friedel−Crafts alkylations are also successfully catalyzed by clays and pillared clays. In these reactions the larger pore of the PLS are fully involved in the alkylation of aromatics such as benzene, toluene, and biphenyl with olefins and alcohols.[145−150] In general, processes which are catalyzed by concentrated sulfuric acid can also be catalyzed by PLS,[151] but as noted in the reactions described above, it is necessary to reduce the water content of the PLS in order to avoid undesired hydrolysis reactions.

In the last years, special emphasis has been placed on using natural renewable products as raw materials or building blocks to obtain higher value added products. In this sense terpenes, sugars, fatty acids, and esters are largely used to produce aromas, food additives, cosmetics, and pharmaceuticals. Many of the desired transformations are catalyzed by acids, and consequently it is worth looking at what has been done with PLS. In the case of terpenes, α-pinene, limonene, and α-terpinene, all have been reacted on alumina-pillared clays and also on a layered α-tin phosphate analogue. α-Pinene is found to be the most reactive one, giving camphene as the major product (>50%) at 100 °C.[152] In reactions such as these where many products can be formed, the fine-tuning of acidity and pore dimensions are mandatory if selective catalysts are to be prepared.

Glucose, an abundant natural raw material, can be transformed into other valuable products by glycosidation with alcohols, or dehydration to form organic acids. The glycosidation allows one to obtain fully biodegradable surfactants by generating a molecule with two hydrophobic and hydrophylic moities:

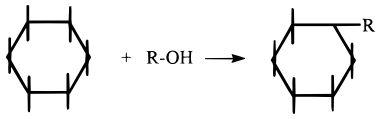

PLS are able to perform this reaction with minimum formation of the ether of the alcohol.[153] Fe-, Cr-, and Al-pillared montmorillonite can also promote the shape-selective partial dehydration of glucose to organic acids. Pore widths of at least 1.0 nm allowed the 0.86 nm glucose molecule to diffuse and react directly within the micro- and mesopores of the catalyst, the principal reactions occurring in this example being the isomerization of glucose to fructose, partial dehydration of glucose to 5-hydroxymethylfurane (HMF), rehydration and cleavage of HMF to formic acid and 4-oxopentanoic acid, and coke formation.[154] The Fe-pillared montmorillonite provided the highest glucose conversion rate, with 100% glucose conversion at 150 °C, and the lowest and highest selectivities to HMF and formic acid respectively. In the PLS examples studied the fraction of pores in the 1−3 nm range allowed glucose to diffuse but also trapped the bulky HMF intermediate, thereby directing the reaction toward the final organic acid products.

Since the reactions are occurring at relatively low temperatures, the stability of the pillars is not so critical and thus montmorillonite cross-linked by organic cations can be used as catalysts, for example in the oligomerization of oleic acid, as well as for esterification reactions.[155,156] It was observed when montmorillonite cross-linked by $(CH_3)_4\ N^+$ was used to produce dicarboxylic (DCA) acids by oligomerization of oleic acid[155] that the yield of DCA is a funcion of the layer charge density (Figure 8). When the layer charge is high, neighboring oleic acid molecules are separated by the high density of pillars, and bimolecular reactions are thus disfavored. Conversely with one decreases the density of pillars, the pore volume increases and dimerization can occur. If the pillar density is decreased still further the available void space increases again and then trimers can be formed. This is a good example of restricted transition state selectivity in PLS.

When the montmorillonite was pillared with the diamine 1,4-diazabicyclo[2.2.2]octane[156] the resultant material can catalyze the esterification of carboxylic acids with alcohols. Again in this case the density of pillars should allow the reactivity among reactants with different size to be differentiated. Indeed, in Figure 9, the data conclusively show that the reactivity decreases with increasing size of the alcohol molecule. Along these lines, it would certainly be of interest to investigate the possibilities of PLS for the esterification of fatty acids (for instance oleic acid) with linear alcohols, since it should be possible to produce esters analogous to jojoba oil and whale sperm oil which are of interest to the cosmetic industry.

I do not want to finish this chapter on acid-catalyzed reactions on PLS without briefly introducing another type of pillared layer materials, pillared zirconium phosphates, which can also be used for acid catalysis particularly for processes requiring low temperatures. Layered phosphates containing tetravalent metals such as Zr, Ti, Pb, and Ge have been

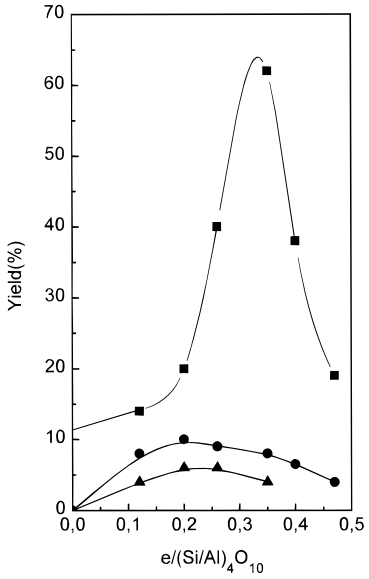

Figure 8. Effect of charge density of montmorillonite on oligomerization of oleic acid: (■) dicarboxylic acid, (●) tricarboxylic acid, and (▲) oligocarboxylic acid.

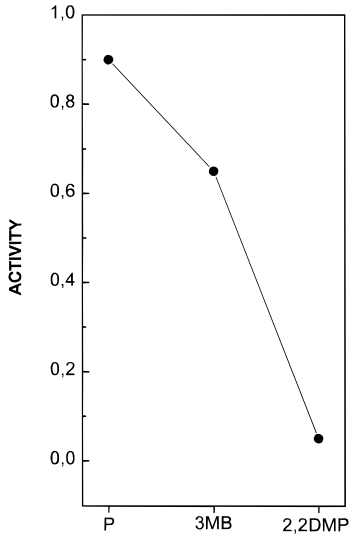

Figure 9. Relative rate of esterification of acetic acid with *n*-pentanol (P), 3-methylbutan-1-ol (3MB), and 2,2-dimethylpropan-1-ol (2,2-DMP).

synthesized,[157−165] but the zirconium phosphates are the most stable to hydrolysis, and they have been pillared successfully with aluminum and chromium oxides, giving materials with good surface area, porosity, and thermal stability up to 400 °C.[160,166−168]

The pillared zirconium phosphates can catalyze isomerization, dehydration and alkylation reactions,[169−172] and when they are pillared with organic pillars of the phosphonate or sulfonic acid type, acidic properties are generated. These type of materials are denoted MELS (moleculary engineered layered structures) and look like inorganic−organic acid resins and, as such, can catalyze reactions including butene isomerization, methanol dehydration, MTBE synthesis, aromatics alkylation and cracking.[173−178]

While the expectations for MELS were high, their use in acid catalysis seems to be limited today, probably due to problems derived from diffusion and regenerability of the catalysts. In general, we believe that the use of pillared zirconium phosphates, at least

in acid catalysis, will be limited to some very special cases.

B. Pillar Layered Silicates as Redox Catalysts

It appears logical from the knowledge that since it is possible to generate stable pillars with a large variety of transition metals, one should be able to use those as the centers of catalytic activity for redox type reactions. This has been tried out and the selective catalytic reduction (SCR) of NO by NH_3 was successfully carried out on titanium pillared montmorillonite.[179−181] Since it has been claimed[182,183] that Brønsted sites are important for SCR of NO by NH_3, the acidity was modified by sulfation and catalysts having high resistance to SO_2 were prepared.

The Ti-pillared montmorillonite in combination with Pd metal can selectively carry out the hydrogenation of 3-butenonitrile and 2-butenonitrile, to butyronitrile without isomerization. However, progressive poisoning of the catalytic sites and possible diffusional limitations decrease the activity of the catalyst.[184]

Ti-pillared montmorillonites together with chiral auxiliaries in the presence of stoichiometric amounts of tertiary butyl hydroperoxide were able to enantioselectively oxidize prochiral sulfides to sulfoxides.[185] The authors claim that the Ti-PLS, possessing optimum Lewis acidity, form complexes with bridged tartrates of alkoxides reactant and oxidant (Figure 10), as inhomogeneous analogue which facilitates the oxygen delivery stereospecifically to afford higher enantioselectivity and activity.

Elimination of contaminants by photocatalytic oxidation has also been carried out on TiO_2-pillared clays. When montmorillonite was pillared with TiO_2 particles and supercritically dried, the resultant PLS has porosities in the order of 0.6 mL g^{-1} and showed little hysteresis on the nitrogen adsorption−desorption isotherms. After photoelectrochemical deposition from hexachloroplatinic(IV) acid solution was performed, the resultant material was very active for the photocatalytic oxidation of CO in a stream of air. The high catalytic activity was attributed to the high dispersiveness of the TiO_2 sol particles between the silicate layers and the smallness of the Pt particles effectively loaded on the sol particles.[186] Phenol, an important contaminant in some residual waters, has also been oxidized photochemically on small TiO_2 crystallites pillared in between the clay interlayers.

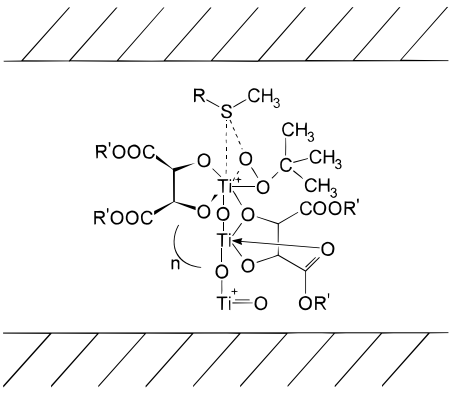

Figure 10. Transition state of asymmetric sulfoxidation.

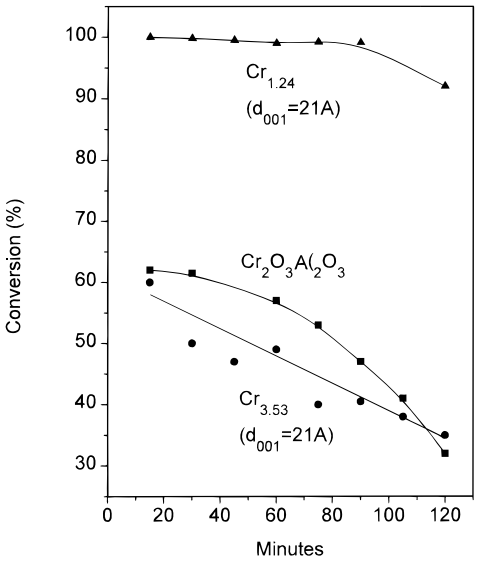

Figure 11. Dehydrogenation of cyclohexane to benzene on Cr-montmorillonite containing 1.24, 3.53 Cr per unit cell, and also on a commercial Cr_2O_3/Al_2O_3 catalyst.

Cr-pillared clays[187] have also been used in catalysis for reactions such as dehydrogenation and hydrodesulfurization. In this sense Tzou and Pinnavaia[188] have studied the dehydrogenation of cyclohexane by a chromium-pillared montmorillonite. Results from Figure 11 show that when the dispersion of the chromium was high (1.24 Cr per unit cell) in the montmorillonite the results were better than for the corresponding commercial catalyst on the basis of Cr_2O_3/Al_2O_3. When Cr-montmorillonite was presulfided it was furthermore able to desulfurate a stream containing thiophene. However, the activity decreased slowly with time, and no possibilities for commercial use are envisaged.[189] Other metals such as Fe when was used to pillar clays have a high resistance to reduction and are stable when heated (500 °C) in a reducing atmosphere. It is therefore not surprising that these Fe-PLS have been studied for their acidity to convert synthesis gas into olefins.[190−193] The selectivity for lower olefins, i.e. ethene (16.0%) and propene (38.0%), was particulary noteworthy. These results show that the iron oxide-pillared clay is in fact a shape-selective catalysts a feature which can be attributed to steric factors originating in the micropores of the pillared clay. However, increasing iron content resulted in an excess of iron outside the pillars, and conversion and selectivity to longer olefins increases.

C. New Perspectives for Pillared Materials

Recently, multilayered nanostructured materials were prepared from macromolecular precursors by modifying some of the techniques used in the semiconductor industry.[194] It is known that molecular adsorbates can form densely packed monolayers and multilayers on solid substrates by spontaneous self-assembly (SA).[195] The synthesis itself involves a series of adsorptions with poly(diallyldimethylammonium chloride) (PDDA), and exfoliated sheets of synthetic hectorite. The procedure uses silicon wafers and involves the slow addition of PDDA to the silicon wafer, followed by a fast washing with water and drying. After this, a diluted dispersion of hec-

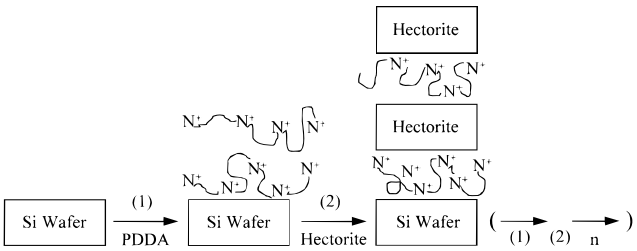

Figure 12. Synthesis of multilayer structures on silicon wafers.

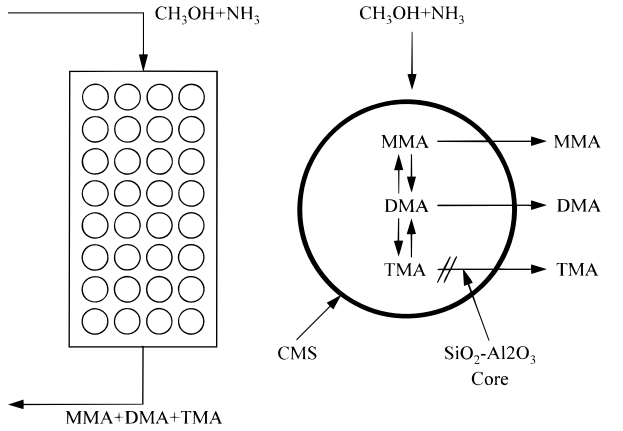

Figure 13. Shape-selective production of MMA and DMA in a composite SiO_2-Al_2O_3/CMS.

torite in H_2O is added to the surface, rinsed quickly, and dried. By repeating the process layers thicker than 2 nm could be prepared (Figure 12) and XRD provides evidence for structural order in PDDA-hectorite multilayers.

Deposition of crystalline materials onto sheet silicates including oxides, indicates that the technique could be used for substrate growth of other materials. This method opens up a strategy for building ordered organic−inorganic layers with control over the structure and thickness. In line with this work it has been shown[196] that new materials could be formed by combining and flocculating two different single layer suspensions with opposite charges, and in this way $MoWS_4$ which is an ordered compound was prepared by alternating MoS_2 and WS_2. In an analogous way a random interstratified solid was prepared from separate dilute suspensions of two layered materials, $Li_{0.25}MoO_3$ and Na montmorillonite.[197]

Composite catalysts formed by a layered silica-alumina with carbogenic molecular sieves (CMS) have been prepared by coating the silica-alumina with a polyfurfuryl alcohol carbon molecular sieve (PFA-CMS).[198] The resultant material was shape selective for the preparation of monomethylamine (MMA) by reaction of ammonia with methanol, at 400 °C and 200−400 psig. In this case, the ratio of the sum of MMA and dimethylamine (DMA) to trimethylamine (TMA) was between 3 and 5, compared to a lower ratio obtained when using silica-alumina as the catalyst. Thus by coating the SiO_2-Al_2O_3 with layers of PFA-CMS high selectivity to MMA is achieved by a diffusion shape-selective process (Figure 13).

The possibilities of producing new materials via a biomineralization process has been brought to light very recently.[199] In this sense porous lamellar silicas, structurally similar to pillared clays, have been synthesized.[200] The procedure is concerned with the hydrolysis and cross-linking of a neutral inorganic alkoxide precursor in the interlayer region of multilamellar vesicles of a neutral bolaamphiphile surfactant. These materials may offer new possibilities as catalysts.

There is the possibility to modify the chemical composition and the pore size of dense layered metal oxides[201] by preswelling and pillaring with silica or alumina pillars.[202] By changing the size of the preswelling agent, the d spacing can be changed allowing pillared products with a wide range of pore sizes to be produced, which can be adapted to take into account the size of the reactant molecules during a catalytic process. For instance, layered silicic acids which can be prepared by proton exchange starting from layered silicates, such as ilerite,[203,204] magadiite, kenyaite, and kanemite, are useful hosts in the formation of pillared materials because of the presence of reactive silanol groups on their interlayer surfaces.[205] Silanol groups, which are acidic enough to allow proton transfer to an amine group, are oriented in a crystallographically regular manner on the interlayer surface,[206] and consequently, it should be possible to generate a porous material with a high degree of uniformity during pillar formation.[201,207] Using this strategy a layered silicic acid of ilerite was preswelled with octylamine and tetraethylorthosilicate (TEOS) was added, and a silica-pillared product was obtained by calcination in air at 600 °C.[208] The surface area of the resultant material after calcination at 600 °C was 1152 $m^2\ g^{-1}$.

Materials of this type while they can be used as molecular sieves for adsorption and also act as supports for the specific catalytic active components, they cannot be used as molecular sieve acid catalysts. It would be then of interest to prepare such a class of materials which possessed in addition relatively strong acid sites in the layers. We can envisage one way to achieve this; the method consisting of preparing similar materials but containing layers of silica-alumina instead of silica. This could be achieved for instance, by starting with a layered compound such as MCM-50 within which the amorphous layers are formed by silica-alumina. One may attempt to pillar a layered material of this kind using TEOS and in this way generate an extremely high surface area silica-alumina with molecular sieve properties. If this is indeed a plausible solution, it can be improved if the layers instead of being amorphous are crystalline. This can be attained by taking into consideration the observation that some zeolites go through a layered intermediate phase during their synthesis. There is then the possibility of preswelling these intermediates and pillaring them, giving rise to a whole series of new pillared compounds with controlled pore dimensions in which the composition of the layers (Si/Al) as well as the nature of the pillars can be adapted to suit the particular reaction to be catalyzed. This has in fact been done with a laminar precursor of the MCM-22 zeolite, which has been pillared with TEOS, producing the MCM-36 molecular sieve. The procedure can also be applied to other layered zeolite precursors such as that formed during the preparation of ferrierite.[209] By this procedure one should obtain a pillared material combining both micro- and mesopores, and produce as a result

crystalline layers, with higher thermal and hydrothermal stability.

In conclusion, new possibilities for engineering pillar layered materials are opened, which should allow us to design a catalyst with regular pores in the micro- to mesoporosity range, and to adapt them to our catalytic needs in the domains of oil refining and petrochemistry, as well as for chemicals and fine chemicals production.

III. Silica-Aluminas with Narrower Pore Size Distribution

Up to now we have described in this review how it is possible to go toward mesoporous materials starting from microporous ones. However, there is another approach aimed to produce mesoporous materials with a narrow pore size distribution, by means of preparation techniques closer to those of classical silicas or silica-aluminas. Indeed, silica-aluminas have been prepared which have catalytic properties similar to zeolites but without the zeolite pore restrictions. They have been synthesized by hydrolysis of bulky organosilanes in the presence of aluminum salts,[210] followed by introduction of an aging step into the standard technique of Co-gelalumiminate,[211] and finally cogelation of silica and alumina hydrosols in the presence of K^+.[212]

More recently, it was thought that one could perhaps control the pore size of the amorphous silica-aluminas by preparing them exclusively in the presence of tetraalkylammonium cations, and thus by changing the size of these one should change the size of the pore.[213] This type of synthesis should also direct the aluminum to be Al^{IV} and to an Al−Al separation that will be controlled by the size of the organoammonium cation. As organoammonium cations, typically tetramethyl-, tetraethyl-, tetrapropyl-, and tetrabutylammonium ions were used.

The derivatives of the pore size distribution (Figure 14) indicate that when tetraalkylammonium cations are used alone the average pore size obtained is inversely related to the size of the cations used. The pores are in the mesoporous region and a quite regular distribution is obtained with total surface area up to 500 $m^2\ g^{-1}$. In contrast when Na^+/NH_4^+ cations were used, a very broad pore size distribution was observed.

The Al_2O_3 content of these samples was in the range of 67 to 93 SiO_2/Al_2O_3. However, it is possible, following this procedure, to prepare samples with higher Al_2O_3 content (6.7 SiO_2/Al_2O_3). In this case,

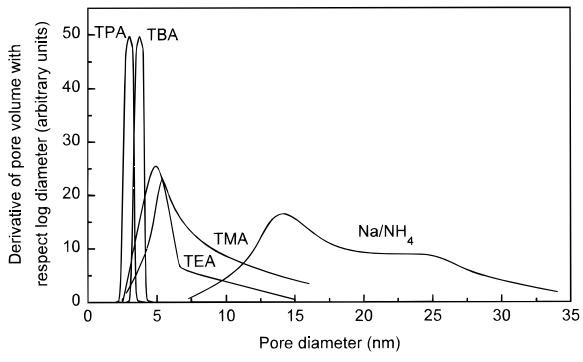

Figure 14. Pore size distribution of Si-Al catalysts, from N_2 adsorption.

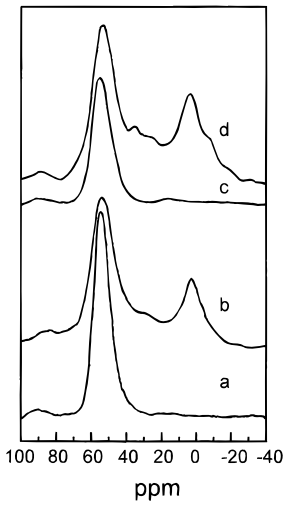

Figure 15. ^{27}Al MAS NMR spectra of sample TMA (a, synthesized and b, after calcination) and sample 2 (c, synthesized and d, after calcination).

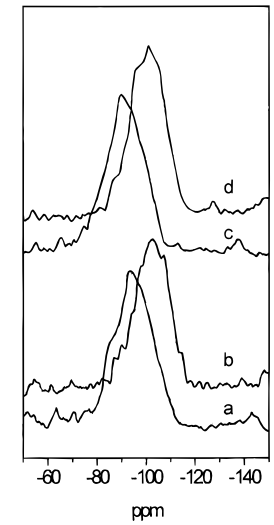

Figure 16. ^{29}Si MAS NMR spectra of sample TMA (a, synthesized and b, after calcination) and sample TEA (c, synthesized and d, after calcination).

narrow pore size distributions were also obtained, and the ^{27}Al MAS NMR indicated that after the synthesis all observable aluminum was as Al^{IV} (54 ppm) and therefore, they have the potential to generate acid sites (Figure 15).[214] After calcination at 550 °C acid samples were obtained and the NMR spectra significantly changes. Three different signals, the first one centered at 57 ppm corresponding to Al^{IV}, a broad band at 30 ppm which can be assigned to strongly distorted Al^{IV},[215] and a line at 0 ppm, corresponding to octahedral aluminum, were observed. With respect to the ^{29}Si MAS NMR spectra (Figure 16), it shows in the precalcined samples a broad resonance line showing several shoulders. This line is centered at −95 ppm, but ranges from −80 to −110 ppm. This is the chemical shift region characteristic of Si atoms surrounded by zero, one, two, three, and four Al atoms. This resonance line shifts to the region −90 to −113 ppm (maximum at −105 ppm), after calcination. No individual contribution of each silicon environment to the total resonance line was detected.

These samples were suitable as acid catalysts for processing large molecules. When calcined they were

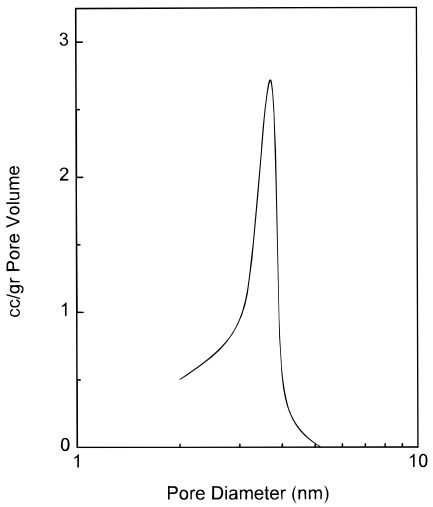

Figure 17. Pore size distribution of silica-alumina prepared with tetrapropylammonium, and in absence of alkalines.

active and selective as gas oil cracking catalysts, with their activity being larger than that of a classical amorphous silica-alumina, showing the benefit of a more narrow and regular pore size distribution. Unfortunately, when the samples were steamed at 750 °C in the presence of 100% steam, most of the pores collapsed and their activity strongly decreased.

Very recently, the preparation of amorphous silica-aluminas with very narrow pore size distribution was revisited, and new materials were obtained from a precursor of ZSM-5, using tetrapropylammonium as template in the absence of alkali ions.[216] The SiO_2/Al_2O_3 of the samples produced were higher than any of the samples prepared before ($80 < SiO_2/Al_2O_3 < 600$), the pore size distribution was very narrow indeed (Figure 17), and the calcined samples were acidic and had very high surface areas (≥ 700 m^2 g^{-1}). Obviously, the first option for catalytic uses was the cracking of gas oil. The results obtained showed that these materials, when calcined, were highly active and selective, with its actual behavior being between that of a conventional amorphous silica-alumina and a zeolite. However, when the catalysts were stabilized by a hydrothermal treatment at 750 °C, the surface area strongly diminished and so did the cracking activity. Under those conditions practically all Al^{IV} (54 ppm) disappeared, being converted into a mixture of tetrahedrally distorted (35 ppm) and octahedral (0 ppm) aluminum.

These results strongly suggested that if catalytic benefit was desired from these silica-aluminas with a narrow distribution of pore size, one had to look to processes requiring less severe reaction or regeneration conditions than cracking. Thus, when they were used as oligomerization,[216] hydroisomerization,[217] and hydrocracking catalysts,[218] the results were very promising showing the catalytic benefits from producing mesoporous materials with a narrow distribution of pore sizes.

IV. Ordered Mesoporous Materials

It is true to say that one of the most exciting discoveries in the field of materials synthesis over the last years is the formation of mesoporous silicate and aluminosilicate molecular sieves with liquid crystal templates. This family of materials generically called M41S have large channels from 1.5 to 10 nm ordered in a hexagonal (MCM-41), cubic (MCM-48), and laminar (MCM-50) array. In essence, they therefore possess both long-range order, and surface areas above 700 m^2 g^{-1}.[219−228]

There is no doubt that the synthesis of these materials opens definitive new possibilities for preparing catalysts with uniform pores in the mesoporous region, which should importantly allow the relatively large molecules present in crude oils and in the production of fine chemicals to react. Obviously when a new type of materials such as these are discovered, an explosion of scientific and commercial development swiftly follows, and new investigations on every conceivable aspect of their nature, the synthesis procedures and synthesis mechanisms, heteroatom insertion, characterization, adsorption, and catalytic properties, rapidly occurs. The advances carried out in these areas form the subject to review in this chapter.

A. Synthesis of Silica M41S Molecular Sieves Materials

1. Direct Synthesis

The system with a hexagonal array of pores, known as MCM-41, is the most important member of the family, and can be prepared by what was originally described as a liquid crystal templating mechanism where surfactant molecules act as templates.[225] Surfactants such as $C_{16}H_{33}(CH_3)_3NOH/Cl$ in solution were added to a sodium silicate in acid solution, to form a gel which was mixed with water and heated to 100 °C for 144 h. Of course to prepare aluminosilicate MCM-41 a source of Al must be added, to a solution of $C_{16}H_{33}(CH_3)_3NOH/Cl$. To the resulting solution, ultrasil silica, tetramethylammonium silicate solution, and tetramethylammonium hydroxide solutions were added while stirring. The mixture was then heated in a stirred autoclave to 100 °C for 24 h. The conditions reported here are only particular examples, since M41S materials can be synthesized from a variety of silica and alumina sources, surfactant to silicon ratios and within a broad time/temperature range.

In order to explain the synthesis mechanism and the observation that the microscopy and X-ray diffraction results presented for MCM-41 are similar to those obtained from surfactant/water liquid crystals or micellar phases,[229,230] Beck et al.[225] proposed a liquid crystal templating (LCT) mechanism. They proposed that the structure is defined by the organization of surfactant molecules into liquid crystals which serve as templates for the formation of the MCM-41 structure. In other words, the first step in the synthesis would correspond to the formation of a micellar rod around the surfactant micelle which in a second step will produce a hexagonal array of rods, followed by incorporation of an inorganic array (silica, silica-alumina) around the rodlike structures (Figure 18).

However, considering that the liquid crystal structures formed in surfactant solutions are highly sensitive to the overall characteristics of the solution, the authors[225] also account for the possibility that the

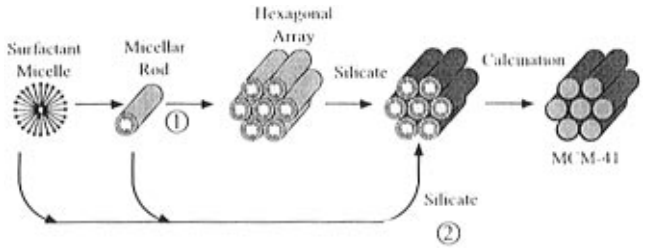

Figure 18. Possible mechanistic pathways for the formation of MCM-41: (1) liquid crystal initiated and (2) silicate anion initiated.

addition of the silicate results in the ordering of the subsequent silicate-encaged surfactant micelles. In a more recent paper, the authors[227] carried out the synthesis of MCM-41 using surfactants with different alkyl chain lengths from C_6 to C_{16} and worked at different synthesis temperatures. They found that only in the cases where the surfactant and synthesis conditions allow the formation of well-defined liquid crystal hexagonal structures, is the synthesis of MCM-41 successful. For instance, when C_6 and C_8 alkyl chain surfactants were used, MCM-41 was not formed, in agreement with the fact that the solubilities of these short chain quaternary ammonium are high, and aggregated structures are not necessary to minimize hydrophobic interactions. It is then concluded that M41S materials are formed through a mechanism in which aggregates of cationic surfactant molecules in combination with anionic silicate species form a supramolecular structure.

Davis et al.,[231] by carrying out in situ ^{14}N NMR spectroscopy, concluded that the liquid crystalline phase is not present in the synthesis medium during the formation of MCM-41, and consequently, this phase cannot be the stucture-directing agent for the synthesis of the mesoporous material in agreement with the already proposed mechanism through route 2. Thus, the randomly ordered rodlike organic micelles interact with silicate species to yield two or three monolayers of silica around the external surface of the micelles. Subsequently, these composite species spontaneously form the long-range order characteristic of MCM-41 (Figure 19). If one tries to remove the surfactant by calcination, just at the point when the long-range order is achieved, i.e. short synthesis times, the material is not stable as a consequence of the still large number of noncondensed silicate species. Longer synthesis time and/or higher temperature increases the amount of condensated silanols giving as a result stable materials.

Stucky and coworkers[232−239] have developed a model that makes use of the cooperative organization of inorganic and organic molecular species into three dimensionally structured arrays. They divided the global process into three reaction steps: multidentate binding of the silicate oligomers to the cationic surfactant, preferential silicate polymerization in the interface region, and charge density matching between the surfactant and the silicate (Figure 20). Furthermore, they state that in this model, the properties and structure of a particular system were not determined by the organic arrays that have long-range preorganized order, but by the dynamic interplay among ion-pair inorganic and organic species, so that different phases can be readily obtained through small variation of controllable synthesis parameter including mixture composition and temperature. This was proved by examining the structures in their final form and at various stages during their synthesis, by means of small angle neutron scattering (SANS).[240] The scattering contrast of the aqueous medium used in the synthesis was varied to enhance or diminish the scattering associated with the organic or inorganic precursor phases, allowing a probe of the component structures as they changed during the synthesis reaction. The SANS results verify that nucleation, growth, and phase transitions are not directed by a preassembled micellar arrays mimicking the final hexagonal pore structure. Similar conclusions have been achieved by Calabro et al. by carrying out an "in situ" ATR/FTIR study of M41S-type mesoporous silicate synthesis.[241]

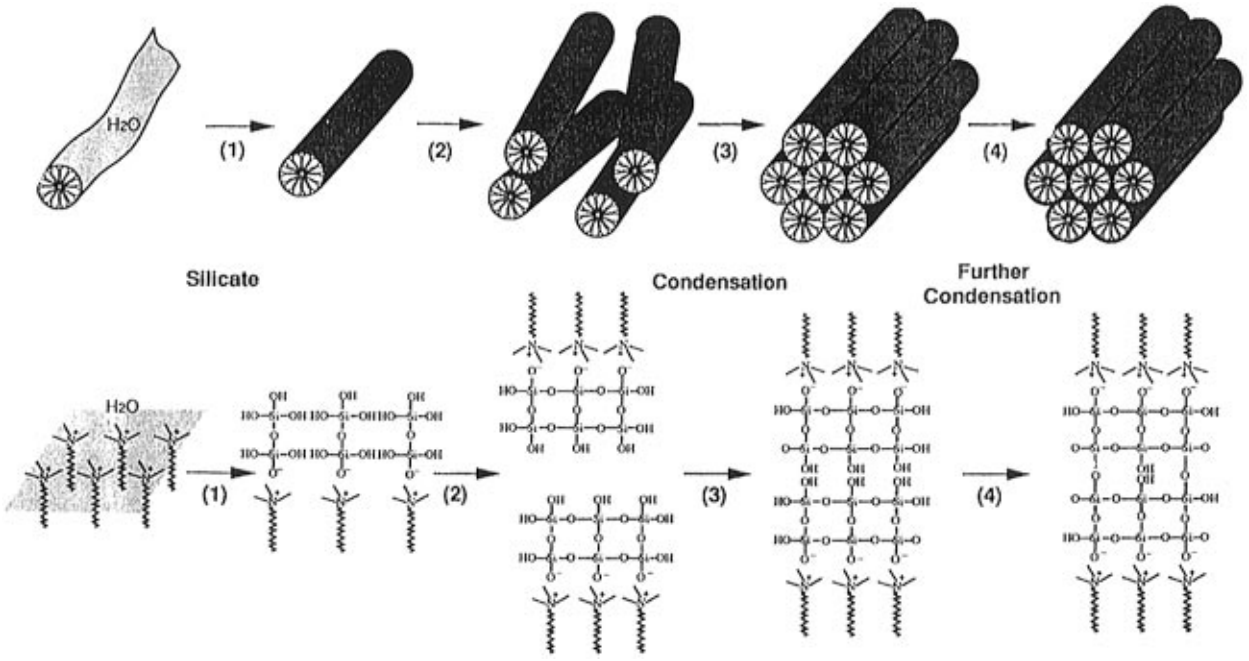

Figure 19. Mechanism for the formation of MCM-41.

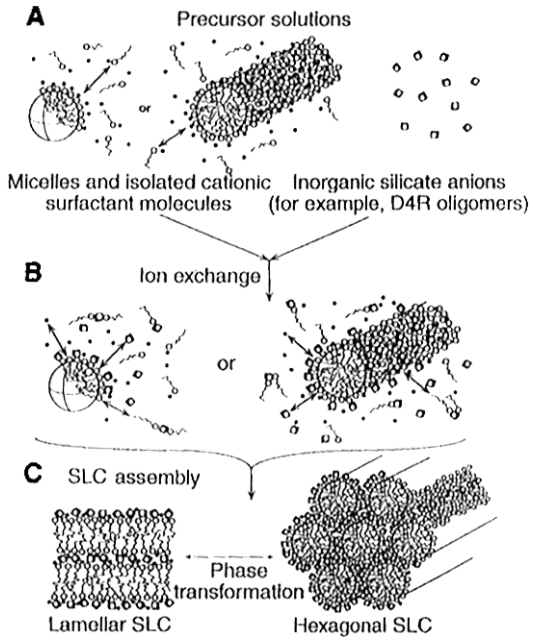

Figure 20. Schematic diagram of the cooperative organization of silicate-surfactant mesophases.

Following this mechanism, the criteria of charge density matching at the surfactant inorganic interfaces governs the assembly process, and consequently, the final type of structure generated. From this, it can be seen how the principle methodology can be extrapolated to prepare mesophases with different metal oxides as far as there is an electrostatic complementarity among the inorganic ions in solution, the charged surfactant head groups, and, when these charges both have the same sign, inorganic counterions.[233] These authors have presented four pathways to the synthesis of mesostructured surfactant−inorganic biphasic arrays (Figure 21).

In this way, cationic surfactants S^+ are used for the structuring of negatively charged inorganic species I^- (S^+I^- mesostructures). On the other hand, anionic surfactants (S^-) are employed for structuring cationic inorganic species (I^+) (S^-I^+ mesostructures). Organic−inorganic combinations with identically charged partners are possible, but then the formation of the mesostructure is mediated by the counter-charged ions which must be present in stoichiometric amounts ($S^+X^-I^+$, and $S^-M^+I^-$ mesostructures). In cases where the degree of condensation of the oligomeric ions which form the walls is low, the removal of the template leads to the collapse of the ordered mesostructure. It would then be of both fundamental and practical interest to develop new synthetic routes which allow the template to be more easily removed. Following this line, neutral amine template surfactants have been used[242] to prepare mesoporous molecular sieves (HMS) that have thicker pore walls, higher thermal stability, and smaller cyrstallite size than MCM-41 materials produced with highly charged surfactants. The neutral charge of the template allows for easy recovery. One has however to be aware that at the pH at which the synthesis was done (pH = 6) the amine can be protonated and, therefore, this is not a real neutral template system.

Nonionic polyethylene oxide surfactants[243] and ethylene glycol hexadecyl ether at high concentrations[244] can also act as structure directors. When one considers these neutral templating routes the interaction at the S° I° interface probably occurs through

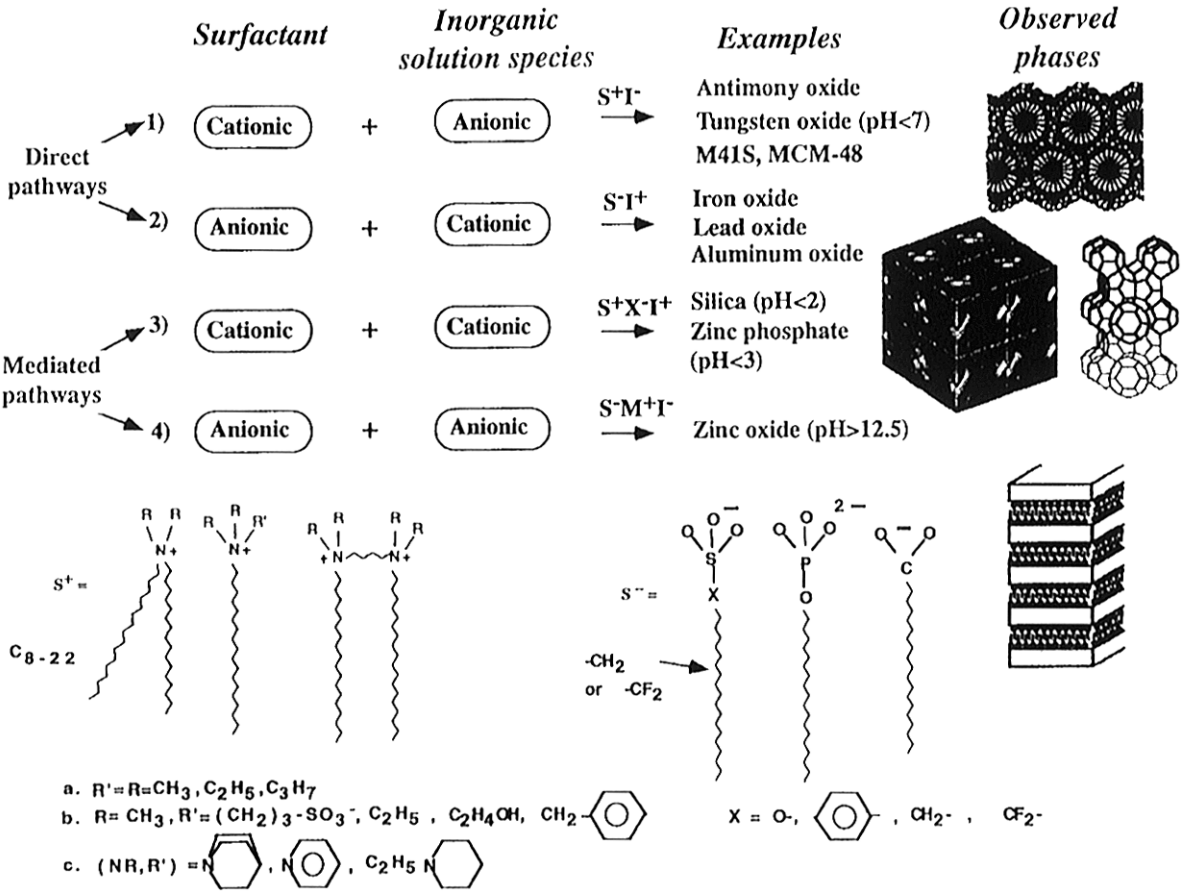

Figure 21. A general scheme for the self-assembly reaction of different surfactant and inorganic species.

Table 8. Elemental Analysis of the MCM-41 Samples Synthesized in a Highly Acidic Media: HCl (Sample 1) and HNO_3 (Sample 2)

	C (wt %)	H (wt %)	N (wt %)	C/N	CTMA/N
sample 1	34.09	6.91	2.11	18.8	0.99
sample 2	37.46	7.40	5.10	8.57	0.45

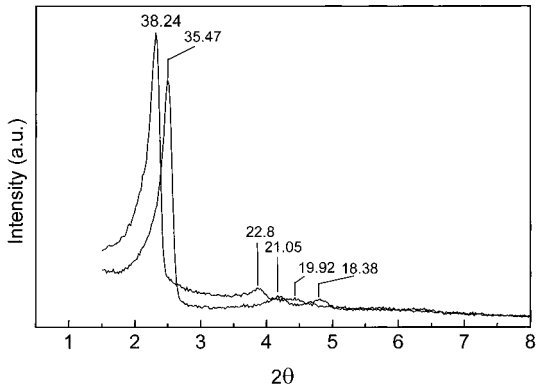

Figure 22. XRD (Cu Kα) of MCM-41 prepared in strong acid media generated by HCl and HNO_3.

hydrogen bonds which, by being weaker than electrostatic interactions, allow the extraction of the neutral template molecules by washing with ethanol.[245]

It is worth discussing here a new procedure for synthesizing silica and silica-alumina MCM-41 materials, which involves highly acidic synthesis conditions instead of the basic or mildly acid conditions commonly used. Maintaining consistencies with the charge density matching principle, it has been proposed[233] that the templating mechanism during the acid synthesis of MCM-41 follows a path in which $S^+X^-I^+$ mesostructures are involved, where I^+ is a positively charged silica precursor, S^+ is the alkyltrimethylammonium cation, and X^- is the compensating anion of the surfactant. If this were true it would be expected that samples prepared using different acids will give MCM-41 mesostructures with different final chemical composition, d spacings, and pore diameters. In order to check this, we have carried out the synthesis of MCM-41 in highly acidic media using two different monoprotic acids: HCl and HNO_3.[246] The gel composition used in the synthesis of the sample was 1:9.2:0.12:130 TEOS:HX:CTMABr:H_2O, where TEOS is tetraethyl ortosilicate, CTMABr is cetyltrimethylammonium bromide, and HX is HCl (sample 1) or HNO_3 (sample 2). The elemental analyses of the synthesized samples are given in Table 8.

The results from Table 8 indicate that sample 2 has a lower C/N ratio than sample 1. Moreover the CTMA/N ratios obtained strongly suggest that the liquid crystals are $CTMA^+Cl^-SiO^+$ and $CTMA^+NO_3^-SiO^+$ for samples 1 and 2, respectively. The presence of NO_3^- in sample 2 was proven from the presence of an IR band at 1383 cm^{-1} which can be assigned to the stretching vibration of NO_3^- groups. The XRD patterns of samples 1 and 2 (Figure 22) show that the typical reflections of MCM-41 are shifted to lower 2θ angles in the sample prepared in presence of HNO_3, giving a unit cell parameter of 4.4 nm instead of the 4.1 nm value found for sample 1. This expansion of the unit cell size could be easily explained by considering that NO_3^-, which has a larger size than Cl^-, is located between the silica layer and the surfactant core.

Up to this point in the discussion everything appears to be simply explained by assuming the predicted $S^+X^-I^+$ mesostructures to be correct. However, there is one experimental observation which makes us reconsider the above model. This is the fact that in the samples prepared under a highly acidic synthesis medium, the template can be removed from the core of the MCM-41 by a simple washing with water at room temperature. The removal of the liquid crystal template is accompanied by a decrease in the structural order of the MCM-41 and by a polymerization of the silica layer. The easy removal of the template indicates that the interaction between the silica layer and the surfactant should be very weak and more probably associated with the van der Waals interaction between oligomers of silicic acid-like species and the anions that compensate the surfactant cation. Therefore, we think that in this case the mesostructure should be written as $I^\circ X^- S^+$, giving a neutral structure instead of the positively charged one previously proposed.[233]

Recent work on synthesis of mesoporous molecular sieve silicates has focused on improving the synthesis by decreasing the temperature and synthesis time, as well as by controlling the crystal size and pore dimensions. In this way, the synthesis of MCM-41 at room temperature (25 °C) in alkaline media was achieved,[234] but the silica groups of the material were poorly condensed, and the resultant product was much less thermally stable than the ones obtained at higher temperatures. Other synthetic efforts[247,248] have succeeded in preparing stable MCM-41 samples at room temperature. In this case, some condensation of silanol groups should be already achieved either during an aging process or during the synthesis itself, while a further polymerization should occur during drying and calcination of the sample.

The control of crystal size can be of paramount importance when mesoporous molecular sieves with unidirectional channels, such as MCM-41, are to be used in catalytic processes. In principle and if diffusion limitations can exist, one should decrease as much as possible the length of the pores, and this is achieved synthetically, by decreasing the crystal size of the product. In the case of zeolites this can be done by changing the relative rate of nucleation vs the crystal growth and/or by adding seeds to the synthesis media. However, when mesoporous materials are to be synthesized the methods used for zeolites cannot be easily applied, even though conceptually they should work. However, by carrying out the synthesis of zeolites and zeotypes by microwave heating, it is found that this homogeneous heating consequently results in more homogeneous nucleation and shorter crystallization times compared to conventional autoclaving. When microwave heating was applied to the synthesis of MCM-41,[249−253] high-quality hexagonal mesoporous materials of good thermal stability were obtained by heating precursor gels to about 150 °C for 1 h or even less. Calcined samples had a uniform size of about 100 nm.[254] The homogeneousness and small crystal sizes obtained are probably the result of the fast and

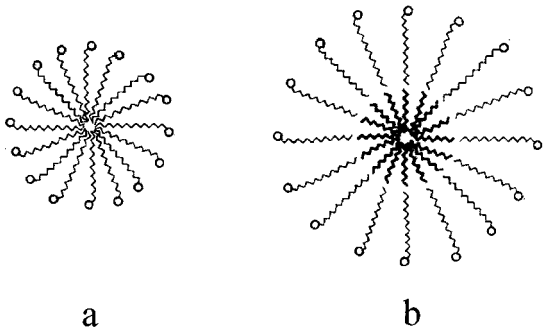

Figure 23. Schematic drawing of a micelle of surfactant molecules: (a) in the absence of a solubilizing agent and (b) in the presence of *n*-alkanes as solubilizing agents.

homogeneous condensation reactions occurring during the microwave synthesis. This fast condensation should also be responsible for the high thermal stability of the resultant materials.

Again from the point of view of catalytic application, it would be of interest not only to have shorter length pores but, if possible, to have them communicated through a tridimensional pore network, instead of the unidirectional pore system of the MCM-41. Very recently, it has been shown[255] that it is possible to obtain mesoporous silica material with a tridimensional disordered network of short wormlike channels, with uniform diameters. It is claimed that the fully disordered channel branching system similar to a three-dimensional fractal with truly uniform channel widths, distinguishes the present material with respect to the ordered MCM-41. This material was synthesized by an electrostatic templating route using sodium silicate (CTMACl) and ethylenediaminetetraacetic acid tetrasodium salt. The silicate was hydrothermally polymerized surrounding CTMA micelles in aqueous solution at 370 K, similar to hydrothermal synthesis of MCM-41 using repeated pH adjustment.[256,257]

One possibility for the M41S mesoporous materials, and more specifically the MCM-41 structure, is to be synthesized with different pore diameters, which can range from 1.5 to 10 nm. In the original work, the pore size in mesoporous silica was expanded by changing the chain length of the surfactant, and also by the addition into the synthesis medium of organic molecules, in particular 1,3,5-trimethylbenzene (TMB), the hydrophobic solvation interactions of the aromatic molecules playing the key role.[225] Very recently[258] alkanes of different chain length have been used together with the surfactant to synthesize MCM-41 with different pore diameter. The XRD patterns of the resultant samples suggest that the surfactant molecule in the micelle is fully extended (Figure 23a), and the size of such micelle increases with the chain length of the *n*-alkane (Figure 23b), at least until the molecule has 15 carbon atoms. However, it is obvious that the introduction of large amounts of organic (up to 20 wt % in the case of TMB)[259] in order to swell the original liquid crystals is not an appropriate procedure, since their use involves not only a larger reaction volume, but also additional separation processes. It would be highly desirable to increase and control the pore size of the mesoporous materials without introducing organic swelling agents. This has been recently achieved[260] by adjusting the composition of the gel and the

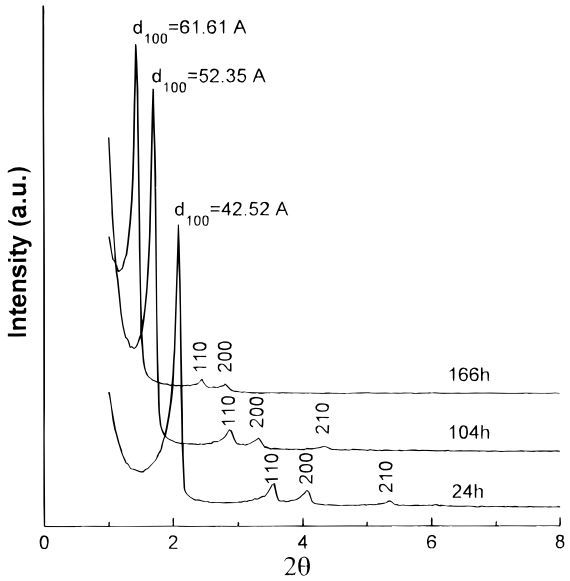

Figure 24. XRD (Cu Kα) of MCM-41 samples with different pore diameter.

crystallization variables. In this way, pure siliceous MCM-41 with different pore diameters were hydrothermally synthesized with the following molar composition: SiO_2:XCTMABr:0.14M_2O:26.2H_2O, where X was varied between 0.06 and 0.15, and M represents cations such as tetramethylammonium (TMA^+), tetraethylammonium (TEA^+), or Na^+, which were added as hydroxides. In a typical synthesis, an aqueous solution of tetramethylammonium silicate obtained from the reaction between Aerosil silica, and TMAOH solution (25% TMAOH, 10% SiO_2) was added to an aqueous solution containing 9.86 wt % CTMABr. Amorphous silica was then added under continuous stirring. The homogeneous gel (pH ~ 13.8) was sealed in Teflon-lined stainless steel autoclaves and heated at 150 °C under static conditions, allowing the crystallization time to be varied between 1 and 10 days. The resultant MCM-41 was stable to calcination.

The results in Figure 24 nicely show that a typical MCM-41 material with $d_{100} = 4.25$ nm is formed in the presence of TMA^+ when the crystallization time was 24 h. Longer crystallization times under these conditions increase the pore diameter of the sample, until reaching a maximum of 7.0 nm after 10 days. If crystallization is prolonged beyond that a loss of crystallinity accompanied by a decrease in the pore volume of the mesoporous material was observed. In Figure 25 a correlation between the unit cell parameter (a_0) of the resultant MCM-41 sample and the crystallization time is given. Variables such as temperature, CTMA/SiO_2 ratio, and nature of the cation (TMA^+, TEA^+, Na^+) are all important for controlling the process. The swelling mechanism observed may be related to the replacement of some $CTMA^+$ by tetraalkylammonium cations in the interphase formed between the liquid crystal and the silica surfaces.

2. Indirect Synthesis

Practically at the same time that researchers from Mobil discovered the synthesis of the mesoporous materials M41S, MCM-48, and MCM-50 by using surfactants and a solubilized silica source, Kuroda et al.[261,262] reported the preparation of highly ordered

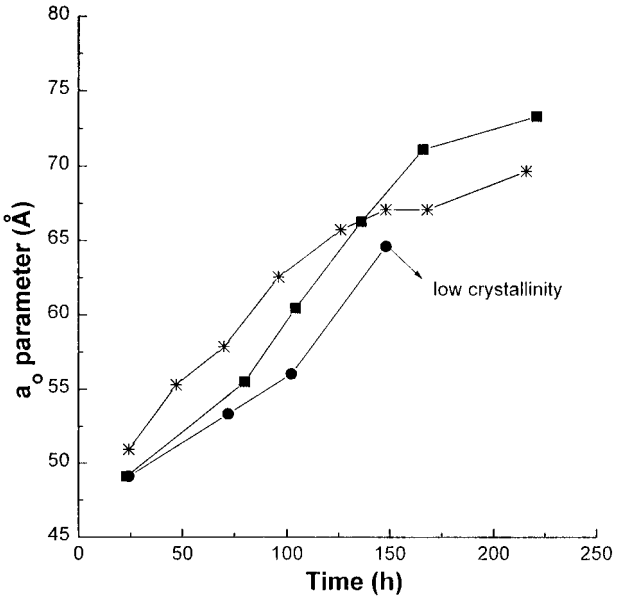

Figure 25. Correlation between the unit cell parameter (a_0) of MCM-41 and the crystallization time.

mesoporous FSM-16 materials derived from a layered polysilicate. In this case a mesoporous silica with uniform pore size was prepared by ion exchange of interlayer Na ions of the layered polysilicate kanemite for surfactants. The benefit of using kanemite is due to the fact that this layered material is extremely flexible owing to the relatively low degree of polymerization in its structure, as it is demonstrated by the high Q_3/Q_4 ratio observed by ^{29}Si MAS NMR (3:1). Then, upon intercalation with the surfactant the highly flexible sheets of kanemite are folded and cross-linked to each other to form the three-dimensional framework (Figure 26).[263] In agreement with this mechanism, the pore size could be changed by varying the alkyl chain length of the surfactant, and a more precise pore-size control was achieved by trimethylsilylation of the inner surface of the pores.[264]

The high pH used in the ion exchange of the surfactant molecules at which silica from the kanemite can in fact be dissolved reveals the distinct possibility that, essentially, this synthesis procedure is the same as that previously reported by Mobil researchers, in the sense that kanemite was just a source of silica. However, recent studies of FSM-16[226,263,265] have shown that despite the fact that MCM-41 and FSM-16 have similar pore size and surface areas, their mechanism of formation is different. Indeed, the MCM-41 is formed from a silicate anion initiated liquid crystal templating mechanism, while the layered silicate derived materials are formed by intercalation of the layered silicate using the surfactant present in the synthesis mixture.[266] Rheological data on the surfactant solutions used to form both materials indicate the presence of micelles in the MCM-41, while no micelles were observed at the low surfactant concentrations used with the layered silicates. There is a particularly interesting study which follows the formation of silica−surfactant mesophases by real time in situ X-ray powder diffraction.[267] These authors clearly demonstrate the different synthesis mechanism for MCM-41 and FSM-16, by finding evidence for the formation of an intermediate lamellar silica−surfactant intercalate during the synthesis starting from kanemite, whereas no intermediate phases are observed during the formation of MCM-41 by the direct synthesis. Vartuli et al.[226] found that the pore size distribution is broader in the case of FSM-16, where the total pore volume and hydrocarbon sorption capacity is about 5 times higher in the case of the MCM-41 materials. On the other hand, due to a higher degree of condensation in the silica walls in the FSM-16, this has a higher thermal and hydrothermal stability than MCM-41.[266]

It can be then concluded that FSM-16 and MCM-41 are probably different materials, and further detailed characterization will be necessary in order to see possible advantages of each one of them for different applications.

B. Synthesis of Mesoporous Molecular Sieves Containing Elements Other Than Silica

The success achieved in preparing silica mesopores was the starting point for using the concept to produce materials with potential catalytic applications. The first of which was to produce mesoporous acid materials which could be used for cracking large molecules present in vacuum gas oil and residues. Thus, in order to produce acidic mesostructured materials, MCM-41 and MCM-48 with walls of silica-alumina, where the Al was tetrahedrally coordinated, were synthesized.[231,268−271]

In general, it appears from the XRD data that the introduction of Al on the walls during the synthesis decreases the order in the material.[269,272] It has been claimed that the order could be improved in the presence of aluminum, if instead of SiO_2 one uses sodium silicate as the Si source for the synthesis.[273,274]

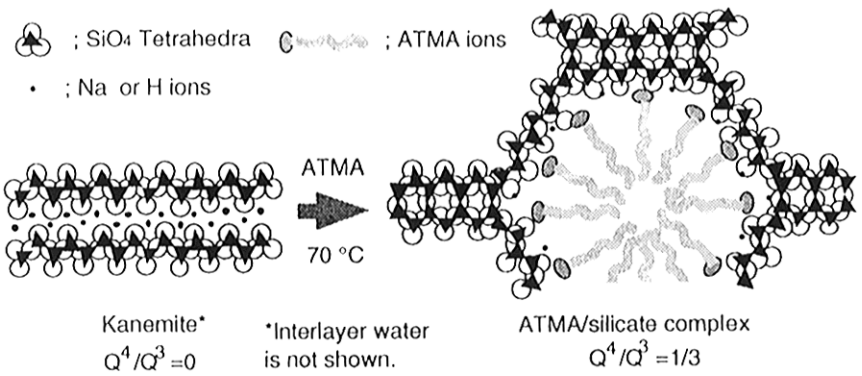

Figure 26. The model of folding silicate sheets of kanemite.

Table 9. Reports on the Incorporation of Al to the Structure of MCM-41

author	source of Al	Si/Al	OH_{ef}/SiO_2	Na/Al	Al coordination
Reddy, K. M.	$(SO_4)_3Al_2$	25	0.10	4.32	tetrahedral
	$(C_3OH_7)_3Al$	25	0.22	4.32	tetra + octa
	$Al_2O_3{\cdot}xH_2O$	25	0.22	4.32	octahedral
Luan, Z.	$(SO_4)_3Al_2$	2.5−60	11.5 (ph)	not specified	tetrahedral
	$NaAlO_2$	15	11.5 (ph)	not specified	tetra + octa
	Al orthophospate	15	11.5 (ph)	not specified	tetra + octa
	Al acetylacetonate	15	11.5 (ph)	not specified	tetra + octa
	Al isopropylate	15	11.5 (ph)	not specified	tetra + octa
	$Al_2O_3{\cdot}xH_2O$	6−90	11.5 (ph)	not specified	octahedral
Schmidt, R.	$NaAlO_2$	8.5	0.26	1.4	tetrahedral
Borade, R. B.	$NaAlO_2$	2	0.31	1.1	tetrahedral

Table 10. Effect of the Compositional Synthesis Variables on the Incorporation of Al in MCM-41

	Al-MCM-41												
	$Al_2O_3{\cdot}xH_2O$								$NaAlO_2$		Al°	$Al(C_3OH_7)_3$	
	Al15	Al4	Al8	Al9	Al7	Al6	Al5	Al14	Al10	Al13	Al11	Al12	Al16
OH_{ef}/SiO_2	0.30	0.19	0.19	0.19	0.16	0.10	0.08	0.06	0.16	0.08	0.16	0.16	0.17
Na/Al[a]	3.3	0	0	3.6	0	0	0	1.9	1.1	1.1	0	0	2.4
Si/Al[b]	15.8	12.8	16.1	14	15.8	13.5	18.5	13.7	15.7	13.4	14.6	18	13.6
Al^{tetr}	0.2	1	1	0.1	1	0.9	0.66	0.1	1	1	1	1	0.75
Al^{tetr}/Al^{oct}													
ppc[c] (%)	15.1	20.0	19.6	11.9	22.5	19.0	19.4	8.0	23.3	19.8	19.0	20.0	16.7

[a] Ratio in gel. [b] Ratio in the solid [c] Weight lost at temperatures above 300 °C.

However, it should be taken into account that in this synthesis, a part of the aluminum is not incorporated as Al^{IV} but remains as Al^{VI}, and consequently, the "framework" Si/Al ratio in the walls is much lower than the one given by the chemical analysis. On the contrary, we believe that the apparent "worse" XRD pattern obtained when introducing aluminum, is not a result of a less ordered material but due to the formation of smaller crystallites of MCM-41. The precise nature of the aluminum source can also play, an important role on the type of final incorporated species obtained.[272] For instance, it has been claimed that when Catapal alumina or sodium aluminate is used, virtually all the Al in the solid is hexacoordinated. In contrast by employing instead aluminum sulfate or aluminum isopropoxide, MCM-41 can be easily prepared with Al in tetracoordination. While this is true in general terms, it has to be pointed out, that it is possible, regardless of the aluminum source, to incorporate all of it as Al^{IV} if the synthesis conditions are properly optimized.

In Table 9 we have summarized the most significant reports highlighting the synthesis variables for the incorporation of Al into the wall of MCM-41.

Owing to the importance of the incorporation of Al in a tetrahedral coordination in the walls of MCM-41 for its final catalytic properties, we decided to carry out a synthetic investigation in which the most important variables, i.e. OH/SiO_2, Na/Al, and alumina source, were systematically varied (Table 10). When the results were plotted (Figure 27), it could be clearly seen that when the aluminum source is polymeric (pseudobohemite), the incorporation of Al in the framework of the MCM-41 decreases with decreasing OH/SiO_2 ratio in the gel. It appears that for $OH/SiO_2 < 0.13$ not all the alumina is depolymerized in AlO_2^- species, and consequently, it will be impossible to incorporate all the aluminum in the framework as Al^{IV}. Thus, consequently in those synthesis where one needs to work at pH values

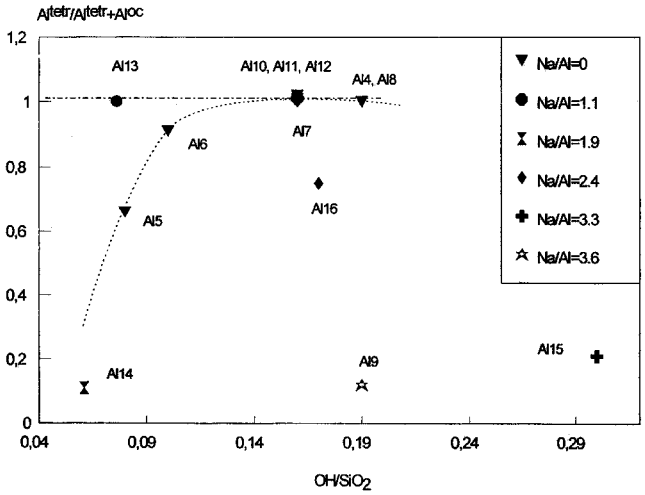

Figure 27. Influence of the OH/SiO_2, and alumina source on the ratio of $Al^{IV}/Al^{IV}+Al^{VI}$ in the MCM-41 formed.

below 0.13, sodium aluminate has to be used if the purpose is to introduce all Al as Al^{IV}.

It can also be observed that if the level of Na^+ in the synthesis gel is too high (Na/Al ≥ 1.9) the isomorphic substitution of Si for Al is impeded, regardless of the Al source. For instance, a sample prepared from aluminum isopropoxide at a OH/SiO_2 ratio for which the incorporation of Al as Al^{IV} would be complete in absence of Na^+, only 75% of the Al was incorporated when Na^+ was introduced in a Na/Al ratio of 2.4. When pseudobohemite is used as a source of aluminum and the Na/Al ratio is increased up to a value of 3.6, only 10% of the total aluminum is incorporated as Al^{IV} (Table 10).

Attempts have also been made to prepare samples with a high aluminum content. In this direction, it has been suggested[271,274] that MCM-41 with a Si/Al ratio of 4 can be prepared using sodium silicate and sodium aluminate as sources of Si and Al, respectively. However, the ^{27}Al MAS NMR of such samples indicates that this particular MCM-41 contains sig-

nificant quantities of aluminum within octahedral coordination. More recently, Borade and Clearfield[275] have synthesized MCM-41 with Si/Al ratios as low as 2 without observing the presence of octahedral aluminum by ^{27}Al MAS NMR, using sodium aluminate and fumed silica as the sources of aluminum and silicon, respectively.

Even though, it is possible to prepare low Si/Al ratio MCM-41 and MCM-48 samples with the aluminum being tetrahedrally coordinated, what is important, from a catalytic point of view, is the amount of Al^{IV} left after the calcination procedures necessary to activate the catalysts. In this sense, it appears that after calcination at temperatures above 500 °C the intensity of the NMR peak corresponding to tetrahedral aluminum decreases, while Al^{VI} is formed.[268,276−278] The results can be explained by assuming that upon calcination the Al^{IV} either becomes distorted or is removed from the aluminosilicate structure. Experiments indicate that when calcined samples are subjected to deep hydration the NMR peak of tetrahedral aluminum can be restored. In our opinion it is more likely that a part of the original Al^{IV} whose coordination was distorted by the thermal treatment could be restored by hydration, but it is certainly true that there is also a part of the aluminum which came out of the silicate structure and which remains as Al^{VI}.

If the introduction of Al in the mesostructure was important from the point of view of acid catalysis, it is also very important to introduce, transition metal elements such as Ti, V, and Cr in order to prepare mesoporous catalysts with redox properties. Following the interest stemming from the synthesis of Ti-zeolites and their application as selective oxidation catalysts[279−281] it was thought that it would be of great interest to incorporate Ti in mesoporous MCM-41, for reasons of its activity in oxidation reactions while allowing larger molecules to diffuse.[282] Thus Ti was incorporated in a mesoporous structure by direct synthesis working in absence of alkaline ions and using a cationic[282] or a neutral surfactant.[283,284] It was demonstrated by means of UV−vis spectroscopy and EXAFS that Ti was not in the form of anatase, but it was incorporated into the silicate wall, in the form of isolated tetrahedrally coordinated titanium, with some small amount of dimers of the type Ti−O−Ti also identified to be present.[285,286] Ti−Si−MCM-41 materials were active catalysts for reactions which will be described later such as the epoxidation of olefins and oxidation of sulfides to sulfoxides and sulfones. Titanium has also been introduced by direct synthesis in a MCM-48 structure, using TEOS and tetraisopropyl titanate as the sources of Si and Ti, respectively.[287,288]

Vanadium-containing MCM-41 structures could also be used as a selective oxidation catalyst, as far as the vanadium atoms were incorporated into the silicate walls and isolated one from another. This has also been achieved,[287,289] as ^{51}V NMR demonstrated the presence of vanadium in the framework of the MCM-41. Raman and NMR methods have been further used to support the above conclusions proving that V_2O_5 was not present.

Finally, it has also been intended to introduce Cr in the structure of MCM-41.[287] However, unlike Ti, only a few Cr^{3+} ions, similar to what occurs in zeolites,[290] will properly substitute isomorphously for Si in the walls, as was proven by the fact that when the Cr-MCM-41 was washed with diluted acetic acid, approximately half the amount of Cr is depleted from the sample.

Mesoporous manganosilicates having hexagonal, cubic, and lamellar structures have been synthesized at a low surfactant/Si ratio (0.12), and with a broad range of Mn/Si ratios (0.0004−0.09).[291,292] The phase formed depends on temperature and NaOH content, but the addition of Mn ions induced the formation of the cubic phase also at low surfactant to Si ratio. With respect to the state of the Mn in the resultant material, it appears from EPR studies that at room temperature it is located in the walls or interface region of the mesoporous materials. Unfortunately after calcination, the manganese ions migrate into the pores.

From the mechanism of formation of mesostructures, it should be possible, in principle, by the adequate selection of a cationic or anionic surfactant, to synthesize a large variety of metal oxide/surfactant composite materials. One can easily imagine the interest of these types of materials in catalysis just by considering the benefit of a stable mesoporous alumina with very high surface area as catalyst support, or the preparation of a high surface area zirconia with regular pores that can act as a catalyst support,[293] and also as zirconia-based solid acids.[1,295−297] If a mesostructure of pure TiO_2 could be prepared, it will certainly be of use not only as a support but also for application in photocatalytic processes.

The first attempt to form mesostructured pure oxides other than SiO_2 was done with tungsten, iron, and lead. In this case, even though the mesostructure was formed, attempts to remove the surfactant within the channels caused the pore structure to collapse.[298] A similar approach to alumina-based mesoporous material, resulted in the formation of lamellar phases.[233] However, very recently Yada et al.[299] have found that an aluminum-based dodecyl sulfate mesostructured material with a hexagonal framework can be obtained by the homogeneous precipitation method using urea and converted into a mesoporous alumina with some structural disorder but with the hexagonal structure of its retained principal framework. So far the results show that after calcination at 600 °C the washed composite solid with hexagonal structure is deorganized into a completely disordered form but preserves the narrow distribution of pores. If the calcination is done at 1000 °C the material is converted into α- and γ-alumina. When calcination was avoided and the anionic surfactant was removed by washing with ethanol or acetone, the hexagonal structure collapsed. This collapse could be avoided if a mesostructure of alumina was formed via S°I° and N°I° pathways. This has been very recently shown, and mesoporous alumina molecular sieves have been prepared by a N°I° assembly process.[300] Three forms of mesoporous aluminas, named MSU-1, MSU-2, and MSU-3, have been prepared by the hydrolysis of tri-*sec*-butoxyaluminum at room temperature in the presence of nonionic polyethylene oxide (PEO) surfactants. PEO-

based surfactants adopt spherical to long "wormlike" micellar structures in aqueous solution, and the wormlike structure is hence adopted by the MSU-X alumina structures. However, even if the channels in MSU-X are more or less regular in diameter, they have no discernible long-range order, unlike the MCM-41 structure.[300] The walls of the channels in the case of MSU-X are larger for aluminas than for silicas, resulting in lower surface areas (420−535 $m^2 g^{-1}$) for the former. The coordination of aluminum in the as-synthesized samples corresponds to Al^{IV}, Al^{V} and Al^{VI}, Al^{VI} being dominant. After calcination at 500 °C the 4- and 5-coordinations increase at expense of the Al^{VI} sites.

Alumina mesophases have also been synthesized by reacting aluminum alkoxides and carboxylic acids with controlled amounts of water in low molecular weight alcohol solvents. These materials give after calcination high surface area alumina (up to 710 $m^2 g^{-1}$) with pores in the mesopore region centered around 2.0 mm. However, in this case the pores were not ordered within any type of symmetry.[301]

Further work should be done on these aluminas, and to particularly test them as supports for preparing HDS and hydrogenation catalysts, as well as, when conveniently doped, for base-catalyzed reactions.

As mentioned above, it is of considerable interest for catalysis to prepare large surface area mesoporous zirconia, and therefore, it is not surprising that this has been studied by several groups. Schüth et al.[302] were the first reporting on the synthesis of mesoporous zirconia, while Hudson and Knowles[303] have shown that cationic quaternary ammonium surfactants can be used to prepare zirconia in the mesoporous range. The authors have pointed out that the conventional templating mechanism of mesopore formation is not operative in their case, and a scaffolding mechanism was invoked in order to explain the ordering. The pore size distribution increases with the chain length of the surfactant, and BET surface areas of 240−360 $m^2 g^{-1}$ can be obtained depending upon the chain length of the incorporated surfactant. What can be of interest from the viewpoint of the catalytic use of these materials as zirconia-sulfated solid acids, is the observation that it is possible to prepare them in the form of tetragonal zirconium(IV) oxide, by calcination at 650 °C. The one-step preparation of sulfated mesoporous zirconia with good acidic properties has been performed by using lauryl sulfate as surfactant. This preparation route could avoid further synthetic wet steps after the synthesis.[304] The samples prepared with high concentrations of this surfactant (SZ-848) give, after calcination at 575 °C, a broad tetragonal zirconia XRD fingerprint, while mesoporosity was not lost. The resulting samples were indeed active for low temperature *n*-butane isomerization and cracking.

Up to this point we have described synthetic routes to mesoporous zirconia which are based on expensive alkoxides, relying alternatively on the sulfate ion to link the surfactant and zirconium, or do not involve self-assembly. There are however two new synthesis routes which involve: a self-assembly of a soluble zirconia precursor with an amphoteric surfactant template,[305] and a neutral amine route.[306] The amphoteric surfactant, cocamidopropylbetaine (CAPB), which has quaternary ammonium and carboxylate groups, can bond to both negatively and positively charged inorganic species. Additional benefits arising from this surfactant is that it does not need a bridging anion for the formation of the surfactant−Zr complex, and can also be used in a wide pH range. Thus, when the synthesis is carried out at low pH, the quaternary ammonium group of CAPB is positively charged, the carboxylic group is protonated, and the positively charged inorganic species attack to the surfactant by reaction with the carboxyl group. Concurrent surfactant bonding with the inorganic component and aggregation of the micellar structures leads to formation of the hexagonal mesophase[305] (Figure 28). This work opens new possibilities in mesoporous synthesis specially for those involving cationic inorganic species.

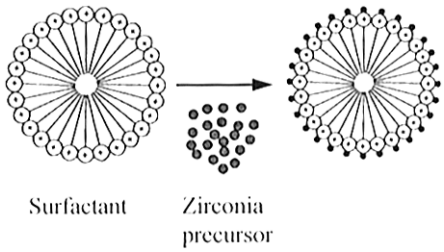

Figure 28. Proposed amphoteric surfactant templating route for hexagonal mesophase formation where the carboxylate group provides for the bonding of the surfactant with the inorganic species and the quaternary ammonium group maintains a large head group area for hexagonal mesophase formation.

When zirconia mesostructures were prepared with neutral amines, lamellar phases were obtained using C_8 to C_{16} alkylamines. However, these lamellar phases changed to a hexagonal structure when water was introduced in the reaction mixture.

In the case of titania mesoporous solids, only partial success has been obtained in preparing stable surfactant-free materials. A hexagonal phase of mesoporous TiO_2 was prepared with alkyl phosphate surfactants,[307] in which the alkyl phosphate could be partially removed from the pores, with the phosphate units being retained in the oxide phase. Others[308] have used a neutral surfactant (decyl- or hexadecylamine), together with titanium alkoxide in a mixture of isopropyl alcohol and water. After aging at room temperature for 18 h or in a hydrothermal treatment at 90 °C for 18 h, mesoporous structures with pores of 2.9 and 3.2 nm for decylamine and hexadecylamine surfactants, respectively, were obtained. Unfortunately, removal of the amine from the pores, either thermally or by using solvents, results in the destruction of the mesoporous structure. More success was obtained when the surfactant was partially removed in an acidified dilute alcohol medium.[308]

By using an anionic surfactant such as sodium dioctylsulfosuccinate (AOT), it was possible to obtain a mesostructure SnO_2-AOT. However, it has not been possible up to now, to remove the template without destroying the mesophase.[308]

Before finishing the chapter devoted to the synthesis of mesoporous molecular sieves, two novel mesoporous compounds should be introduced. In one case, the authors[309] proposed that since there are microporous aluminophosphates (AlPOs), it also

could be of interest and benefit to extend the liquid crystal templating approach to the synthesis of mesoporous $AlPO_4$. They used long-chain primary and tertiary amines, but at the present time only lamellar $AlPO_4$ materials were obtained which did not allow template removal without structural collapse.

In an analogous way and from the prior knowledge achieved in vanadium phosphorous oxides (VPO) containing micropore[310] and lamellar compounds formed by intercalation of organic molecules,[311−313] a novel three-dimensional ordered mesoporous VPO has been successfully synthesized. Using *n*-tetradecyltrimethylammonium chloride as surfactant, and $VOHPO_4$ and heating at 76 °C for 48 h, a layered structure was formed which contained the surfactant. When this was suspended in water and hydrothermally treated at 170 °C for 48 h, the layered VPO was transformed into another mesoporous material with hexagonal structure. The evolution in this case bears same resemblance to the synthesis of MCM-41 from kanemite, in the sense that the surfactant remaining in the layer forms a micelle in water and forces the layer to bend. We do not know from the report if the mesoporous VPO compound remains stable after removing the surfactant.

In conclusion, it can be said that despite a period of very intensive work over the last two years in the synthesis of mesoporous molecular sieves using liquid crystals as templates, the field is in its infancy. Still much effort is needed in many cases to produce samples in which the surfactant could easily be removed and recovered without losing order or even destroying the pore structure. Furthermore it will be of great scientific interest and practical use to synthesize well-structured mesoporous materials with a tridirectional system of communicating channels which will enhance the diffusivity of bulky reactants and products. Finally, it is easy to understand that the synthesis of mesoporous materials of the M41S type but with crystalline microporous walls will generate highly thermally stable systems with a well-defined bimodal pore system will certainly be of much interest for catalytic and membrane applications. In any case, it is possible to forecast that the possibilities for synthesizing new materials based on these concepts is immense and only limited by the scope of our imagination.

C. Characterization of Mesoporous Molecular Sieves

When one suspects that a mesoporous molecular sieve has been synthesized a well-established methodology must be followed to demonstrate that this is indeed the case. The procedure involves, first, the use of XRD and synchrotron X-ray powder diffraction which should be carried out at low angles. The XRD powder d spacings of well-prepared MCM-41 and MCM-48 (Figure 29) can be indexed on a hexagonal and cubic lattice, respectively.[225,314−318] XRD combined with other techniques, such as HRTEM,[220,225] electron diffraction,[220] and lattice images,[319] have been key methods for the characterization of these materials and identification of the phase obtained, i.e. cubic (MCM-48), hexagonal (MCM-41), and lamellar (MCM-50). From a combination of these techniques, two structural models with an amorphous wall have been constructed for MCM-41 as shown in Figure 30.[320]

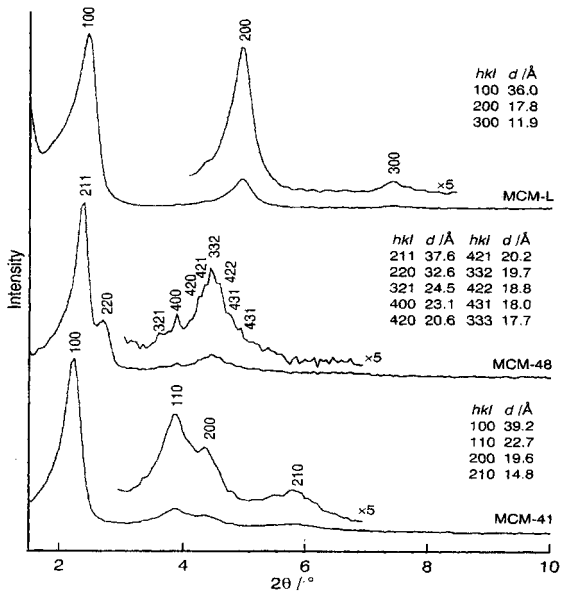

Figure 29. Powder X-ray diffraction paterns (Cu Kα) of as prepared MCM-41 (hexagonal), MCM-48 (cubic), and MCM-50 (lamellar) materials.

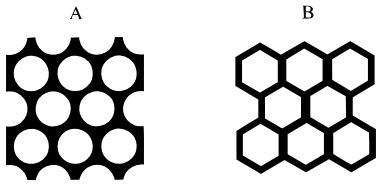

Figure 30. Structural model of MCM-41 with cylindrical pore (A) and hexagonal pore (B).

In model A, a cylindrical pore structure, with a lattice constant of 4.46 nm and a wall thickness of 0.84 nm, was proposed by Feuston and Higgins[319] by a classical molecular dynamics simulation approach. The authors simulate 10^3-10^4 atoms to model MCM-41 and analyzed models with different lattice constants and wall thicknesses. When comparing their simulation with experimental values, they found that the simulated X-ray patterns of amorphous silica with wall thickness larger than 1.1 nm agreed well with the experiments. The percentage of silicon in the form of silanols obtained from the model (17−28%) also agrees fairly well with the observed diffraction pattern. It has to be pointed out, however, that an inverse relationship between the diameter of the micelle template and the wall thickness of the pores was found. Thus, decreasing the template diameter leads to thicker walls between hexagonal packed cylindrical pores. For model B, a hexagonal pore structure with an interpore distance of ∼3.5 nm was proposed by Behrens et al.[321] Both the cylindrical and hexagonal pore structures have been visualized by HRTEM.[322]

A unified model based on the void fraction and structure of nanoporous materials structures has been proposed by Garcés.[323] The author reduces the pores to spheres, plates, and cylinders with dense shells and inner cores. Most of the material mass is assigned to the surfaces of the geometrical forms with empty spaces inside. This gives rise to a single

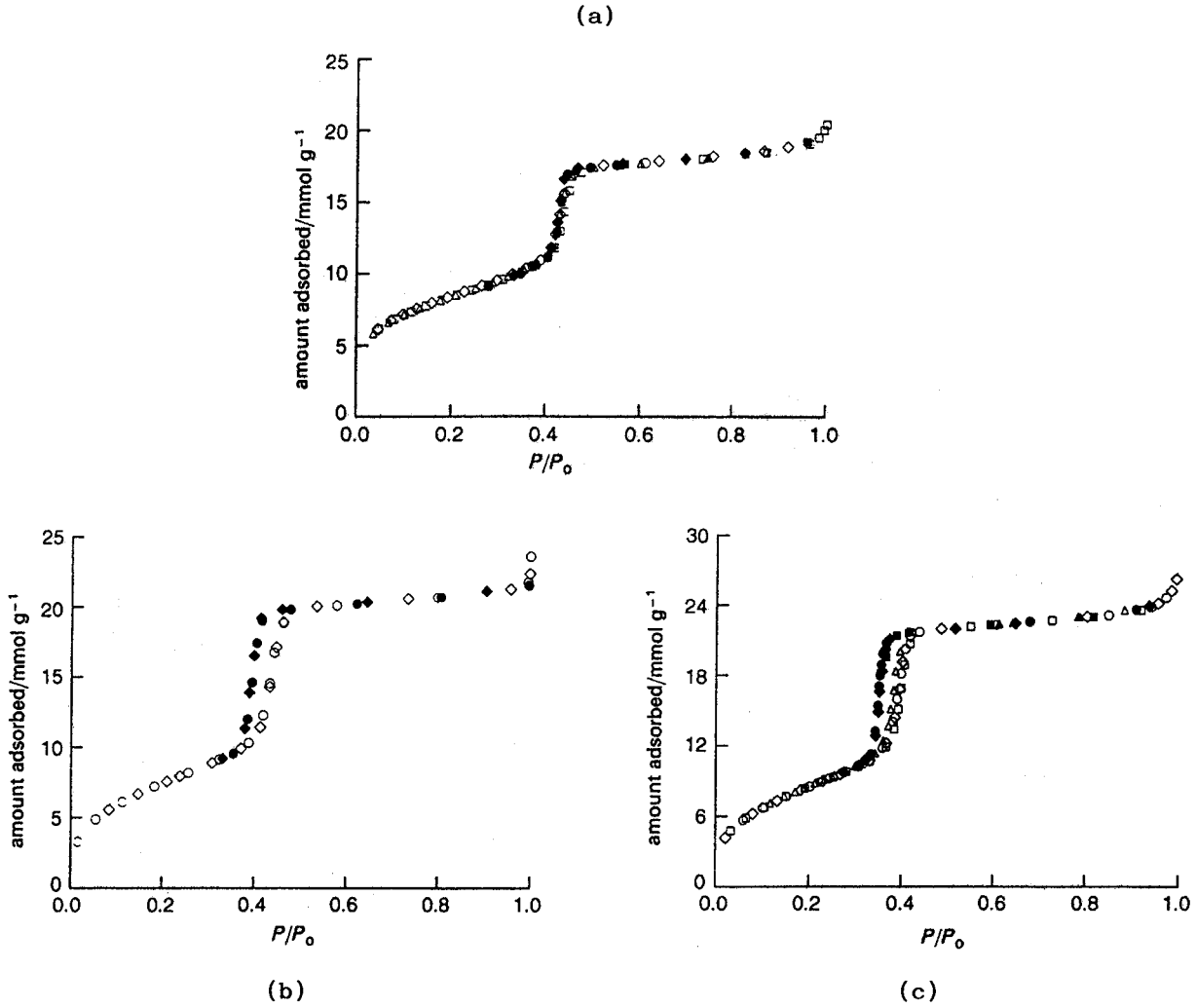

Figure 31. Adsorption isotherm of nitrogen (a), argon (b), and oxygen (c) on MCM-41 at 77K. Different symbols denote different runs; filled symbols denote desorption.

sphere representing the structure. The radius of the empty interior space is adjusted so the void in the center matches experimentally found void fractions. When this model is applied to MCM-41, the author finds that a spherical fits most closely, which implies that instead of smooth cylindrical channels, the pores of MCM-41 can be seen as spherical cages connected by narrower necks.

Adsorption of molecules has been widely used to map the pore size distribution of solid catalysts. In this sense the physisorption of gases such as N_2, O_2, and Ar have been used to characterize the porosity of M41S samples and more specifically MCM-41.[324−327] When adsorption was carried out on a MCM-41 sample with 4.0 nm pore diameter (Figure 31), it was found that the isotherm for N_2 is type IV in the IUPAC classification, and no adsorption−desorption hysteresis was found at the boiling temperature of N_2 (77.4 K). In the case of Ar and O_2 the isotherm is also of type IV, but they exhibit well-defined hysteresis loops of the VI type. These results can be attributed to capillary condensation taking place within a narrow range of tubular pores with effective width of 3.3−4.3 nm,[328] confirming both the high degree of pore uniformity and the dimension of the pore determined by HRTEM.[325] Further adsorption studies under different experimental conditions and on samples with different pore diameters showed that the presence and size of the hysteresis loop depend on the adsorbate,[325] pore size,[329,330] and temperature.[331] In this respect, no nitrogen hysteresis loops were found for materials with pore sizes of 2.5−4.0 nm, but a nitrogen isotherm on a 4.5 nm material showed hysteresis. Finally, adsorption of cyclopentane at different temperatures showed that the presence and size of hysteresis depends on the temperature.

These samples with monodispersive pore channels represent a beautiful model for standardizing adsorption measurements and methods for characterization of porous solids.[332] In fact, when N_2 adsorption isotherms are modeled using nonlocal density functional theory (NLDFT) over a wide range of pore sizes (18−80 Å), it is found[326] that the theoretical thermal dependence of the thermodynamic adsorption−desorption hysteresis predicted by NLDFT is confirmed by the experimental measurements.

We have here then a type of material with a regular pore structure in the mesoporous region where the pore diameter cannot only be perfectly measured by gas adsorption, but the materials themselves can serve as models for adsorption of gases in porous solids. Owing to the success of N_2 and Ar adsorption in terms of the determination of the pore diameter, one can combine the XRD results together with the pore size determined from gas adsorption experiments to find the thickness of the wall. When this is done, it is found that in the regular MCM-41

samples the wall thickness varies little around 1.0 nm. We will see later that the value can be changed, having as a consequence important implications on the stability of the sample.

Adsorption studies, besides their convenience for measuring the textural properties of these materials, can also be used to study the interaction of molecules with the walls of the pores, a feature of particular importance from the point of view of the diffusion and catalytic properties of the material. In this sense, adsorption studies of polar and nonpolar molecules can be quite useful for measuring the hydrophobic and hydrophilic properties of M41S mesoporous materials. When H_2O was adsorbed at 297 K on a MCM-41 sample,[333] the isotherm obtained showed a fairly narrow hysteresis loop but with no identifiable B. The isotherm is of type V in the IUPAC classification, indicating relatively weak adsorbent−adsorbate interactions. From these results,[333] one would conclude that the MCM-41 surface is quite hydrophobic, with an uptake of water similar to that given by hydroxylated silica and many carbons.[334] This conclusion is nevertheless surprising if one considers the high number of silanol groups present in these materials. However, the hydrophobic character of MCM-41 has been clearly demonstrated by carrying out the adsorption of cyclohexane and water, and benzene and H_2O.[335,336] The results obtained show that while in a hydrophilic zeolite, such as faujasite, large amounts of benzene and H_2O are adsorbed, when the same adsorbates were used on a sample of siliceous MCM-41, much larger amounts of benzene than H_2O were adsorbed. This adsorption characteristic is of vital importance when reactants with different polarities, for instance H_2O or H_2O_2 and olefins, have to react and certainly it will control the rate of the diffusion−adsorption reaction in those cases.

Another powerful technique for the characterization of M41S mesoporous materials is NMR spectroscopy. Its benefits include the determination of the pore size and the mechanism of formation of the material, to the study of the diffusion of molecules in the pores, and finally, to the organization of the walls in the pure silica and in the isomorphous substituted materials, before and after calcination pretreatments.

A large amount of effort was directed at inferring the pore size distribution of solids from NMR relaxation time data (T_1 and T_2).[337−339] Recently, interesting work on MCM-41 has been published,[340] in which the effect of pore size on the freezing−melting transition of water confined in porous materials has been investigated using ^{1}H NMR. In this work, ^{1}H NMR intensity vs temperature data of water confined in MCM-41 materials with different pore sizes were obtained. Thus, by comparing the NMR, with N_2 adsorption and HRTEM results, a correlation between freezing point depression of frozen pore water, ΔT, and the pore radius (R_p) was established, with this shown to have the following form: $\Delta T = K_f/(R_p - t_f)$; where t_f and K_f are constants. The authors tentatively proposed the t_f factor to be identical to the thickness of a nonfreezing pore surface water. This method thus allows the determination of pore size distribution in materials with pore diameters larger than 1.0 nm, from ^{1}H NMR intensity vs temperature measurements of water-saturated porous materials. There is no doubt that this is a valuable method for the people working on catalysis and adsorption who need to know the effective pore diameter of the solids.

In the case of MCM-41 materials, the self-diffusion coefficient of water was derived[341] from NMR spin−echo experiments using the Carr−Purcell−Meiboom−Gill pulse sequence[342] and a model proposed by Doussal and Sen.[343] It has to be pointed out that the found diffusion coefficients (D) are somewhat surprisingly, of the same order as the value for the diffusion of water in ferrierite determined by molecular dynamics[344] (0.8×10^{-6} cm^2 s^{-1}). The authors explain the rather small diffusion coefficient, relative to bulk water (2×10^{-5} cm^2 s^{-1}), by a strong interaction of water molecules with the pore surface. This, however, would be in contradiction with the small interaction with the walls observed (recall the hydrophobic nature of the MCM-41) during adsorption experiments.

It has to be noted that most of the NMR work has been performed to determine the state of Si and Al in the walls of the M41S materials, with some incursion into the mechanism of formation.[236] We have already described in a previous section how ^{27}Al MAS NMR was used as a technique to follow the incorporation of aluminum in the walls of the M41S materials. In this sense, the first studies[231,268] of the Bloch decay (BD) and cross polarization (CP) ^{29}Si NMR spectra of two MCM-41 samples with relatively low (28) and high (189) SiO_2/Al_2O_3 ratios indicated (Figure 32) that while in the first sample some Si (2Si, 2Al) and Si (3Si, 1Al) sites were present, in the high-silica MCM-41 material practically all sites correspond to Si(4Si) with very little Si (3Si, 1Al). When the sample containing more Al was calcined, a substantial intensity loss of the Si (2Si, 2Al) and Si (3Si, 1Al) occurred, while octahedral aluminum appeared (Figure 32); these results could be explained by assuming that upon calcination "dealumination" occurs. Similar results were obtained in B-MCM-41.[345] It is important to bear in mind these results when considering using these materials for acid-catalyzed reactions, in which the Brønsted acidity should be associated to the presence of tetrahedral aluminum.

The acidity of Al-containing MCM-41 samples has been measured by adsorption−desorption of bases such as pyridine and NH_3.[231,269] The calcined silicoaluminate samples have both Brønsted and Lewis acidity as determined by pyridine adsorption[269] (Figure 33), and the amount of Brønsted acidity increases with the aluminum content of the sample.[269] When the acidity of silicoaluminate MCM-41 was compared with that of a USY and an amorphous silica-alumina, it was found (Figure 34) that the acid strength of the MCM-41 is weaker than in the zeolite and appears more similar to that of an amorphous silica-alumina.[269] From these results, we can conclude that the MCM-41 silicoaluminate corresponds closely, from the point of view of its acidity, to amorphous silica-alumina with regular pores.

In the case of the transition metal-substituted M41S samples, their principal interest resides in

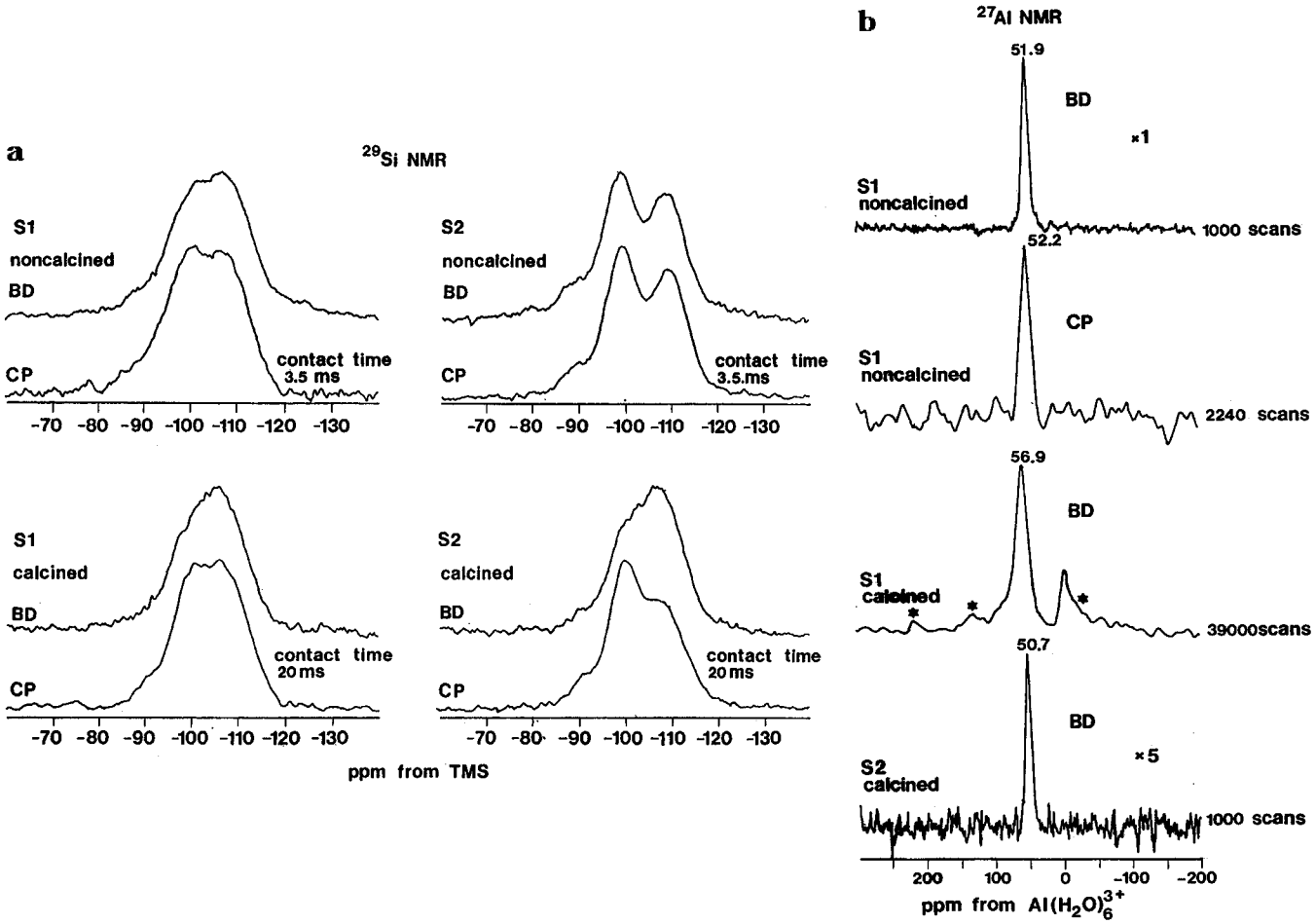

Figure 32. (a) Bloch Decay (BD) and cross polarization (CP) ^{29}Si MAS NMR spectra of MCM-41. The CP spectra were recorded with the optimum contact times. (b) BD and CP ^{27}Al MAS NMR spectra of MCM-41. Note the different intensity scaling factors for the BD spectra of the uncalcined samples. Asteriks denote spinning side bands.

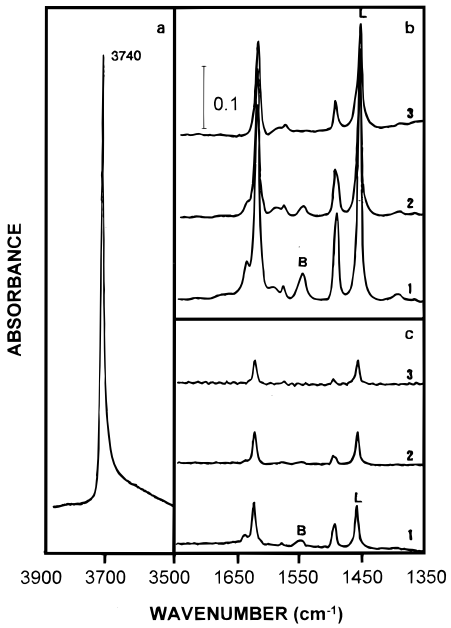

Figure 33. IR spectra of MCM-41 samples (a) hydroxyl range, (b and c) pyridine adsorbed on high Al content, S1 (b), and low Al content, S2 (c) samples and desorbed in vacuum at different temperatures: (1) 423 K; (2) 523 K; (3) 623 K.

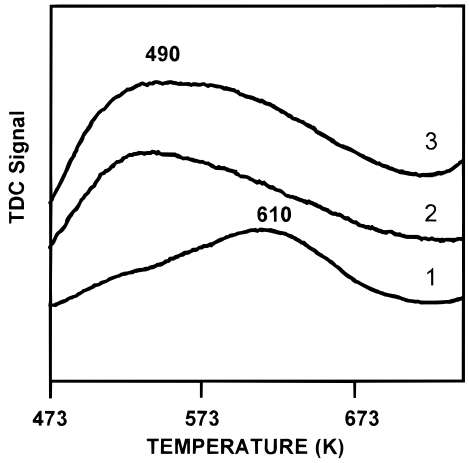

Figure 34. TPD NH_3 spectra of USY (1), calcined S1 sample (2), and amorphous silica alumina (3).

their potential use as oxidation catalysts, with this particularly true for the Ti- and V-substituted MCM-41 materials.[269,289] In these two cases, the isomorphous substitution and, therefore, the incorporation of these elements in the framework is not easy to ascertain, and hence, a combination of several techniques is required to provide the necessary information. In the case of Ti-substituted MCM-41, spectroscopic and catalytic techniques should be used to show the incorporation of Ti in the silica framework. Previous work on the characterization of Ti-zeolites[346,347] can be used as a guide for characterizing the Ti-MCM-41 samples. Thus, an IR absorption band at ~960 cm^{-1} attributed to Si−O−Ti stretching with Ti in tetrahedral coordination[348] was used to identify the incorporation of Ti in zeolites and,

similarly, has also been used to show the presence of Ti in the framework of Ti-MCM-41. However, this has been questioned[280] on the basis of more recent IR studies on as-made and calcined Ti-β-zeolite, the authors of which have concluded that the band at $\sim$960 cm^{-1} can instead be due to the Si−O stretching vibration in the Si−OR group, R being H^+ in the calcined state and TEA^+ in the as made material. Thus, we have to say that while all the properly prepared Ti-zeolites and Ti-MCM-41 show the presence of this band, the reverse is not neccesarily true.[280]

Raman spectroscopy, while having the limitation of its relatively high detection limit (0.5 wt %), has the advantage that it can visualize if some or all of the Ti has or has not been incorporated and whether indeed some is segregated as TiO_2 anatase (140 cm^{-1}). On the other hand, UV−vis spectroscopy gives very valuable information on the coordination of the Ti. A sample containing only framework titanium should give an optical transition at $\sim$210 nm, which is assigned to a charge transfer (CT) in [TiO_4] and [O_3Ti-OH] moieties.[349] Isolated extraframework hexacoordinated Ti would give a CT at about 225 nm.[349] Partially polymerized hexacoordinated Ti species, which contain Ti−O−Ti bonds and belong to a silicon-rich amorphous phase, would give a broad band at $\sim$270 nm.[350] Finally, for TiO_2 in the form of anatase the transition occurs in the $\sim$330 nm region. We see then that UV−vis spectroscopy, which is a widely available technique, is a very useful tool for characterizing Ti-MCM-41 samples since, besides its low detection limit (0.03 wt %), it can give information on framework and extraframework Ti.

The definitive proof in favor of the tetrahedral coordination of Ti in MCM-41 came from the application of X-ray absorption spectroscopy (EXAFS/XANES). When this technique was applied to TS-1 and Ti-β-zeolites,[347,351,352] it was found that in anhydrous samples titanium is tetrahedrally coordinated, and the first coordination shell of titanium consists of oxygen atoms only. In hydrated samples penta- and hexacoordinated species are present, corresponding in this case to a titanium atom coordinated with four oxygens from the framework and two molecules of water.

We have carried out recently an EXAFS-XANES study of well-prepared Ti-MCM-41,[347] and the XANES spectra of a calcined Ti-MCM-41 sample (1.7 TiO_2 wt %), and calcined and subsequently rehydrated is shown in Figure 35. We note that the XANES region of the X-ray absorption spectrum is sensitive both to the oxidation state of the absorbancy atom (in this case Ti) as well as to its local coordination geometry. A clear change in the preedge feature is observed after dehydration, indicating a modification in the site symmetry of Ti atoms (see the characteristics of the prepeaks in Table 11). The prepeak intensity in the calcined material suggests a distorted octahedral environment for Ti. The energy position and intensity of the preedge suggest mainly octahedral coordination for Ti, as observed for Ti-zeolites when exposed to the atmosphere. However, when Ti-MCM-41 was dehydrated a sharper and more intense prepeak at lower energy is observed in the XANES spectrum, indicating a decrease in the coordination

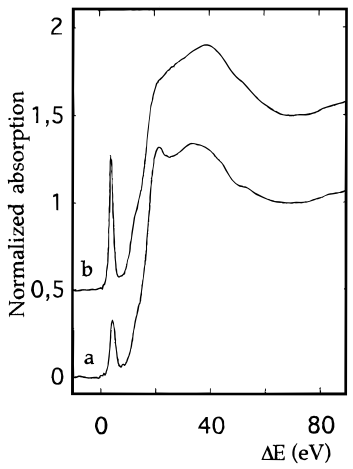

Figure 35. Ti K-edge XANES spectra of Ti-MCM-41 sample: (a) calcined and (b) calcined and dehydrated.

Table 11. Ti Preedge Peak Parameters for Ti-MCM-41 Sample

compound	peak position[a] (±0.2 eV) $A_1/A_2/A_3$	intensity (height) ± 5%	FWHM[b] (± 0.2 eV)
calcined	4.2	0.33	2.0
calcined dehydrated	3.8	0.77	1.2

[a] Relative to the first inflection point for Ti metal. [b] The full width at half maximum.

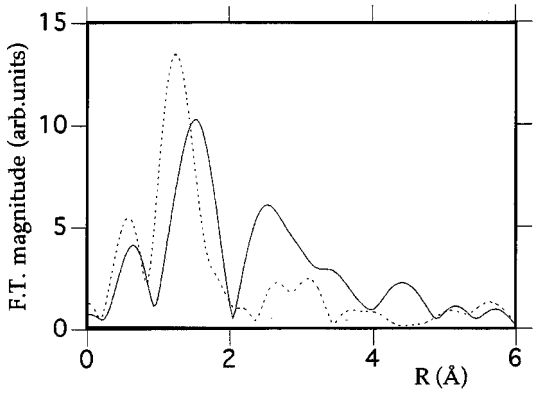

Figure 36. Fourier transform magnitude of the K^3-weighted EXAFS signals of anatase (solid line) and calcined, dehydrated Ti-MCM-41 sample 2 (dashed line).

Table 12. EXAFS Simulation Parameter for the First Shell of Calcined Dehydrated Sample

neighbor	N (± 0.5)	R (Å)	$\Delta\sigma^2$ (Å^2)	ΔE_0 (eV)	fit value
oxygen	4.3	1.81 ± 0.02	4×10^{-4}	0.8	5×10^{-3}

of Ti toward tetrahedral coordination, feature which has also been previously observed in TS-1 and Ti-β.

To obtain further insight into the coordination of Ti, the analysis of the EXAFS data of the Ti-MCM-41 sample after calcination and dehydration was carried out (Figure 36), and the coordination number and the Ti−O distance for the calcined and dehydrated samples are given in Table 12. From these, it can be concluded that when the sample is dehydrated, Ti becomes tetrahedrally coordinated.

The observations from EXAFS-XANES complement the IR and UV−vis spectroscopic results (Figures 37 and 38). Indeed the sample showed a band at about 960 cm^{-1} in the IR spectra, this band disappears, and the material becomes yellow when

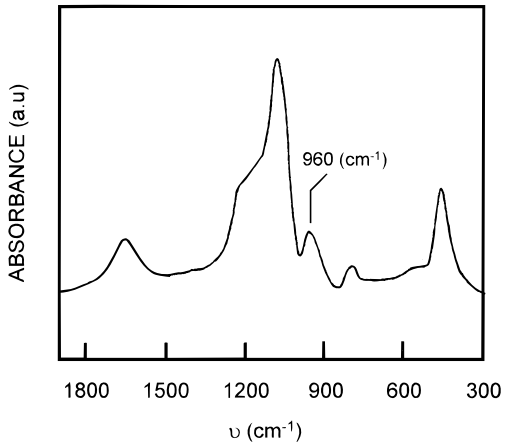

Figure 37. IR spectra of calcined Ti-MCM-41.

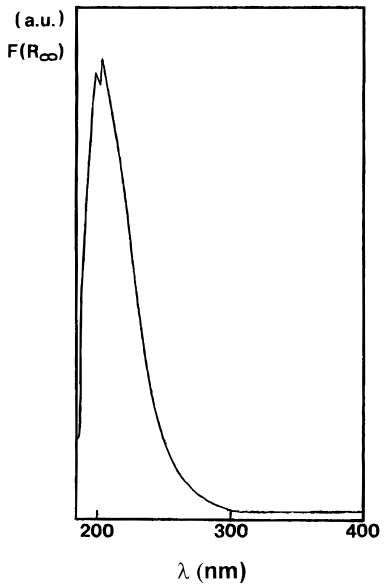

Figure 38. DR-UV spectra of calcined Ti-MCM-41.

adding H_2O_2. The initial conditions are restored by heating the sample at 353 K overnight. The diffuse reflectance spectra in the UV−vis region of the calcined Ti-MCM-41, does not show the ∼330 nm band associated to anatase, but a band at 210−230 nm associated to isolated Ti in tetrahedral (∼210 nm) and hexacoordination (∼230 nm). Then we can certainly conclude that in well-prepared Ti-MCM-41 samples, isolated Ti^{IV} and Ti^{VI} species are present, and therefore the incorporation of Ti to the framework of the walls occurs. This fact opened the possibility of using these materials as catalysts for the selective oxidation of large molecules.

In an analogous way to Ti, vanadium was also incorporated in relatively low amounts in the framework of zeolites[353,354] and MCM-41.[289,355] In well-prepared V-MCM-41 samples, ^{51}V NMR and EPR characterization show that V is, at least in part, incorporated in the framework and consequently can also play a role in catalysis. However, attention should be paid to the fact that leaching of active vanadium species from the silicate matrix during reaction may occurred depending on the nature of the substrate, the solvent, and the oxidant.[356]

Since Ti- and V-substituted mesoporous materials are the best documented and also those already proven to be catalytically active, we have limited our characterization discussion to these two materials only. In the next section we will discuss the catalytic activity of mesoporous materials with long-range crystallinity.

D. Catalytic Properties of Mesoporous Materials with Long-Range Crystallinity

We have seen during this review that mesoporous molecular sieves present very high surface areas with very regular pore size dimensions. These properties alone, even if no catalytically active sites can be generated in the structure, are already of great utility for producing carriers on which catalytically active phases such as heteropolyacids, amines, transition metal complexes, and oxides can be supported. Besides their characteristics as supports, we have seen that it is possible to generate Brønsted acid sites on the surface of the mesoporous structures, which opens new possibilities for producing monofunctional acid as well as acid/metal oxide bifunctional catalysts. If Brønsted acidity is generated, one can immediately think of the posibility of increasing the basicity of the conjugated base by exchanging the protons by alkaline ions. This certainly will introduce mild basicity to these materials, which will be useful for less demanding base-catalyzed reactions. Finally, the possibility of introducing transition metals in the walls will give catalytic redox properties which are of use in selective oxidation as well as for air pollution abatement. The versatility of active sites which can be introduced in these materials clearly extends the catalytic possibilities of the microporous zeolites.[356]

Thus, in this section, we are going to show the possibilities of these materials as acid, base, and redox catalysts, as well as supports for acid, base, hydrogenation, HDS-HDN, and oxidation functions.

1. Acid Catalysis

The large pores of MCM-41 combined with acidity on the walls were specially conceived to carry out catalytic cracking of large molecules. These materials were thought to represent an extension of zeolites and should allow us to deal with large molecules whose diffusion was strongly impeded in the micropores of zeolites such as for instance USY zeolites. Thus, a cracking catalyst was prepared in which the USY zeolite was substituted by Al-MCM-41 (35 wt %) in a silica-alumina-kaolin clay matrix, and the results indicated a higher selectivity of the MCM-41-containing catalyst toward liquid fuels than the one containing the USY zeolite.[357] In the general literature, polyethylene,[358] *n*-heptane, and a vacuum gas oil,[359] have been cracked on Al-MCM-41, amorphous silica-alumina, and USY zeolite, in a microactivity test (MAT) unit. It has been found that with a small reactant (*n*-heptane), which can easily diffuse inside the pores of the three catalysts (Table 13), the intrinsic activity of the USY zeolite is 139 times larger than MCM-41. This difference in activity is not only due to the larger amount of Brønsted acid sites present on the zeolite, but it is also a consequence of the stronger acid sites present in the zeolite (Table 14). On the other hand, when the large reactant molecules present in the gas oil were cracked, we can see that the activity of MCM-41

Table 13. First-Order Kinetic Rate Constants for *n*-Heptane Cracking

sample	first-order kinetic rate (h^{-1})[a]	*K* Al(Al + Si)
MCM-41.1	0.6211	8.873
amorphous Si-Al	3.20	35.56
USY1	12.37	1237

[a] Calculated from plot stop of $-\ln(1 - x)$ vs $WHSV^{-1}$.

Table 14. IR Intensity of the Pyridinium Bands and Pyridine Coordinate to Lewis Site on the Different Catalyst Samples

	desorption temperature (K)		
	423	523	623
	Brønsted Acidity		
MCM-41.1	12	6	3
MCM-41.2	1.5	0.6	0.3
MCM-41.3	n.d.	n.d.	n.d.
ASA	12	6	3
USY1		21	9
	Lewis Acidity		
MCM-41.1	47	34	24
MCM-41.2	3.1	2.3	1.5
MCM-41.3	2.3	1.5	1.5
ASA	37	23	2
USY1		11	8

Table 15. First-Order Kinetic Rate Constants for Gas Oil Cracking

sample	first-order kinetic rate (K)[a]	*K* Al(Al + Si)
MCM-41.1	2.04	29.14
ASA	1.71	19.00
USY1	3.22	322

[a] Calculated from a first-order rate expression ln (1 - *x*) at cat/oil ratio of 4.

Table 16. BET Surface Area ($m^2\ g^{-1}$) of the Samples

	Si/Al	calcined	steamed
MCM-41.1ST	14	837	81
MCM-41.2ST	100	1031	84
MCM-41.3ST	143	877	347
ASA.ST	100	551	116
USY1.ST	2.5	268	213

approached that of the USY zeolite and is higher than that of amorphous silica-alumina (Table 15).

Comparing gas oil cracking selectivity results (Figure 39), it was seen that MCM-41 produces more liquid fuels and less gases and coke than amorphous silica-alumina. When compared with USY zeolite, MCM-41 is more selective toward diesel formation and gives less gasoline and more coke. These results would suggest that if not present as the main active cracking component of the FCC catalyst, MCM-41 could probably be used as an active component of the matrix. Indeed, mesoporous silica-aluminas are active for performing a precracking of the largest feed molecules, facilitating the ulterior action of the USY zeolite.[360] A clever use of the MCM-41 in this respect was reported by Schipper et al.[361] who prepared a cracking catalyst comprising a core of a zeolite (USY, ZSM-5) and a shell of MCM-41.

However, if one takes into account that in a FCC unit the catalyst is subjected in the regenerator to temperatures close to 800 °C in the presence of steam, it is easy to understand that for FCC cracking catalysts more important than the initial activity is the hydrothemal stability of the catalysts. It is for this reason that work reporting only on the cracking activity of fresh catalysts becomes limited.[362−364]

To find if a given cracking catalyst is suited to resist at a reasonable level, the hydrothermal deactivation in the regenerator of the FCC unit, this is calcined at 750 or 815 °C in the presence of 15 psig of steam. When the MCM-41, amorphous silica-alumina and the USY zeolite discussed before were steamed at 750 °C, their surface area decreases, this effect being much larger in the case of the MCM-41 samples (Table 16). The observed decrease in MCM-41 indicates two things: First of all that the samples are not stable enough to resist the inferno of the regenerator, and secondly, that the MCM-41 sample containing the lowest Al content is the most stable one. Unfortunately, if MCM-41 is more hydrothermally stable when it contains less Al, it will contain, as a result, a lower number of acid sites when the Si/Al increases and consequently, its catalytic activity decreases. Nevertheless, the gas oil cracking activity of the steamed samples was measured (Figure 40) and the results show that MCM-41 is much less active than either USY or amorphous silica-alumina.[359] Similar results on the hydrothermal stability of MCM-48 have also been found.[365]

At this point, it becomes clear that even though the characteristics of MCM-41 for cracking vacuum gas oil and straight run naphtha[366] are good, unless more hydrothermally stable samples are prepared the possibilities of using MCM-41 in the actual crackers themselves will be limited. Thus, due to its practical importance the stability of MCM-41 has been studied in a number of publications.[367−371]

The most fruitful direction for increasing the stability of these solids consist of increasing the diameter of the walls. In this way pore diameters up to 2.0 nm have been claimed, and the resultant samples show very good thermal stability.[370,371] Unfortunately, the hydrothermal stability of the resultant samples was not checked. It appears to us that an increase in hydrothermal stability will be achieved if MCM-41 samples, with more ordered walls, are synthesized. The ideal will be to synthesize MCM-41 with crystalline walls, since if this were achieved the madelung energy will increase the hydrothermal stability of the crystalline samples.

Meanwhile, one can look into refinery processes which require a catalyst with mild acidity and are less demanding from the point of view of the hydrothermal stability. In this sense, processes such as hydroisomerization, hydrocracking and demetalization, and olefin oligomerization appear as good candidates.

Resids or shale oils can be upgraded by using a catalyst comprising MCM-41 and nickel and molybdenum,[372] with the peculiarity that the mesoporous MCM-41 is used in decreasing pore sizes from the top to the bottom of the reactor[373] (Table 17).

A recent development consists of perfoming hydrocracking in reactors commonly used for carrying out hydrodesulfurization of the feed and which works at pressure below 100 bars. By working under these conditions one can perform some hydrocracking of the feed, increasing therefore the amount of diesel pro-

Table 17. Residue Upgrading Process with Decreasing MCM-41 Pore Size

	1st stage	2nd stage	3rd stage
MCM-41 pore size maximum catalytic activity	• demetalization • asphaltene conversion	• demetalization • asphaltene conversion	• desulfurization • CCR reduction

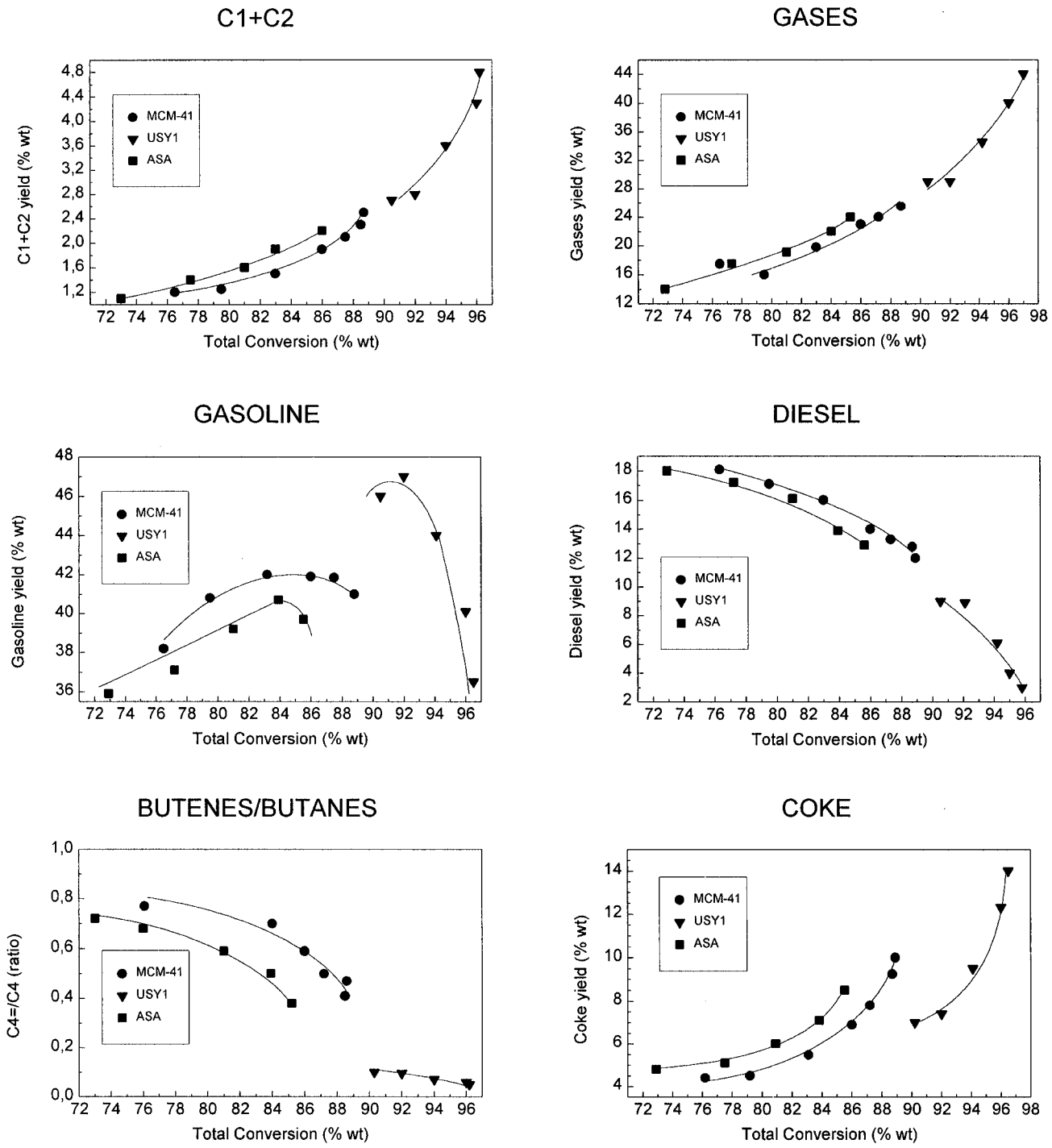

Figure 39. Selectivity to different products vs total conversion for cracking of gas oil for MCM-41.1, ASA, and USY1.

duced while achieving the desired HDS of the feed. This process is called mild hydrocracking (MHC) and requires as a carrier a mildly acidic support on which NiO and Mo_2O_3 are incorporated. Typical catalysts used in MHC include acidic carriers such as halogen-doped alumina, silica-alumina, or zeolites, which allow conversion of heavy hydrocarbons via carbenium ion cracking. The zeolite-containing catalysts are now used extensively in MHC. The amorphous-based hydrocracking catalysts are more sensitive to deactivation by coking and by organic nitrogen compounds and ammonia, formed in the hydrodenitrogenation (HDN) reactions, than zeolite-based catalysts.[374] However, because of their very high cracking activity, zeolite-based hydrocracking catalysts show a higher selectivity to LPG, gasoline, and lower to middle distillates than the amorphous systems.[375] Moreover, an important aspect of hydrocracking catalysts which takes on special relevance when processing heavy feedstocks is the distribution of the

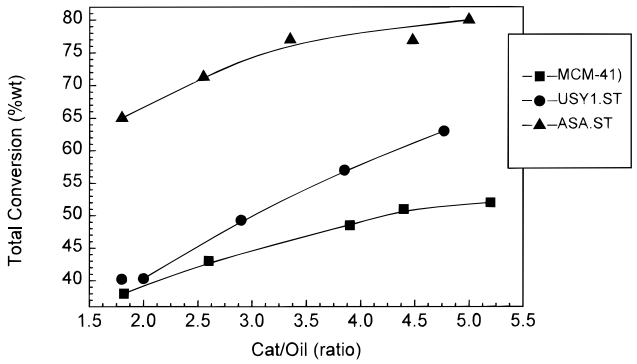

Figure 40. Activity for cracking of gas oil for steamed MCM-41.1, ASA, and USY1.

Table 18. Textural Properties of Unsupported and NiMo-Supported Catalysts

sample	BET surface area ($m^2\ g^{-1}$) micropore	BET surface area ($m^2\ g^{-1}$) total	pore volume ($cm^3\ g^{-1}$) micropore	pore volume ($cm^3\ g^{-1}$) total	APD[a] (nm)
MCM-41	0	648	0	0.54	3.3
NiMo/MCM-41	0	519	0	0.60	4.6
SiO_2-Al_2O_3	21	268	0.01	0.31	4.6
NiMo/SiO_2-Al_2O_3	15	171	<0.01	0.29	6.8
USY	362	551[b]	0.18	0.41	2.1
NiMo/USY	179	283	0.09	0.29	2.9

[a] Average pore diameter. [b] The PQ data specifies a surface area of 720 $m^2\ g^{-1}$.

metals on its surface, and their proximity to the acid sites where cracking will occur. This is a serious problem for zeolite-based hydrocracking catalysts, even if a large pore Y-type zeolite with enhanced mesoporosity is used. Taking all this into account, MCM-41 appears as a well-suited carrier for this process since it has high surface area for achieving good dispersion of the transition metal oxides, and at the same time the aluminum form of the mesoporous material presents mild acidity.[376,377]

In a recent work,[377] the MHC performance of a NiMo/MCM-41 catalysts was compared with that of amorphous silica-alumina and an ultrastable low unit cell size Y zeolite (USY) having the same Ni and Mo contents (Table 18). From the point of view of the acidity of the carrier, USY zeolite showed the highest amount of Brønsted acidity, most of the sites having medium-strong acid strength. The acidity of MCM-41 was similar to that of amorphous silica-alumina, both in number and acid strength distribution. Moreover, most of the Brønsted acid sites in the two mesoporous silica-alumina carriers are of weak-medium strength, as is required for producing diesel in MHC operation. However, it should be taken into account that the acid characteristics of the support are modified when supporting the metals, and in this particular case, the Mo strongly interacts with the acid sites, making the strongest acid sites disappear from MCM-41 and amorphous silica-alumina samples.[377] A vacuum gas oil containing 2.53 wt % of sulfur and 2900 ppm of N_2 was hydrotreated on the above bifunctional catalysts and their performance for hydrodesulfurization (HDS), hydrodenitrification (HDN), and hydrocracking are given in Figure 41a–c.

The results show that the MCM-41-based catalyst gives better performance from the point of view of

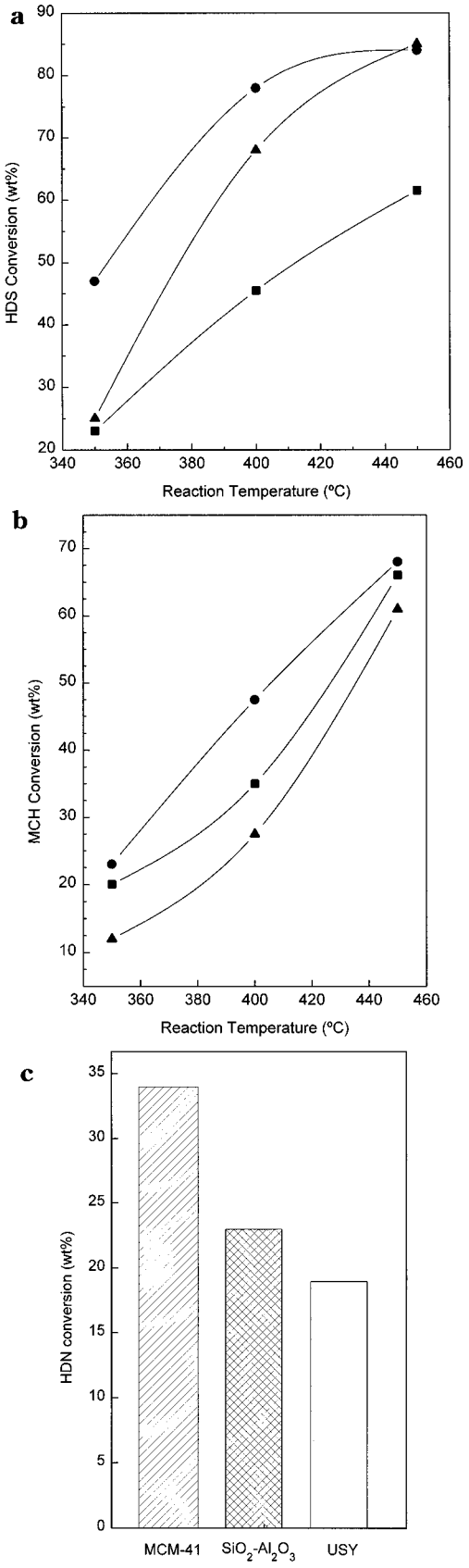

Figure 41. (a) Hydrodesulfurization (HDS) conversion of feed A as a function of reaction temperature for (●) NiMo/MCM-41, (▲) NiMo/SiO_2-Al_2O_3, (■) NiMo/USY catalysts. (b) Hydrocracking (MHC) conversion of feed A as a function of reaction temperature. Same symbols as in a. (c) Hydrodenitrogenation (HDN) conversion of feed A obtained at 400 °C reaction temperature on the different supported catalysts.

Table 19. Product Distribution Obtained in the Mild Hydrocracking of Vacuum Gas Oil (Feed A) at About 50 wt % Hydrocracking Conversion to Products Boiling Below 360 °C on the Different NiMo Catalysts

	distribution of products boiling below 360 °C (wt %)		
catalyst	C_1-C_4	naphtha[a]	middle distillates[b]
NiMo/MCM-41	16.2	25.8	58.0
NiMo/SiO_2-Al_2O_3	18.9	23.1	57.9
NiMo/USY	19.7	27.3	52.0

[a] Naphtha: C_5 to 195 °C bp. [b] Middle distillates: 195−360 °C bp.

HDS, HDN, and hydrocracking conversion. This is probably due to the very high surface area and regular pore dimensions of the MCM-41 aluminosilicate, which favors a high dispersion of the active species while increasing the accessibility of the large molecules of the gas oil feed containing heteroatoms to the catalyst active sites. In the case of the MHC, as important as the total conversion is to obtain a good selectivity to middle distillates. The product distribution obtained is given in Table 19 and shows that the NiMo/MCM-41 catalyst produces the lowest amount of gases and consequently the highest to liquid fuels, with diesel production also being maximized. Since the acidities are very similar on the two mesoporous catalysts, the differences in selectivities were related to the regularity, size, and dimensionality of the pores present in MCM-41.[377] When the hydrocracking catalysts were used in a hypothetical two-stage operation, using a pretreated feed with lower sulfur and nitrogen contents and with the boiling range of the feed shifted to lower boiling point products, the USY-based catalyst shows its superior hydrocracking activity, while MCM-41 is more selective toward middle distillates than the zeolite and similar to amorphous silica-alumina.

It appears, then, that NiMo/MCM-41-type materials may be used in the next generation of MHC catalysts. In this respect it would be worth studying the influence of the pore size of the mesoporous material on the final hydrocracking behavior. This could be relevant, if one takes into account that the reaction network involves a series of consecutive reactions. Therefore, the relative rates for formation of diesel, kerosene, naphtha, and gases should be quite sensitive to the existence of diffusional problems and, consequently, to the diameter of the pores.

When deep hydrocracking is desired and the highest possible activity together with the highest possible middle distillate selectivity are to be achieved, then the process is carried out at pressures above 100 bars and temperature range of 230−450 °C, on catalysts comprising as the support silica-alumina dispersed in an alumina matrix, or silica-alumina and zeolite within an alumina matrix. As the hydrogenation−dehydrogenation component, a group VII metal and a group VIB metal are introduced. A hydrocracking process has been developed using mesoporous MCM-41.[378−380] In this case hydrotreated vacuum gas oil feed was hydrocracked on a three-component catalyst: NiW, MCM-41, and USY/ZSM-5. The metal components of the catalyst are preferably associated with the high-surface area mesoporous component and high metal loadings can be achieved in order to give good hydrogenation activity to the catalyst. The zeolite (USY or ZSM-5) provides a higher level of acidic functionality than the mesoporous component, allowing metal loadings and acidic activities to be optimized for good catalyst selectivity and activity. The catalyst that include MCM-41 instead of amorphous silica-alumina allows similar distillate selectivity but with an improved conversion activity.

The acid form of Al-MCM-41 together with nickel and tungsten can also be used to hydrocrack heavy waxes.[381] The selectivity of this catalyst toward lube oils is higher than that of fluorinated NiW/Al_2O_3, specially at levels of conversion above 50%.

The mild acidity of Al-MCM-41 can also be useful for isomerizing normal paraffins into isoparaffins on bifunctional Pt/MCM-41 catalysts.[382,383] In the case of a bifunctional mechanism the generalized steps are outlined in the following scheme:

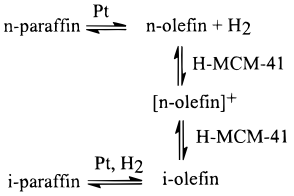

The first reaction step occurs on the metal function and corresponds to the dehydrogenation of the paraffin yielding the corresponding olefin. The high reactivity of olefins toward acid catalysts allows the mildly acidic MCM-41 to isomerize the normal olefin to the isoolefin, which is finally hydrogenated on the metal function and desorbed as an isoparaffin. In comparison to Pt-silica-alumina catalysts the Pt/MCM-41 produced less cracked products, probably due to its effectively greater Pt dispersion.

A combination of hydrocracking plus hydroisomerization in a two-step process based on a MCM-41 catalyst is able to convert wax feeds to high viscosity index lubricants.[384] In the first step the wax feed is hydrocracked under mild conditions (70 bar), with a conversion to nonlube range products lower than 40% of the feed, on an acidic mesoporous MCM-41 based catalyst. The effluent of the first stage is hydroisomerized in a second step using a low acidity hydroisomerization Pt/MCM-41 catalyst to produce less waxy branched paraffins.

Since olefins can easily be activated by solid catalysts containing mild acid sites, H-MCM-41 has been used for upgrading olefins in several different processes.[385] In one of these routes, C_3, C_4, or C_5 olefins are oligomerized to $C_6-C_{18}^+$ hydrocarbons which are then recycled and cracked in a multistage process to form C_3-C_5 range olefins.

Olefins can also be disproportionated on H-MCM-41 to produce isobutylene and isoamylenes that are reactants for the production of MTBE and TAME.[366]

Production of fuel and lubricants can also be obtained by direct oligomerization of olefins[386−390] on metal-containing MCM-41. Cr, Ni, and Fe are suitable metals to carry out the oligomerization of ethylene and propylene. In general, it can be said that the catalytic activity of mesoporous materials was lower than MFI-metallosilicates,[391] particularly when the purpose is to produce oligomeric gasoline.

However it has been shown[391] that a considerable amount of oligomers is produced from propene at low temperatures on MCM-41-type catalysts, and in this case the pore size of the mesoporous material can make a difference when the objective is to oligomerize larger olefins, or in general, to produce large lubricant molecules. As an example the oligomerization of propylene on different acid catalysts is given in Figure 42.[390]

When discussing the advantages of mesoporous materials for acid-catalyzed reactions, the benefit of the large regular pores better allowing the diffusion of the reactants and conversely the fast diffusion of the products out, minimizing unwanted consecutive reactions and catalyst decay by the large sizes of the adsorbed molecules, is a recurring theme. If this feature was useful in the field of oil refining and petrochemistry, it becomes of paramount importance when dealing with the synthesis of fine chemicals. Indeed, these reactions, often involve bulky reactants and products, and in many cases they are carried out in liquid phase where diffusional problems can be enhanced. It is not then surprising that acidic mesoporous materials have enjoyed considerable success in the field of organic synthesis, even though the applications are still in their infancy. Up to now most of the work published in the application of acidic MCM-41 materials for the production of fine chemicals comes principally from two research groups from Delft and Valencia Universities. Friedel−Crafts alkylations and acylations are successfully carried out on aluminosilicate MCM-41.[392−398] The shape selectivity of the H-MCM-41 was demonstrated during the alkylation of 2,4-di-*tert*-butylphenol with cinnamyl alcohol. Even though a large-pore HY zeolite has adequate acidity to carry out this reaction, only very minor amounts of the Friedel−Crafts product **3** were observed, while this was the major product on MCM-41 (Table 20).[3924]

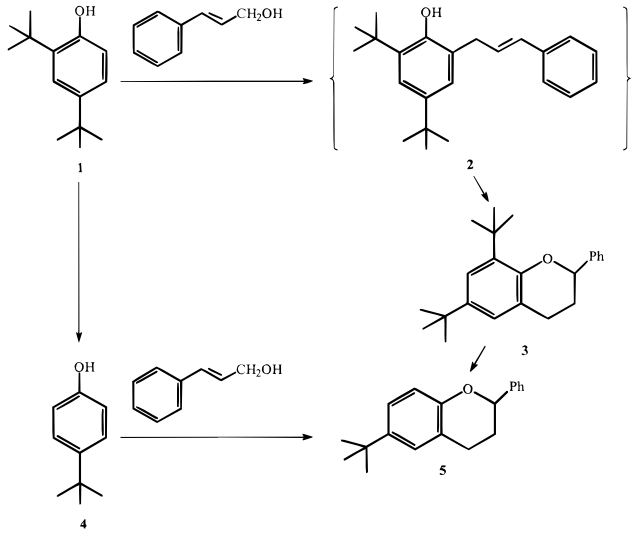

An explanation for this is the possibility that dihydrobenzopyran (**3**) would be produced via the intermolecular ring closure of the primary cinnamylphenol (**2**), arising from the Friedel−Crafts alkylation of phenol (**1**). On the other hand, compounds **4** and **5** would be formed by acid-catalyzed dealkylation, a process which is generally observed in *tert*-butyl substituted aromatics and has been

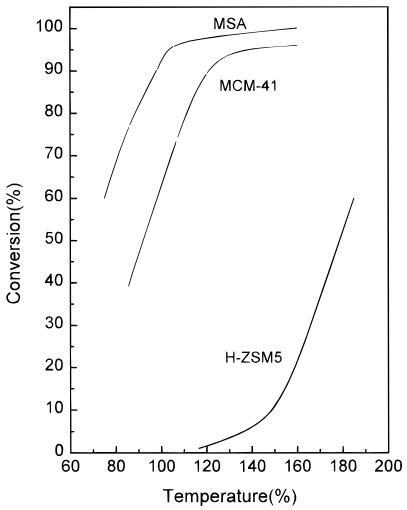

Figure 42. Propylene oligomerization on different acid catalysts.

Table 20. Results of the Reaction of 2,4-Di-*tert*-butylphenol (206 mg) with Equimolar Amounts of Cynnamyl Alcohol (134 mg) in Isooctane (50 mL) at 90 °C in the Presence of Solid Catalyst (250 mg) or Sulfuric Acid (20 mg)

	products, yield (%)			
catalyst	**1**	**3**	**4**	others
HY	89	<1	5	−
HYM	75	9	−	12[a]
MCM-41	20	35	25	**5**(6)
Si/Al	56	6	−	−
H_{2SO4}	73	12	9	3[b]

[a] Dicinnamyl ethers plus diphenylpentadienes. [b] Tri-*tert*-butylphenol.

reported to occur on zeolites.[399−401] Thus, owing to the diffusional problems of the reactant **1** through the windows of the zeolite, benzopyran (**3**) will only be formed on the surface of the faujasite, while it will easily diffuse and react in the pores of MCM-41. Analogous pore size effects were observed during the *tert*-butylation of anthracene, naphthalene, and tianthrene.[394]

Acylation reactions are of general use in the production of fine chemicals. In most processes $AlCl_3$ is still used in stoichiometric amounts to "catalyze" this type of reactions. Very recently, the economic as well as waste disposal problems associated with the use of $AlCl_3$ are trying to be overcome through the use of easy separable and regenerable solid catalysts. In this sense researchers from Rhône-Poulenc have claimed the use of acid zeolites for the Friedel−Crafts acylation of aromatics,[402] and some of the results have now been commercialized. The work of Spagnol et al., however, certainly opens up the possibility of exploring MCM-41 for carrying out acylation reactions of more bulky reactants.

The synthesis of aromatic ketones is an important process in the preparation of synthetic fragrances and pharmaceuticals which involves an aromatics acylation step. More specifically in this area, work has been reported[396] on the acylation of 2-methoxynaphthalene with acetic anhydride, with the aim of achieving the highest acylation at the 6 position which is of particular interest for the production of the anti-inflamatory drug Naproxen.

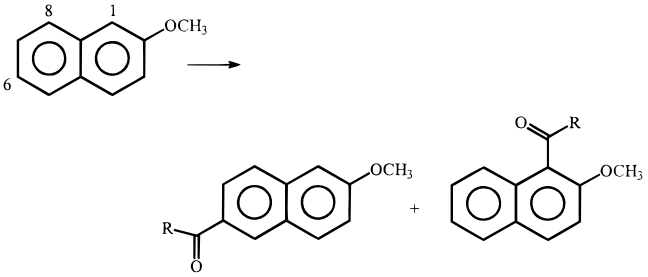

In this respect, H-MCM-41 was found to be an active catalyst giving at 132 °C in chlorobenzene, turnover numbers of 20, 17, and 11 when using acetic, benzoic, and isobutyric anhydride, respectively, as acylating agents. With respect to the product distribution it was observed that at moderate temperatures (up to 100 °C) the selectivity to the 1-acylated product was practically 100%. At higher temperatures, the preferential deprotodeacylation of the 1 position, with respect to the 6 or 8 position, leads to a decrease in the selectivity for the 1 position. Nevertheless selectivities to the acylation in the 6 position were always below 10% on the H-MCM-41 catalyst. What is remarkable in this system is that the catalyst can be easily regenerated. It appears then that the mildly acidic H-MCM-41 mesoporous material is a suitable Brønsted acid catalyst for the Friedel−Crafts acylation of 2-methoxynaphthalene using anhydrides as acylating reagents.

This mild acidity combined with the large pores has been especially useful for carrying out reactions such as acetalyzations,[403] Beckman rearrangements,[404] glicosidation,[405] and aldol condensation.[406] The catalytic preparation of acetals is of interest for their use in pharmaceuticals[407,408] and as fragrances in perfumes and detergents.[409] Since the reaction does not need strong acid sites and on the other hand it frequently deals with bulky reactants, H-MCM-41 appeared as a good choice of catalyst. The acetalization of aldehydes with different sizes, i.e. *n*-heptanal (1), 2-phenylpropanal (2), and diphenylacetaldehyde (3), with trimethylorthoformiate (TOF) was carried out on different acid catalysts going from microporous (*β*-zeolite) to mesoporous amorphous silica-alumina (Si-Al), and long-range ordered MCM-41 silica-alumina.[403] The rates of acetalization obtained on these catalysts are given in Table 21.

It can be seen once again in this case that when working with reactants of smaller size, the zeolite is the most active catalyst. However when the size of the aldehyde increases, the diffusional restrictions imposed by the zeolite pores strongly decrease the observed rate of reaction, while in the case of the MCM-41 catalyst the ratio remains very close, regardless of the size of the reactant aldehyde. This makes the ordered mesoporous acid catalyst a very convenient one for carrying out, acetalization reactions, especially when bulky reactants and products are involved. If the catalytic activity is important for these reactions, it is also very important to avoid, or at least to slow down, the deactivation of the catalyst during the process. The acetalization of the bulkiest diphenylacetaldehyde is a very nice example of the importance of the fast diffusion of the products to slow down the catalyst deactivation. Indeed, the results presented in Figure 43 indicate that while the initial rate of acetalyzation is larger on HY zeolite this becomes rapidly poisoned due to the products which are not able to diffuse outside building up in the α cavities resulting in conversions no greater than 60%. On the contrary, in the case of the MCM-41 catalyst even though the initial rate is slightly lower, the catalysts decay is slower than in the case of HY zeolite, and consequently practically 100% conversion is achieved within three hours of reaction time.

Table 21. Influence of the Catalyst Pore Size on the Rate and Conversion in the Acetalization Reaction of 1, 2, and 3

	r_0 (mol h^{-1} g^{-1}) × 10^3		
catalyst	**1**	**2**	**3**
1-MCM-41	2500	2480	2340
2-*β*H			180
Si-Al	1500	1600	460

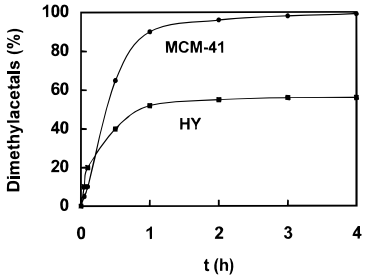

Figure 43. Synthesis of dimethyl acetals on HY and MCM-41 acid catalysts.

The Beckman rearrangement of cyclohexanone oxide has been carried out on medium and large pore zeolites,[410−414] and it has been concluded that weak acid sites, as weak as silanols, can carry out the reaction.[412] Then MCM-41 with its low acidity can also catalyze a reaction of this type[404] but the yields and selectivity are lower than those obtained with zeolites.

It is remarkable, taking into account the general properties of mesoporous materials, how little work was undertaken in applying acidic mesoporous molecular sieves to the preparation of fine chemicals. We are convinced that in the next few years, when more information on these materials will be available to organic chemists, the number of applications of MCM-41 type materials in organic synthesis will strongly increase. This review is aimed, in part, to show the readers who are nonspecialized in materials preparation but who are potential users of MCM-41 derivatives that they are relatively easy to make and their potential, at least in catalysts, is still largely unexplored.

2. Base Catalysis

It was previously reported that microporous aluminosilicates can be used as base catalysts when the negative charge on the aluminum was compensated by alkaline ions.[415,416] Furthermore the smaller the charge to radius ratio of the compensating cation is, the stronger the basicity of the associated framework oxygen is.[415,416] In an analogous way to that of zeolites, the negative charge of the tetrahedrally coordinated aluminum atom in MCM-41 was compensated by Na^+ and Cs^+ and the resultant samples were active and selective for carrying out the base-

Table 22. Knoevenagel Condensation of Benzaldehyde and Ethyl Cyanoacetate with Different MCM-41 Catalysts

catalyst	amount (% m/m)	t (h)	conversion (% m/m)	selectivity (%)	A_{alk} (mol h^{-1} $mol^{-1}_{alk.met.}$)	A_{wt} (mmol h^{-1} g^{-1})[c]
Na-MCM-41[a]	5	7	81	75	2.3	11.8
Na-MCM-41[b]	5	3	72	99	4.7	15.5
HNa-MCM-41[b]	5	3	61	95	24.9	14.1
Cs-MCM-41A[a]	1.6	7	67	60	5.3	12.9
Cs-MCM-41A[b]	5	3	72	98	7.5	18.4

[a] Solvent free at 150 °C, 20 mmol of ethyl cyanoacetate and 26 mmol of benzaldehyde. [b] THF-H_2O at 70 °C, 15 mL of each and 10 mmol of each reactant. [c] Specific activity at t.

Table 23. Catalytic Oxidation of Hex-1-ene with H_2O_2 on Ti-MCM-41 Zeolite

t (h)	conversion (H_2O_2)	selectivity (H_2O_2)	selectivity (% molar)		
			epoxide	glycol	ether
0.50	3.9	60	100		
2.00	23.4	70	95.7	1.7	2.6
3.50	28.9	70	94.4	1.6	4.0
5.00	39.9	75	91.2	3.1	5.7

catalyzed Knoevenagel condensation of benzaldehyde with ethyl cyanoacetate:[417]

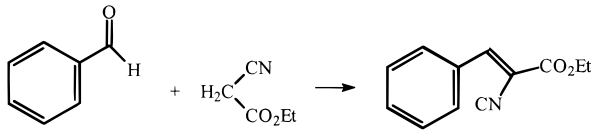

As expected, the H-MCM-41 was not able to catalyze the reaction, while the Na^+-exchanged sample could perform the reaction. The Cs^+-exchanged sample was more basic and therefore, it was more active than the Na^+-exchanged sample (Table 22).

When the Na-MCM-41 sample was tested on a more demanding reaction such as the condensation of benzaldehyde with diethyl malonate, it was found that the reaction occurs, but at a much smaller rate. For instance, only 6% conversion was observed after 3 h at 150 °C. When an excess of alkaline with respect to the exchange capacity is introduced, Na_2O and Cs_2O particles can be formed and then the resultant catalysts show a stronger basicity than caesium- and sodium-exchanged MCM-41.

In our opinion alkaline-exchanged MCM-41, especially those with a high Al^{IV} content, can extend the possibilities of alkaline exchanged zeolites toward reactions catalyzed by weak bases and involving large size reactant molecules. On the other hand, the very large surface area of Al-MCM-41 can be an adequate support to generate, after impregnation with cesium salts followed by calcination in an inert atmosphere, a high amount of small Cs_2O particles, which will be able to perform reactions demanding strong basicities.

3. Redox Catalysis

After the seminal work on the selective oxidation of paraffins, olefins, and alcohols on Ti-silicalite[418−420] and its extension to a large pore Ti-β-zeolite,[421−423] the door was opened to introduce active Ti in the walls of MCM-41. The first report on the successful preparation of Ti-MCM-41 was published in early 1994,[282] and the resultant material was able to epoxidize selectively olefins to epoxides using H_2O_2 as the oxidizing agent (Table 23).

The activity of Ti-MCM-41 to epoxidize small linear olefins with H_2O_2 was lower than when using Ti-silicalite and Ti-β-zeolite catalysts, indicating that the intrinsic activity of Ti in the MCM-41 was lower than in ZSM-5 and β-zeolites, at least under the reaction conditions used. However the advantages of Ti-MCM-41 as epoxidation catalyst was in its ability to oxidize large molecules which cannot diffuse in the pores of microporous materials, as well as to use organic hydroperoxides as oxidants.[282,424] For instance Ti-MCM-41 was found to be much more active than Ti-β-zeolite to oxidize α-terpineol and norbornene at 70 °C using *tert*-butyl hydroperoxide as oxidant (Table 24).

Two months later, another paper on the synthesis of a mesoporous Ti-containing material called Ti-HMS appeared,[283] showing a surprisingly high catalytic activity for the hydroxylation of benzene to phenol using acetone as the solvent. However, it was shown later[425] that the phenol yields were overestimated, due to the fact that the competitive oxidation of the acetone was not taken into account and the products formed were not separated chromatographically from phenol. When the reaction was carried out properly it was shown that Ti-HMS has very low activity for the hydroxylation of phenol, and in any case much lower than Ti-MCM-41.[425] Other papers have expounded on the subject.[426−428] Recently it has been proposed that Ti-HMS prepared with a neutral surfactant (S°I°) exhibits greater catalytic activity for the liquid-phase peroxide oxidations of methyl methacrylate, styrene, and 2,6-di-*tert*-butylphenol than Ti-MCM-41 assembled by electrostatic S^+I^+ and $S^+X^-I^+$ pathways. The difference in activity is larger when bulkier reactants are used. This difference in activity cannot be related to differences in the intrinsic activity of Ti, since this is in the same environment in the walls of the structure (see earlier discussion) and thus has been related to the greater interparticle mesoporosity observed in Ti-HMS which should facilitate substrate transport and access to the framework confined mesopores.[286]

Amines have also been oxidized on Ti-MCM-41 and Ti-HMS mesoporous materials.[429,430] The products formed are of interest in several fields including chemical and pharmaceutical industries.[431,432] While Ti-MCM-41 has little activity to convert primary aliphatic amines into the corresponding hydroxylamine, the mesoporous Ti-HMS is active for the oxidation of arylamines in the liquid phase. The success observed from using the mesoporous material was again related to the larger pores and the possibility of using organic peroxides as oxidants. On a similar basis, Ti-MCM-41 is able to oxidize bulky sulfides to the corresponding sulfoxides and sulfones,

Table 24. Oxidation of α-Terpineol and Norbornene on Ti-Containing Materials

		α-terpineol			norbornene epoxides		
catalyst sample	reaction time (h)	product 3	others	reaction time (h)	exo	endo	alcohol
Ti-MCM-41	3	23.8	4.02	5	21.7	4.7	3.1
	8	31.5	8.6	11	30.0	12.3	6.4
Ti-Beta	3	4.1	2.5	5	4.7	5.6	6.6
	8	7.6	5.8	11	11.2	7.1	12.8

better than the large pore Ti-β-zeolite.[433] Indeed, the results show that while Ti-β-zeolite is more active in reaction 1, the order of reactivity is reversed when a bulkier sulfide is involved (reaction 2).

Reaction 1

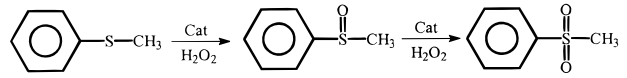

Reaction 2

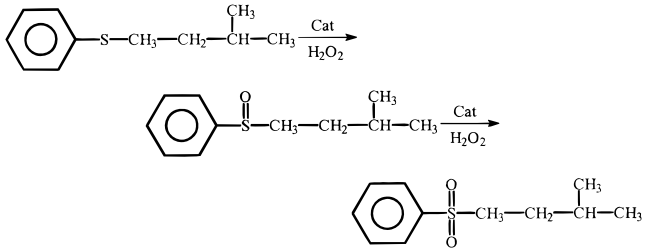

Up to now most of the work on Ti-M41S mesoporous molecular sieves has been carried out on the MCM-41 structure and very few on Ti-MCM-48.[287,434] In those cases a Ti-containing mesoporous material isomorphous to the cubic MCM-48, silicate structure has been synthesized by using surfactants. It was claimed that since the unit cell has been enlarged and UV−vis, IR, and Raman characterization showed that titanium was well dispersed, the guest metal should probably be located in the wall of the mesoporous structure substituting for part of the silicon. However, when one looks closer at the synthesis procedure reported, it can be seen that the high pH synthesis (pH = 11) is achieved by adding NaOH. It is well known in the literature that in order to incorporate Ti in micro- and mesoporous materials in tetrahedral coordination in the final structure, alkalines metal hydroxides should be avoided in the synthesis otherwise alkaline metal titanates will be formed. Thus it may occur that under the reported synthesis conditions only a small amount of the Ti should be in tetrahedral coordination within the walls of the MCM-48. An indication that this may be the case is the fact that the increase in unit cell size in the case of the Ti-containing sample is only of 0.3 Å.[287] Taking all this into account it is certainly remarkable that the resultant Ti-MCM-48 is able to selectively oxidize methyl methacrylate and styrene.

Until now we have discussed the new possibilities opened by Ti-M41S mesoporous materials in the field of selective oxidation of bulky reactants using H_2O_2 and organic hydroperoxides. These possibilities have been expanded by the observation that it is possible to prepare bifunctional acid oxidation catalysts which are able to perform two different reaction steps on the same catalyst.[435] In that work a MCM-41 structure was prepared which contained in the walls both Ti and Al sites. In essence the catalyst now has both the Ti^{IV} oxidation sites, in addition the H^+ associated to the Al^{IV} as acid sites, which enables us to carry out in one pot and using *tert*-butyl hydroperoxide, the multistep oxidation of linalool to cyclic furan and pyran hydroxy ethers with 100% selectivity and in ratio of 0.89. This method somewhat resembles the case where epoxidase enzyme is used instead (∼0.7) and is much better than the less friendly conventional process involving performic acid:[436]

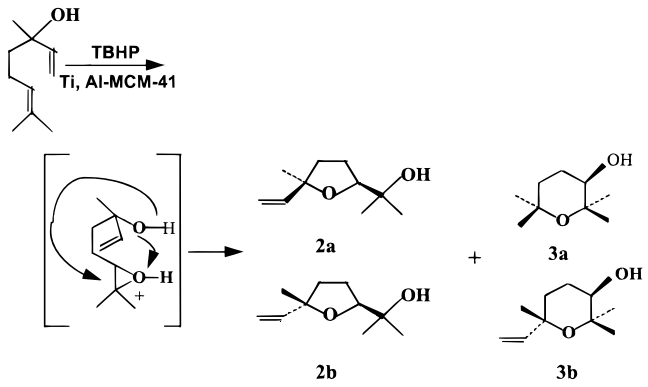

At this point one can ask why should we use long-range-ordered mesoporous catalysts which require the use of surfactants during the synthesis of Ti-containing silicas if they can be prepared by a sol-gel synthesis and hence no surfactant is required. In trying to answer this question we report here on the comparison of the catalytic characteristics of Ti-containing mesoporous molecular sieves with mesoporous titania-silica aerogels with highly dispersed titanium as prepared by an alkoxide sol-gel process.[437−442] In this case it was found that, at least for lower Ti contents, Ti is tetrahedrally coordinated and is able to epoxidize selectively alkenes using organic hydroperoxides. However unlike Ti-MCM-41 they cannot be used when H_2O_2 is the oxidant. An optimized preparation involves a sol-gel technique combined with ensuing supercritical drying at near-ambient temperature.[438] This treatment produces a high density of the desired Ti−O−Si centers, while producing a good mesoporous texture which allows accessibility to bulky olefins and organic hydroperoxides. A titania content of ∼20 wt % has been found to be the optimum for catalytic purposes.

When this catalyst was compared with an optimized Ti-MCM-41 containing ∼2 wt % of TiO_2, it is found that the olefin epoxidation activity per Ti atom is larger on Ti-MCM-41, but since the titania-silica aerogel has a much larger titanium content the conversion achieved on this sample is higher.[443] It can be concluded here that it is well worthwhile to carry out further research in the preparation of titania-silica aerogels by the sol-gel route, since the

Table 25. Oxidation of 2,6-Di-*tert*-butylphenol and Phenol

substrate	sample no.[a]	conv (%)	H_2O_2 eff (%)[b]	product selectivity (%)[a] quinone	CAT	HQ
2,6-DTBP[d]	4	70	64	92		
2,6-DTBP	4[e]	95	95[f]	100		
2,6-DTBP	6[g]	24	22	92		
2,6-DTBP	6	3	3	100		
2,6-DTBP	7	2	2	100		
2,6-DTBP	no catalyst	2	2	100		
2,6-DTBP	Ti-HMS[h]	26	7	54		
2,6-DTBP	Ti-HMS[i]	15	48	93		
phenol[j]	4[k]	13.4	69		58	42
phenol	4[l]	11.7	59		57	43

[a] All the catalysts were used in the calcined form unless otherwise stated. [b] H_2O_2 efficiency = (moles of H_2O_2 utilized for the formation of quinone/moles of H_2O_2 added) × 100. [c] CAT = catechol; HQ = hydroquinone. [d] Catalyst (0.1 g), 2,6-di-*tert*-butylphenol (1.03), hydrogen peroxide (30 mass %) (1.7 g), acetone (7.8 g), 335 K, reaction time 2 h. [e] *tert*-Butyl hydroperoxide was used as the oxidant. [f] TBHP efficiency. [g] As-synthesized catalyst. [h] Reference 12 (Si:Ti = 100). [i] Reference 8 (Si:Ti = 100). [j] Catalyst (0.5 g), phenol (5.0 g) hydrogen peroxide (30 mass %) (2.0 g) solvent (15 g) 353 K, reaction time 15 h. [k] Solvent water. [l] Catalyst was regenerated and reused.

synthesis procedure is relatively easy and avoids the use of organic templating agents and samples can be prepared with larger amounts of titanium. In particular the three aspects to be improved involve the long-term leaching of titanium (one should take into account that for practical industrial application the minimum usage time is 1000 h), the use of H_2O_2 as oxidant, and finally the possibility of regenerating the catalyst by a calcination process in the presence of air.

Owing to the success in the incorporation of Ti and its relatively good behavior as a selective oxidation catalyst, other transition metal elements with potential catalytic activity were also intended to be introduced on the walls of the MCM-41. An interesting study of MCM-41 incorporating Ti, Fe, Cr, V, and Mn was reported,[444] and by means of X-ray absorption spectroscopy the authors were able to show the relative tendencies of the different metals to remain in the framework when the material was subjected to calcination. It was found in this respect that Ti was the most stable in the structure, the majority of Fe also remains in the framework, whereas in the case of vanadium and chromium these were found to increase in their oxidation state to +5 and +6, and especially chromium was found to be in highly dispersed oxidic species. These results are of paramount importance in order to discuss what the active species are and where they are located during the catalytic reactions carried out on mesoporous materials containing transition metals. For instance, a vanadium-containing mesoporous catalyst was used for the hydroxylation of 2,6-di-*tert*-butylphenol (2,6 TBP) into 2,6-di-*tert*-butyl-1,4-benzoquinone with high conversion selectivity and efficient H_2O_2 utilization[445] (Table 25). On the other hand a synthesized V_2O_5-SiO_2 aerogel gives considerable conversion of 2,6-DTBP, but after calcination the activity disappeared, indicating that V_2O_5 was formed. This adds one important point to our previous discussion on advantages and disadvantages, of metal transition-aerogels as catalysts, since if they have to be regenerated by calcination their catalytic performance may not be regenerated, as has been observed at least for V_2O_5-SiO_2 aerogels.

In the case of V-mesoporous catalysts, we discussed before the possible leaching of V during the reaction and the homogeneous catalyzed reaction by the dissolved vanadium. This effect has been observed[445] during the hydroxylation of 2,6-DTBP, where it was found that after the reaction was completed and the catalysts subsequently filtered, if fresh reactants were added to the filtrate it was able to react again. Furthermore the spent catalyst was calcined and then the catalytic activity disappeared. On the other hand no leaching was observed during hydroxylation of phenol, indicating that the substrate can induce the leaching of vanadium.

Hydroxylation of phenol on Ti, V, Mn, and Cr in MCM-41 and HMS has also been attempted, and it was shown that metal-MCM-41 materials are more active than Metal-HMS, except for the chromium-containing samples where the reverse was true. Unfortunately it was not checked in this paper if leaching of any of the metals had occurred during the reaction.

Tin-substituted mesoporous silica molecular sieves have been synthesized with cationic[446] or neutral surfactants.[447] The former material was used to hydroxylate phenol and 1-naphthol and gave much higher activity and selectivity than MCM-41 impregnated with Sn, indicating that during the synthesis the Sn^{4+} active centers were probably incorporated in the lattice of the MCM-41 structure.

Biodegradable lactic acid polymers in the form of semicrystalline (poly-L-lactic acid (PLA)), can be prepared by polymerization of the monomer in the presence of tin(II) salts. However, since the homogeneous catalysts remains occluded in the polymer and this is to be used in biochemical fields, it can give potential toxicological problems due to the presence of the transition metal. Thus, tin-substituted mesoporous silica molecular sieve (Sn-HMS), synthesized using a neutral surfactant, has been used as a heterogeneous catalyst for lactide ring-opening polymerization.[447] The results obtained from the point of view of conversion and product characteristics (reasonably high molecular mass and low polydispersity) look very promising. In this case it appears that the role played by the ordered mesoporous structure lies in improving the average molecular mass and polydispersity in comparison to homogeneous catalysts, by imposing steric constraints on the propagating PLA chains and minimizing "back biting" and the intermolecular transesterification reaction. This outstanding work opens up new possibilities for carrying out other selective ring-opening reactions.

It is known that large cations such as Zr, Mo, and W are active and selective oxidation catalysts in homogeneous systems. Attempts to heterogenize such catalysts by preparing zeolites containing, for instance, Zr gave poor results.[448,449] This is not surprising taking into account the strains on the crystalline framework when the introduction of a large cation such as Zr is intended. On the other hand, Tuel et al.[450,451] have made use of the amorphous character of the mesoporous ordered silicas

which can allow larger cations to be introduced, and have prepared zirconium-containing ordered mesoporous silicas (Zr-MS) which are active and selective for oxidation of a large variety of substrates such as aniline cyclohexane norbonylene, and 2,6-DTBP using both H_2O_2 and *tert*-butyl hydroperoxide. In the case of epoxidation reactions, the selectivity of Zr-MS to the epoxide was always lower than over Ti-MS. We think that the lost selectivity toward the epoxide can be due to the strong Lewis acidity of the Zr^{4+}.

Concerning the redox activity of transition metal-substituted ordered mesoporous solids, we can conclude that they represent a very useful and versatile extension of the redox zeolites. Indeed, zeolites and even AlPOs are limited, due to structural strains, on the size of transition metal which can be introduced. This limitation does not occur, at least to the same extent, in the case of the ordered silica mesopores. It is however a pity that in transition metal-containing mesoporous catalysts the activity and selectivity strongly decrease when increasing the level of the metal. For instance in the case of Ti-MCM-41, the turnover number strongly decreases upon increasing the Ti content in the material. In other words, the conversion during olefin epoxidation increases first with the number of titanium atoms incorporated until reaching a maximum at ~2.0 wt % and then decreases. It appears then that new synthesis procedures have to be developed which allow us to increase the level of active metal on the catalyst. There is another aspect which has been surprisingly neglected and this is the influence of the pore diameter on activity and selectivity of transition metal substituted ordered mesoporous silicas. There is no doubt that even though the substrates studied up to now are smaller than ~3.5 nm, in the case of liquid-phase processes, effectiviness factors lower than one still may exist for molecules with sizes above 1.2 nm.

Finally, we know now that metal leaching strongly depends on the nature of the substrate, solvent-oxidizing agent, and reaction conditions. Care should be taken in testing these materials, and one should check that homogeneous reactions due to leaching of the metal does not occur under each particular set of reaction conditions.

E. Ordered Mesopores as Support

The high surface area of the ordered mesopores together with the presence of groups able to be functionalized have been of great use to support metal oxides and organometalic compounds achieving very high dispersions of the active phase. In this section we will present an overview of the work done to date in this area and discuss future opportunities.

1. Supporting Acids and Bases

It was seen before that the acidity of ordered mesoporous aluminosilicates was mild and, therefore, unable to catalyze reactions demanding strong acid sites. This limitation could be partially overcome using the mesoporous materials as a support for strong acids such as heteropolyacids. Indeed, it has been published that heteropolyacids could be supported on alumina, silica, and carbon, and the resultant materials were active catalyst for reactions such as paraffin isomerization and isobutane/butene alkylation, which require strong acid sites.[1] It was found that supports with basic character such as Al_2O_3 were not appropriate and neutral or mildly acidic supports such as carbon or silica were required. Taking this into account, it was a logical step to make use of the high surface area of pure silica MCM-41 as a support for heteropolyacids (HPA).[452] This was also done by Kozheunikov et al.[453] by supporting $H_3PW_{12}O_{40}$ (PW) on a mesoporous pure silica MCM-41. In this case the HPA retained the Keggin structure on the MCM-41 surface and formed finally dispersed HPA species, without formation of HPA crystals even at HPA loadings as high as 50 wt %. The most remarkable claim is that even with those high HPA contents the resultant materials presented uniformly sized mesopores of ~3.0 nm diameter. This is most surprising considering that the starting MCM-41 used has pores of 3.2 nm and since at HPA contents of 50 wt % the maximum dispersion possible would be close to a monolayer, and hence it would be difficult to obtain pores of 3.0 nm in the resultant material. The textural characterization of the samples (Table 26) clearly shows that the surface area strongly decreased, indicating that some pores are blocked by the HPA, and therefore there is not a uniform distribution of the acid on the surface. Nevertheless the resultant material was quite active as a catalyst, and in any case more active than the bulk HPA and even H_2SO_4 for the liquid phase alkylation of 4-*tert*-butylphenol with isobutene (Table 27):

Table 26. Surface and Porosity of PW/MCM-41

sample	T_{max}[a] (°C)	S_{BET} (m^2/g)	*d* (Å)	V_p (mL/g)
MCM-41	300	1200	32	0.95
20 wt % PW/MCM-41	250	970	30	0.65
40 wt % PW/MCM-41	250	580	30	0.38

[a] Pretreatment temperature.

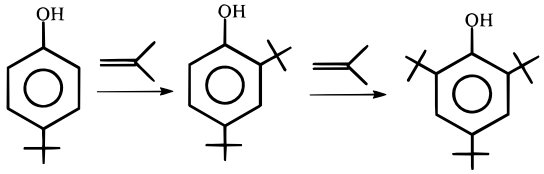

In a second and also interesting report from the same group[454] it was proposed that at lower loadings of HPA (<30 wt %) the predominant species was not the Keggin structure but probably a $H_6P_2W_{18}O_{62}$ species which turned out to be eight times more active catalytically than the Keggin structure, which became the predominant species at higher loading (>30 wt %). However when the impregnation was carried out with a methanol solution of HPA, the Keggin structure was the only observed species in the whole range of HPA loading.

In a similar way to PW heteropolyacids, SiW_{12} heteropolyacids have also been supported on pure silica and aluminosilicate MCM-41. It was also found that SiW_{12} retains the Keggin structure on the mesoporous solids and no HPA crystal phase was developed even when SiW_{12} loadings were as high as 50 wt %. The resultant catalyst was active in the

Table 27. Alkylation of TBP with Isobutene in Benzene (70 °C, TBP/C_6H_6 50/50 wt/wt)

catalyst[a]	amount (wt %)[b]	$\tau_{1/2}$ (min)[c]	selectivity (mol %)[d] DTBP	TTB
97% H_2SO_4	2.5	21	46	54
amberlyst-15	5.0	41	57	43
PW	2.5	15	89	11
20% PW/MCM-41	2.5	20	86	14
40% PW/MCM-41	2.5	11	87	13
50% PW/MCM-41	2.5	8	91	9
20% PW/SiO_2[e]	2.5	20	89	11
20% PW/SiO_2-Al_2O_3[f]	5.0	125	87	13

[a] All the PW catalysts were prepared by impregnation, dried at room temperature in vacuum, and stored over P_2O_5. [b] The percentage of the catalyst based on the total amount of the reaction mixture. [c] The half-time of the TBP conversion. [d] The selectivity based on TBP at 95% TBP conversion, 0.5−1 h. [e] As a carrier Aerosil 380 (Degussa AG) was used. [f] As a carrier an amorphous aluminosilicate LA-SHPV 708 (AKZO) with S_{BET} 539 m^2/g and Si/Al 20 was used.

esterification of acetic acid by 1-butanol in a fixed-bed reactor system. It was interesting to observe that some of HPA was leached during the reaction, with the precise amount leached being lower when the calcination temperature was higher and the lower the loading of HPA.

In our opinion there are two aspects which need to be worked on further in the area of MCM-supported HPA. The first one is achieving a really good dispersion, making available use of all the MCM-41 surface. If this is achieved the predominant species formed, even for higher loading, should be the most active $H_6P_2W_{18}O_{62}$. The second one is that supported heteropolyacids will have a high tendency to leach when polar molecules are used as reactants. However, the supported HPA, if properly attached to the surface should be quite useful when nonpolar molecules are required to react. These two points have been considered in a recent study from our laboratory,[455] in which we have used two MCM-41 materials with different pore sizes to support various amounts of $H_3PW_{12}O_{40}$. The results clearly show that a better dispersion is obtained when MCM-41 with pores with larger diameters are used, and this is positively reflected in the catalytic alkylation of isobutene/butene.

With respect to supported base catalysts, it was shown previously that it was possible to obtain strong basic catalysts by generating highly disperse crystallites of Cs_2O on the surface of MCM-41. This type of catalysts, while they can be active for catalyzing reactions demanding very strong (superbase) base sites, obviously have the inconveniences that they should be prepared and must operate in conditions where no CO_2 and H_2O are present. There is however the possibility of catalyzing a large number of less demanding reactions by using amines with different basicities. Following the tendency of heterogenizing homogeneous catalysts one may think to anchor the amines to the surface of MCM-41 by means of the silanol groups. The techniques for doing this are well known since chromatographic phases are prepared in this way. Very recently Brunel et al.[456,457] have anchored primary and secondary amines to the surface of pure silica MCM-41, and the resultant materials were found to be active and selective for carrying out Knoevenagel condensation reactions, as well as for the preparation of monoglycerids starting from 2,3-epoxy alcohols and fatty acids.[458]

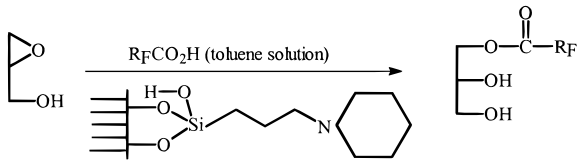

This last reaction represents an alternative to the production of monoglycerides by transesterification of triglycerides with glycerol.

2. Supporting Metals and Oxides

There is a large quantity of accumulated knowledge on supporting metals on carriers, such as Al_2O_3, SiO_2, carbon, and zeolites, among others, and on achieving high metal dispersions. The very high surfaces of ordered mesoporous materials offer new possibilities for obtaining highly dispersed noble metal catalysts. In this respect, Schuth et al.[459] have studied not only more conventional methods such as incipient wetness and ion exchange for incorporation of Pt on MCM-41, but also the direct introduction of Pt during the synthesis of MCM-41. High Pt contents (up to 80% of incorporation) were achieved using the direct incorporation of Pt via the synthesis gel, while small Pt crystallites (40−60 nm) were obtained. A neutral Pt precursor [$Pt(NH_3)_2Cl_2$] results in the formation of the smallest particles. This observation has been explained by Schüth et al.[459] by assuming that during the synthesis, the neutral complex is located in the hydrophobic part of the composite and the individual Pt species are fairly well separated. When the template is removed by calcination, only the Pt particles within one pore coalesce to form a crystallite. This gives a very regular crystal size distribution around 4.0 nm.

Metal dispersion by incipient wetness impregnation or ion exchange gives larger crystallites, with a bimodal distribution of 2 and 20 nm in the former case. While all catalysts were highly active for the oxidation of CO with air the samples prepared by incipient wetness and which have particles of 2 nm were the most active.

The dispersion of Pt by ion exchange from [$Pt(NH_3)$]$^{2+}$ on Al-MCM-41 was improved by using the same exchange, calcination, and reduction methodology used before in the case of Pt/zeolites.[460] Lower calcination temperatures than those used before produced Pt crystallites of 10 nm for 2 wt % loadings of Pt. Thus, highly dispersed Pt/MCM-41 and Pd/Al-MCM-41 catalysts show good catalytic performance for the hydrogenation of benzene, naphthalene, phenantrene, and olefins as well as for hydrocracking of 1,3,5-triisopropylbenzene.[461−463]

The greatest challenge for Pt-supported catalysts is the deep hydrogenation of aromatics in the presence of sulfur compounds. This comes from the fact that future diesel fuels will soon have to meet 50 ppm of sulfur with a cetane number above 40. Then to improve the cetane number of some diesel streams, for instance those from FCC, the aromatics present will have to be hydrogenated. Thermodynamically, hydrogenation is favored at low temperatures and

therefore highly active hydrogenation catalysts as is the case of noble metals would be the most desirable. However, it is well known that noble metals are easily poisoned by sulfur-containing compounds, and some diesel streams can contain up to 2000 ppm of sulfur, while the amount present in the diesel pool is of the order of 200 ppm. Taking this into account, we have studied the possibilities of Pt/MCM-41 catalysts for the hydrogenation of aromatics in the presence of different sulfur levels.[464] In this work, Pt was highly dispersed on ordered (MCM-41) and disordered (MSA) mesoporous solids, and Pt dispersions close to 85% were achieved. A high hydrogenation activity of Pt/MCM-41 was observed when using naphthalene as a model reactant, as well as when employing a light cycle oil refinery stream as the feed. The sulfur resistance (200 ppm) of the Pt on MCM-41 was higher than on other supports such as Al_2O_3 or amorphous silica-alumina, and it is similar to that obtained with Pt on USY zeolites which are well-known sulfur-resistent catalysts.[465,466]

Palladium-titania aerogels with pores in the meso- and macroporous region have been synthesized by the sol-gel-aerogel route.[467] In this case the Pd (crystalline size in the 2−200 nm range) was more active that Pd supported on TiO_2 in the liquid phase hydrogenation of 4-methylbenzaldehyde.

There is one type of supported metal catalyst in which the support can play an important role. This is the ethylene and propylene dimerization on nickel- and chromium-containing catalysts, and more generally oligomerization of α-olefin catalysts containing a VIB metal. MCM-41 has been used as support for the preparation of such a catalyst with preference given to chromium.[386,387] In the case of ethylene dimerization on Ni M41S[468] it was found that the reaction occurs at 70 °C in Ni/MCM-41 and Ni/Al-MCM-41. The active species was Ni(I) and this is probably better stabilized on AlMCM-41. Therefore the formation of *n*-butenes increases with the incorporation of Al into the walls of the MCM-41 structure.[469,470]

In an analogous way to zeolites that have shown great ability as catalysts for the selective catalytic reduction (SCR) of NO_x, the emissions of NO_x to the atmosphere are reduced by treatment of gases containing the above contaminant with a reducing agent such as ammonia in the presence of a catalyst containing a transition metal on MCM-41.[471] A lean NO_x catalyst containing Fe and Pd on a modified MCM-41 allows the control of NO_x, CO, and hydrocarbon emissions generated by oxygen-rich combustion processes. Also, V_2O_5-TiO_2 supported on MCM-41 is an active catalyst for the selective reduction of NO_x using NH_3 as the reduction reagent.

3. Supporting Active Species for Selective Oxidation

The high surface of ordered mesopores, containing silanol groups has been used to inmobilize redox functions following two different techniques. One of them consists on grafting organometallic complexes onto the inner walls of mesoporous MCM-41, while the other involves the functionalization of silanols with silanes, followed by the anchoring of the transition metal complexes to the surface.

With reference to the first technique, the pioneering work involved the grafting of a titanocene complex on the walls of MCM-41 resulted in a material with well dispersed high surface concentration of Ti-containing active sites.[472] This high dispersion was achieved by an elegant procedure which involved the diffusion of a chloroform titanocene dichloride solution into the pores of MCM-41. At that point the surface silanols were activated with triethylamine and grafting occurred. A thorough characterization by X-ray absorption spectroscopy revealed that after calcination the Ti was tetrahedrally coordinated and when exposed to moisture become octahedral.

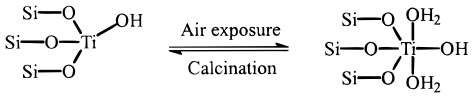

The resultant Ti-grafted material was active for the selective epoxidation of cyclohexene and pinene using *tert*-butyl hydroperoxide (TBHP) as oxidant. When the turnovers are compared with Ti-MCM-41 also using TBHP as oxidant the activities were similar. The Ti-grafted catalyst was deactivated after 90 min of reaction, but it could be regenerated by calcination.

Another grafting procedure used gaseous $Mn_2(CO)_{10}$ which reacts with the silanol groups and leads to a high concentration of manganese-oxygen species on MCM-41. These materials are much more active for catalytic oxidations such as propene combustion than those of bulk manganese oxides.[473]

The silanols of the MCM-48 have been treated with a vanadium alkoxide solution under an inert atmosphere yielding pseudotetrahedral $O_{32}V{=}O$ centers immobilized on the walls of the mesoporous material most probably grafted by three Si−O−V bridges[474] as proposed from various physicochemical techniques (UV−vis, ^{51}V NMR, XRD). Unfortunately, the catalytic performance of the resultant material was not reported.

Transition metal complexes have also been immobilized on MCM-41 by anchoring one of the ligands to the silanol groups of the walls. Following this methodology, Balkus et al.[475,476] have functionalized the surface of MCM-41 with silanes to yield surface-bound chelate ligands that include ethylenediamine (ED), diethylenetriamine (DET), and ethylenediaminetetraacetic acid salts (EDTA). Then, the anchored ligands were used for the preparation of Co(II) complexes covalently bound to MCM-41. These materials have potential use as oxygen carriers and furthermore in catalysis. A $M_3SnMo(CO)_3(\eta\text{-}C_5\text{-}H_5)$ tin−molybdenum complex has also been encapsulated in MCM-41 silicate.[477] Another type of complex manganese(III) Shiff-base are active and selective homogeneous catalysts for the epoxidation of olefins in the presence of an oxygen donor, such as NaOCl, H_2O_2, or PhIO.[478,479] It would be then of interest to attach these complexes covalently to the walls of a solid with high surface area and pores with well-defined sizes such as MCM-41. This was recently performed[480] (see scheme) by functionalizing first the surface of the MCM-41 with (3-chloropropyl)triethoxysilane, and treating the resultant with an excess of 3-[*N*,*N*′-bis-3,3-(3,5-di-*tert*-butylsalicylidenamino)propyl]amine (t-slapr). The introduction of metal atoms was achieved by reacting surface t-salpr ligands with $Mn^{II}(acac)_2$, and then by oxidizing the resultant complex to yield Mn^{III}. The anchored complex was

well characterized by UV−vis diffuse reflectance spectroscopy, and the complex before and after complexation showed similar bands, confirming that its integrity was maintained.

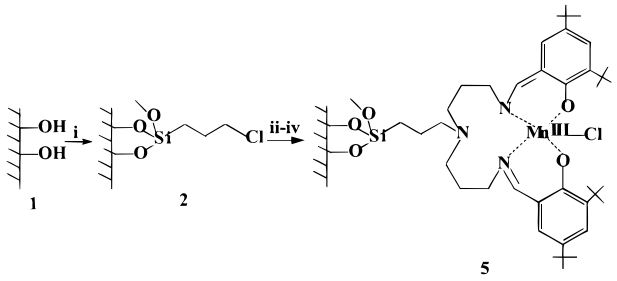

1 2 5

While no catalytic results were given in this work, it is obvious that such a synthetic achievement opens up the possibility of carrying out enantioselective epoxidation of olefins. The reports on enantioselective reactions carried out by anchored complexes are scarce, and only recently it was shown that Rh complexes with a chiral ligand covalently bound to a modified USY zeolite were able to achieve very high enantioselective excesses (>98%) during the hydrogenation of (*Z*)-*N*-acylaminocinnamate derivatives.[481] From the standpoint of enantioselective epoxidation, a salen Mn complex with a chiral ligand prepared by a "ship in a bottle" approach in a Y zeolite has proved to be able to epoxidize enantioselectively a variety of olefins using NaOCl as oxygen donor.[482]

All these results show the real possibilites of obtaining heterogeneized enantioselective catalysts on ordered mesoporous materials. The combination of the properties of the mesoporous materials with the stability of the covalently bonded complexes can offer new possibilities to permit enantioselective reactions without being limited by diffusional problems.

While complexes such as metalloporphyrin can also be attached to MCM-41 via ionic exchange,[483] one has to be careful in this case when using them as catalysts due to the relative ease with which leaching may occur under reaction conditions.

An interesting report employing silica MCM-41 as an entrapping catalyst has been recently reported.[484] In this case the entrapped molecules were not transition metal complexes, but enzymes such as cytochrome *c*, papain, and trypsin. They were entrapped by physical adsorption and consequently the amount and retention strongly depends on enzyme size. The entrapped trypsin enzyme was active for the hydrolysis of *N*-α-benzoyl-DL-arginine-4-nitroaniline.

This work clearly shows that if the pore sizes of the structured silicas could be enlarged to a high limit in the mesoporous region some enzymes that are now immobilized on other supports could also be immobilized through covalent bonding in this type of pore structured materials offering further new possibilities for these systems. However one has to be aware that achieving such high porosities, while keeping the materials stable is not a simple task.

V. Conclusions and Perspectives

In going from microporous zeolites to mesoporous materials one can go through pillared layered materials which have pores in the high limit of microporosity, together with mesopores formed by the arrangement of the layers.

It is possible today to prepare these pillared materials with different interlayer distances and with different layer and pillar compositions. These materials are of great interest in host−guest chemistry. More specifically, in the case of catalysis they are of interest in acid and redox catalysis. Further work is needed to produce materials containing stronger Brønsted sites in the pillars. Finally, new pillared materials in which the layers have a well-defined microporous network will be of much interest. They will not only combine three well-defined porosities in the range of 3.0−6.0, nm (mesopores formed by the ordering of layers), 1.2 nm (corresponding to the galleries between pillars), and 0.4−0.7 nm (pores in the potential microporous layer), but also will improve the stability of the resultant materials. Some steps are being given along this direction as it shown from the synthesis of MCM-36 structures.

When coming into the true mesoporous molecular sieves, the introduction of M41S type materials has opened a very complete new field for preparing materials. We have seen that they are promising catalysts from the point of view of acid, base, and redox catalysis, as well as supports of active phases. Despite the enormous activity developed by researchers in the last five years, there are still some aspects which deserve further and deeper work. Besides an even better knowledge of the mechanism of formation, it would be highly desirable to produce highly thermally and hydrothermally stable materials. Possible research directions include achieving a better polymerization in the walls with fewer connectivity defects and increasing the size of the walls. This certainly will imply further work on the aging synthesis variables as well as on the postsynthesis treatments (maturing, drying, and calcination). In principle, the larger the diameter of the walls is the higher should be the stability, provided that a good polymerization has occurred. Nevertheless, one should take into account that larger walls will preclude a larger number of framework atoms which will not be accessible to reactants. A strong improvement in stability could be obtained if one could make the walls crystalline. If this could be achieved one can dream of producing materials not only more stable and with stronger acidities than the current MCM-41 but also having in the same structure a combination of well-defined micro- and mesopores.

In the case of redox catalysts, while good selective oxidation Ti catalysts have been obtained, there are still several questions to be answered. The first one concerns the impossibility of introducing larger amounts of Ti in the framework without negatively and strongly affecting the activity per Ti site. In this respect one should not forget that when increasing the Ti content a part of the incorporated Ti will be in the walls and, even if it is in the correct coordination, will not cooperate to the final activity since will not be accessible to the reactants. Secondly, a systematic study on the influence of the hydrophobic−hydrophilic properties of the material and the nature of the solvent on the catalytic properties of redox materials is still lacking.

We have seen the importance of the adsorption and diffusion of reactants and products in micro- and mesoporous catalysts on their activity and decay, especially when working in liquid phase, this being particularly important in the field of fine chemicals. It is then remarkable that no studies on the influence of the pore size of MCM-41 have been reported. Along with these lines, it appears very desirable from a diffusional and catalytic point of view to have mesoporous materials with a tridirectional network of pores. While this is barely achieved in variations of MCM-41, it appears (at least theoretically) that MCM-48 can have a tridirectional pore network. It is then surprising the little amount of catalytic work done on MCM-48. This is probably due to the higher difficulty in synthesizing good MCM-48 samples, compared with the much easier synthesized MCM-41. It can be expected that when the synthesis methods for preparing MCM-48 will improve, its interest in catalysis will increase.

It will be of much interest in catalysis to prepare good mesoporous alumina with different pore size, since in this case a high dispersion of Pt, Pd, Pt-Re, and Ni-Mo could be achieved and this could generate new and extremely active hydrogenation, re-forming, and HDS catalysts.

The fact that one can prepare ordered mesoporous materials with pores up to 100 Å gives further possibilities for anchoring transition-metal complexes for carrying out the variety of catalysis that these complexes can give. If on top of that we use those with chiral ligands or chiral assistants, we will be able to carry out enantioselective reactions on heterogeneized catalysts.

From the point of view of the materials discussed, we are in the beginning of an exciting time for those working on materials chemistry and catalysis, and now (more than ever) is time to set our imagination free.

VI. Acknowledgments

The author thanks the financial support of the CICYT, project MAT-97-1016-C02-01.

VII. References

(1) Corma, A. *Chem. Rev.* **1995**, *95*, 559−614.
(2) Mirodatos, C.; Barthomeuf, D. *J. Catal.* **1985**, *93*, 246.
(3) Zicovich-Wilson, C. M.; Corma, A.; Viruela, P. *J. Phys. Chem.* **1994**, *98*, 10863−10870.
(4) Meier, W. M.; Olson, D. H. *Atlas of Zeolite Structure Types*, 3rd Revised ed.; Butterworth-Heinemann: Boston, 1992.
(5) Wilson, S. T.; Lok, B. M.; Flanigen, E. M. U.S. Patent 4,310,440, 1982.
(6) Dessau, R. M.; Schlenker, J. L.; Aiggins, J. B. *Zeolites* **1990**, *10*, 522.
(7) Richardson, J. W., Jr.; Vogt, E. T. C. *Zeolites* **1992**, *12*, 13.
(8) Davies, M. E.; Saldarriaga, C.; Montes, C.; Garcés, J.; Crowder, C. *Nature* **1988**, *331*, 698.
(9) Davies, M. E.; Montes, C.; Garcés, J. M. *ACS Symp. Ser.* **1989**, *398*, 291.
(10) Esterman, M.; McCuster, L. B.; Baerlocher, Ch.; Merrouche, A.; Kessler, H. *Nature* **1991**, *352*, 320.
(11) Merrouche, A.; Patarín, J.; Kessler, H.; Soulard, M.; Delmotze, L.; Guth, J.L.; Jolly, J. F. *Zeolites* **1992**, *12*, 226.
(12) Guth, J. L.; Kessler, H.; Caullet, P.; Hazm, J.; Mewouche, A.; Patarín, J. *Proc. IX th Int. Zeolite Conference*; R. von Ballmoos, et al., Eds.; 1993; p 215
(13) Jones, R. H.; Thomas, J. M.; Chen, J.; Xu, R.; Huo, Q.; Li, S.; Ma, Z.; Chippindale, A. M. *J. Solid State Chem.* **1993**, *102*, 5605.
(14) Huo, Q.; Xu, R.; Li, S.; Ma, Z.; Thomas, J. M.; Jones, R. H.; Chippindale, A.M. *J. Chem. Soc., Chem. Commun.* **1992**, 875.
(15) Freyhardt, C. C.; Tsapatsis, M.; Lobo, R. F.; Balkus, K. J., Jr.; Davies, M. E. *Nature* **1996**, *381*, 295.
(16) Balkus, K. J., Jr.; Gabrielov, A. G.; Sandler, N. *Mater. Res. Soc. Symp. Proc.* **1995**, *368*, 369.
(17) Moore, P. B.; Shen, J. *Nature* **1983**, *306*, 356.
(18) Cartlidge, S.; Nissen, H. U.; Wessicken, R. *Zeolites* **1989**, *9*, 346.
(19) Beyerlain, R. A.; Choi-Feng, C.; Hall, J. B.; Huggins, B. J.; Ray, G. J. *ACS Symp. Series* **1994**, *571*, 81.
(20) Corma, A. *Stud. Surf. Sci. Catal.* **1989**, *49*, 49.
(21) Aracil, J.; Martínez, M.; Sánchez, N.; Corma, A. *Zeolites* **1992**, *12*, 233.
(22) Pinnavaia, T. J.; Kim, H. NATO ASI Series; Kluwer Academic Publishers: Dordrecht, 1992; Vol. 352, p 79.
(23) Pinnavaia, T. J.; Kwanrand, T.; Yun, S. K. NATO ASI Series; Kluwer Academic Publishers: Dordrecht, 1992; Vol. 352, p 91.
(24) *Pillared Layer Structures*; Mitchell, I. V., Ed.; Elsevier: New York, 1990.
(25) Buch, R. *Catal. Today* **1988**, *2*, 1.
(26) *Multifunctional Mesoporous Inorganic Solids*; NATO ASI Series; Kluwer Academic Publishers: Dordrecht, 1993; Vol. 400, p 19.
(27) Grange, P. *J. Chem. Phys.* **1990**, *87*, 1547.
(28) Clearfield, A.; Kuchenmeister, A. *ACS Symp. Ser.* **1992**, *499*, 128.
(29) Barrer, R. M.; McCleod, D. M. *Trans. Faraday Soc.* **1954**, *50*, 980.
(30) Brindley, G. W.; Sempels, R. E. *Clay Miner.* **1977**, *12*, 299.
(31) Vaughan, D. E.; Lussier, R. J.; Magee, J. S. U.S. Patent 4,176,090, 1979.
(32) Casci, J. L. *Stud. Surf. Sci. Catal.* **1994**, *85*, 329.
(33) Vaughan D. E. *Catal. Today* **1988**, *187*, 2
(34) Clearfield, A. *Multifunctional Mesoporous Inorganic Solids*; NATO ASI Series; Kluwer Academic Publishers: Dordrecht, 1993; Vol. 400, p 169.
(35) Clearfield, A.; Tindwa, R. M. *Inorg. Nucl. Chem. Lett.* **1979**, *15*, 251.
(36) Clearfield, A. *Comments Inorg. Chem.* **1990**, *10*, 89.
(37) Alberti, C.; Constantino, U. In *Inclusion Compounds*; Atwood, J. L., Davies, J. E. D., MacNicol, D. D., Eds.; Oxford University Press: Oxford, 1991; Vol. 5, p 132.
(38) Clearfield, A.; Roberts, B. D. *Inorg. Chem.* **1988**, *27*, 3237.
(39) Burwell, D. A.; Thompson, M. E. *Chem. Mater.* **1991**, *3*, 730.
(40) Rosenthal, G. L.; Coruso, J. *Inorg. Chem.* **1992**, *31*, 3104.
(41) Reichle, W. T. *Chemtech* **1986**, 58.
(42) Clearfield, A. *Chem. Rev.* **1988**, *88*, 125.
(43) Kwon, T.; Pinnavaia, T. J. *Chem. Mater.* **1989**, *1*, 381.
(44) Baker, L. C. W.; Figgs, J. S. *J. Am. Chem. Soc.* **1970**, *92*, 3794.
(45) Bradley, S. M.; Kydd, R. A. *Catal. Lett.* **1991**, *8*, 185.
(46) Coelho, A. V.; Poncelet, G. *Appl. Catal.* **1991**, *77*, 303.
(47) Gonzalez, F.; Pesquera, C.; Blanco; Benito, I.; Mendioroz, S. *Inorg. Chem.* **1992**, *31*, 727.
(48) Pesquera, C.; Gonzalez, F.; Hernando, M. J.; Blanco, C.; Benito, I. *React. Kinet. Catal. Lett.* **1995**, *55*, 267.
(49) McCauley, J. R. U.S. Patent 5,202,295, 1993.
(50) Guann, J.; Min, E.; Yu, Z. Proc. 9th Int. Conf. Catal. Calgary 1988, 104.
(51) Ocelli, M. L.; Dominguez, J. M.; Eckert, H. *J. Catal.* **1993**, *141*, 510.
(52) Wu, J.; Rakievicz, E. F.; Gatte, R. R. *Advances in porous materials; Mater. Res. Proc.*; Kiomarneni, S., Smith, D. M., Beck, J. S., Eds.; Materials Research Society: Pittsburgh, PA, 1995; Vol. 371, p 181.
(53) Vaughan, J. S.; O'Connor, C. T.; Fletcher, J. C. *J. Catal.* **1994**, *147*, 441.
(54) Vaughan, D. E. U.S. Patent 5,326,734, 1994.
(55) Occelli, M. L.; Tindawa, R. M. *Clays Clay Miner.* **1983**, *31*, 22.
(56) Tichit, D.; Fajula, F.; Figueras, F.; Bousquet, J.; Gueguen, C. In *Catalysis by acids and bases*; Imelik, B., Ed.; Elsevier: Amsterdam, 1985; p 351.
(57) Poncelet, G.; Schultz, A. In *Chemical Reactions in Organic and Inorganic Constrained systems; Setton, R., Ed.; 1986; p 165.*
(58) Chevalier, S.; Franck, R.; Suquet, H.; Lombert J. F.; Barthomeuf, D. *J. Chem. Soc., Faraday Trans.* **1994**, *90*, 667.
(59) Ming-Yuan, H.; Zhonghui, L.; Enze, M. *Catal. Today* **1988**, *2*, 321.
(60) Ghenciu, A.; Farcasiu, D. *J. Mol. Catal. A: Chem.* **1996**, *109*, 273.
(61) Zubkov, S. A.; Kustov, L. M.; Kazansky, V. B.; Fetter, G.; Tichit, D.; Figueras, F. *Clays Clay Miner.* **1994**, *42*, 421.
(62) Swarnakar, R.; Brandt, K. B.; Kydd, R. A. *Appl. Catal. A* **1996**, *142*, 61.
(63) Moreno, S.; Kou, R. S.; Poncelet, G. *J. Catal* **1996**, *162*, 198.
(64) Bovey, J.; Jones, W. *J. Mater. Chem.* **1995**, *5*, 2027.
(65) Mokaya, R.; Jones, W. *J. Catal.* **1995**, *153*, 76.
(66) Clearfield A.; Aly, H. H.; Serrette, G. P. D.; Shea, W. L.; Tsai, T. Y. *Stud. Surf. Sci. Catal* **1994**, *83*, 433.
(67) Gil, A.; Guin, G.; Grange, P.; Montes, M. *J. Phys. Chem.* **1995**, *99*, 301.
(68) Fetter, G.; Tichit, D.; Denenorval, L. C.; Figueras, F. *Appl. Catal. A* **1995**, *126*, 165.
(69) Bartley, G. J. J. *Catal. Today* **1988**, *2*, 233.
(70) Bradley, S. M.; Kydd, R. A. *J. Catal.* **1993**, *141*, 239.
(71) Ohtsuka, K.; Hayashi, Y.; Suda, M. *Chem. Mater.* **1993**, *5*, 1823.

(72) Kitabayashi, S.; Shindo, T.; Ono, K.; Ohnuma, H. *Nipon Kagaku Kaishi* **1996**, *7*, 624.
(73) Jhonson, J. W.; Brody, J. F.; Soled, S. L.; Gates, W. E.; Robbins, J. L.; Marucchisoos, E. *J. Mol. Catal. A: Chem.* **1996**, *107*, 67.
(74) Auer, H.; Hofmann, H. *Appl. Catal. A* **1993**, *97*, 23.
(75) Sychev, M.; Kostoglod, N.; Vanoers, E. M., Debeer, V. H. J.; VanSanten, R. A.; Kornatowski, J.; Rozwadowski, M. *Stud. Surf. Sci. Catal.* **1995**, *94*, 39.
(76) Yamanaka, S.; Hattori, M. *Catal. Today* **1988**, *2*, 261.
(77) Baksh, M. S.; Kikkinides, E. S.; Yang, R. T. *Ind. Eng. Chem. Res.* **1992**, *31*, 2181.
(78) Kiricsi, I.; Molnar, A.; Palinko, I.; Lazar, K. *Stud. Surf. Sci. Catal.* **1995**, *95*, 63.
(79) Zurita, M. J. P.; Vitale, G.; Goldwaser, M. R.; Rojas, D.; Garcia, J. J. *J. Mol. Catal. A: Chem.* **1996**, *107*, 175.
(80) 80. Ladavos, A. K.; Trikalitis, P. N.; Pomonis, P. J. *J. Mol. Catal. A: Chem.* **1996**, *106*, 241.
(81) Sterte, J. *Clays Clay Miner.* **1986**, *34*, 658.
(82) Barnier, A.; Admala, L. F.; Grange, P. *Appl. Catal.* **1991**, *77*, 269.
(83) Yamanaka, S.; Hattori, M. *Stud. Surf. Sci. Catal.* **1991**, *60*, 89.
(84) Lin, J. T.; Jong, S. J.; Cheng, S. *Microporous Mater.* **1993**, *1*, 287.
(85) Del Castillo, H. L.; Grange, P. *Appl. Catal. A* **1993**, *103*, 23.
(86) Bahranowski, K.; Dula, R.; Komorek, J.; Romotowski, T.; Serwicka, E. M. *Stud. Surf. Sci. Catal.* **1995**, *91*, 747.
(87) Gil A.; Del Castillo, H. L.; Masson, J.; Court, J.; Grange, P. *J. Mol. Catal. A: Chem.* **1996**, *107*, 185.
(88) Takahama, K.; Kishimoto, T.; Yokoyama, M.; Hirao, S. *Nippon Kagaku Kaishi*, **1995**, *4*, 251.
(89) Jong, S. J.; Lin, J. T.; Cheng, S. *Stud. Surf. Sci. Catal.* **1994**, *83*, 33.
(90) Kiricsi, I.; Palinko, I.; Tasi, G.; Hannus, I. *Mol. Cryst. Liquid Cryst. Sci. Technol., Sect. A* **1994**, *244*, 149.
(91) Guin, G., Grange, P. *Mol. Cryst. Liquid Cryst. Sci. Technol., A* **1994**, *244*, A255.
(92) Doblin, C.; Mathews, J. F.; Turney, T. W. *Catal. Lett.* **1994**, *23*, 151.
(93) Occelli, M. L.; Ines, R. A.; Hwu, F. S. S.; Hightowr, J. W. *Appl. Catal.* **1985**, *14*, 69.
(94) Yi, H. X.; Shing, K. S.; Sahimi, M. *AIChE J.* **1995**, *41*, 456.
(95) Yi, H. X.; Shing, K. S.; Sahimi, M. *Chem. Eng. Sci.* **1996**, *51*, 3409.
(96) Vaughan, D. E. W.; Lussier, R. J. Proc. 5th Int. Conf. on Zeolite 1980, 94.
(97) Shabtai, J.; Massoth, F. E.; Takarz, M.; Tsai, G. M.; Mc Cauley, J. *Proc. Int. Congr. Catal.* **1984**, *4* (Berlin), 735.
(98) Pinnavaia, T. J.; Tzou, M. S.; London, S. D.; Raythatha, R. M. *J. Mol. Catal.* **1985**, *27*, 195.
(99) Poncelet, G.; Schultz, A. *Chemical Reactions in Organic and Inorganic Constrained Systems*; Setton, R., Ed.; Elsevier: New York, 1986; p 165.
(100) Ming-Yuan, H.; Zhonghui, L.; Enze, M. *Catal. Today* **1988**, *2*, 321.
(101) Bradley, S. M.; Kydd, R. A. *J. Catal.* **1993**, *141*, 239.
(102) Swarnakar, R.; Brandt, K. B.; Kydd, R. A. *Appl. Catal. A* **1996**, *142*, 61.
(103) Shen, Y. F.; Ko, A. N.; Grange, P. *Appl. Catal.* **1990**, *67*, 93.
(104) Hashimoto, K.; Hanada, Y.; Minami, Y.; Kera, Y. *Appl. Catal. A* **1996**, *141*, 57.
(105) Wong, S. T.; Wong, S. H.; Liu, S. B.; Cheng, S. *Stud. Surf. Sci. Catal.* **1992**, *84*, 305.
(106) Moini, A.; Brewer, T. D.; Tzou, M. S.; Landau, S. D.; Theo, B. K.; Pinnavaia, T. J. *ACS Symp. Ser.* **1989**, *415*, 455.
(107) Molina, R.; Schultz, A.; Poncelet, G. *J. Catal.* **1994**, *145*, 79.
(108) Auer, H.; Ofmann, M. *Appl. Catal. A* **1993**, *97*, 23.
(109) Zhao, D. Y.; Yang, Y. S.; Guo, X. X. *Mater. Res. Bull.* **1993**, *28*, 939.
(110) Isagulyants, G. V.; Chekin, S. S.; Vyunova, G. M.; Sterligov, O. D.; Kapustin, G. I. *Kinet. Catal.* **1993**, *34*, 257.
(111) Sterte, J. *ACS Symp. Ser.* **1990**, *437*, 104.
(112) Guan, J.; Yu, Z.; Fu, Y.; Lee, C.; Wang, X. *Prepr. Am. Chem. Soc. Div. Pet. Chem.* **1994**, *39*, 384.
(113) Kikuchi, E.; Seki, H.; Masudo, T. *Stud. Surf. Sci. Catal.* **1991**, *63*, 311.
(114) Occelli, M. L.; Finseth, D. H. *J. Catal.* **1986**, *99*, 316.
(115) Occelli, M. L.; Landau, S. D.; Pinnavaia, T. J. *J. Catal.* **1984**, *90*, 256.
(116) Chevalier, S.; Franck, R.; Lambert, J. F.; Barthomeuf, D. *Appl. Catal. A* **1994**, *110*, 153.
(117) Vaughan, D. E. W. *Catal. Today* **1988**, *2*, 187.
(118) Molina, R.; Moreno, S.; Vieira-Coelho, A.; Martens, J. A.; Jacobs, P. A.; Poncelet, G. *J. Catal.* **1994**, *148*, 304.
(119) Mendioroz, S.; Gonzalez, F.; Pesquera, C.; Benito, I.; Blanco, C.; Poncelet, G. *Stud. Surf. Sci. Catal.* **1993**, *75*, 1637.
(120) Jiang, D.; Sun, T.; Min, E.; He, M. *Proc. 9th Int. Zeolite Conf.*; Von Ballmos, R., Higgings, J. B., Tracy, M. M., Eds.; Butterworth-Heinmann: Boston, 1993; p 631.
(121) Doblin, C.; Matthews, J.; Turney, T. *Appl. Catal.* **1991**, *70*, 197.
(122) Hernando, M. J:; Pesquera, C.; Blanco, C.; Benito, I.; Gonzalez F. *Appl. Catal. A* **1996**, *141*, 175; *Chemistry Mater.* **1996**, *8*, 76.
(123) Moreno, S.; Kou, R. S.; Poncelet, G. *J. Catal.* **1996**, *162*, 198.
(124) Swarnakar, R.; Brandt, K. B.; Kydd, R. A.; *Appl. Catal. A.* **1996**, *142*, 61.
(125) Lambert, S. L. U.S. Patent 805,752, 1991.
(126) Holmgren, J. S., Gembicki, S. A.; Schoonover, M. W.; Kocal, J. A. U.S. Patent 632,244, 1990.
(127) Holmgren, J. S. U.S. Patent 5,286,368, 1994.
(128) Holmgren, J. S.; Gembicki, S. A.; Schoonover, M. W.; Kocal, J. A. U.S. Patent 5,160,032, 1992.
(129) Gruia, A. J. U.S. Patent 5,007,998, 1991.
(130) Marcilly, Ch. U.S. Patent 860,927, 1986.
(131) Occelli, M. L. U.S. Patent 5,076,907, 1991.
(132) Occelli, M. L. U.S. Patent 5,374,349, 1994.
(133) Occelli, M. L. U.S. Patent 5,023,221, 1991.
(134) Occelli, M. L. Rennard, R. J. *Catal. Today* **1988**, *2*, 309.
(135) Gembicki, J. S. U.S. Patent 5,114,895, 1992.
(136) Sarup, B.; Hommeltoft, S. I.; Sylvest-Johansen, M.; Soegaard-Andersen, P. *Catal. Solid Acids Bases* **1996**, *1*, 175.
(137) Bentham, M. F.; Gajda, G. F.; Jensen, R. H.; Zinnen, H. A. *Catal. Solid Acids Bases* **1996**, *1*, 155.
(138) Oldenberg, T.; Seefeld, V.; Parlitz, B.; Trettin, R. *Catal. Solid Bases* **1996**, *1*, 277.
(139) Krajcovic, J.; Hudec, P.; Grejtak, F. *React. Kinet. Catal. Lett.* **1995**, *54*, 87.
(140) Onaka, M. *J. Synth. Org. Chem.* **1995**, *53*, 392.
(141) Llamas, A.; Bautista, F.; Corma, A.; Martínez, C.; Pérez-Pariente, J. SP Patent 9300828, 1993.
(142) Knifton, J. F. *Appl. Catal. A* **1994**, 109, 247; Knifton, J. F. U.S. Patent 4,870,217, 1990.
(143) Groot, W. A.; Coenen, E. L. J.; Kuster, B. F. M.; Marín, G. B. 11th Int. Conf. Catal. Baltimore, **1996**.
(144) Barlow, S. J.; Bastock, T. W. *Worldwide Solid Acid process Conference*, Houston, TX, Catalyst Consultants Ed., 1993.
(145) Isagulyants, G. V.; Chekin, S. S.; Vyunova, G. M.; Sterligov, O. D.; Kapustin, G. I. *Kinet. Catal.* **1993**, *34*, 257.
(146) Moyaka, R.; Jones, W. *J. Chem. Soc., Chem. Commun.* **1994**, 929.
(147) Kokal, J. U.S. Patent 5,034,564, 1991.
(148) Min, E. *Stud. Surf. Sci. Catal.* **1994**, *83*, 443.
(149) Horio, M.; Suzuki, K.; Masuda, H.; Mori, T. *Appl. Catal.* **1991**, *72*, 109.
(150) Buruille, J. R.; Pinnavaia, T. J. In *Multifunctional Mesoporous Inorganic Solids*; Sequeira, C. A. C., Hudson, M. J., Eds.; NATO ASI Series, Kluwer Academic Publishers: Dordrecht, 1993, p 259.
(151) Gutierrez, E.; Ruiz-Hitzky, E. *Pillared Layered Structures*; Mitchell, I. V., Ed.; Elsevier: New York, 1990; p 199.
(152) Destefanis, A.; Perez, G.; Ursini, O.; Tomlinson, A. A. G. *Appl. Catal. A* **1995**, *132*, 353.
(153) Corma, A; Iborra, S; Miquel, S. Manuscript to be published.
(154) Lourvanij, K., Rorrer, G. L. *Appl. Catal. A* **1994**, *109*, 147.
(155) Weiss, A.. *Angew. Chem. Ind. Ed. Engl.* **1981**, *20*, 850.
(156) Mortland, M. M.; Berkheiser, V. *Clays Clay Miner.* **1976**, *24*, 60.
(157) Alberti, G.; Constantino, S.; Allulli, N.; Tomassini, N. *J. Inorg. Nucl. Chem.* **1978**, *40*, 1113.
(158) Maireles-Torres, P.; Jimenez-López, A.; Sanz, J.; Fierro, J. L. G. *J. Phys. Chem.* **1995**, *99*, 1491.
(159) Tomlinson, A. A. G. In *Pillared Layered Structures*; Mitchell, I. V., Ed.; Elsevier Applied Science: London, 1990; p 91.
(160) Jimenez-López, A.; Maireles-Torres, P.; Olivera-Pastor, P.; Rodriguez-Castellon, E.; Tomlinson, A. A. G. In *Multifunctional Mesoporous Inorganic Solids*; Sequeira, C. A. C., Hudson, M. J., Eds.; NATO ASI Series; Kluwer Academic Publishers: Dordrecht, 1993; p 273.
(161) Alberti, G. In *Multifunctional Mesoporous Inorganic Solids*; Sequeira, C. A. C., Hudson, M. J., Eds.; NATO ASI Series; Kluwer Academic Publishers: Dordrecht, 1993; p 179.
(162) Alberti, G.; Gasciola, M.; Constantino, U.; Vivani, R. *Adv. Mater.* **1996**, *8*, 291.
(163) Jaimez, E.; Bortun, A.; Hix, G. B.; García, J. R.; Rodriguez, J., Slade, R. C.T. *J. Chem. Soc., Dalton Trans.* **1996**, *11*, 2285.
(164) Song, Y. J.; Hui, Z.; Yang, Q. L.; Zhao, A. M. *J. Radioanal. Nucl. Chem.* **1995**, *198*, 375.
(165) Cabeza, A.; Aranda, M. A. G.; Cantero, F. M.; Lozano, D.; Martinez-Lara, M.; Bruque, S. *J. Solid. State Chem.* **1996**, *121*, 181.
(166) Maireles-Torres, P.; Olivera-Pastor, P.; Rodriguez-Castellon, E.; Jiménez-López, A.; Alagna, A.; Tomlinson, A. G. *J. Mater. Chem.* **1991**, *1*, 319.
(167) Maireles-Torres, P.; Olivera-Pastor, P.; Rodriguez-Castellon, E.; Jiménez-López, A.; Alagna, A.; Tomlinson, A. G. *J. Mater. Chem.* **1991**, *1*, 739.
(168) Maireles-Torres, P.; Olivera-Pastor, P.; Rodriguez-Castellon, E.; Jiménez-López, A.; Alagna, A.; Tomlinson, A. G. *J. Solid State Chem.* **1991**, *94*, 368.
(169) Bagnasco, G.; Ciambelli, P.; Turco, M.; La Giniesta, A., Patrono, P. *Appl. Catal.* **1991**, *68*, 69.
(170) Ramis, G.; Busca, G.; Lorenzelli, V.; La Giniesta, A.; Galli, P.; Massucci, M. A. *J. Chem. Soc., Dalton Trans.* **1988**, 881.

(171) La Ginesta, A.; Patrono, P.; Beradelli, M. L.; Galli, P.; Ferragina, C.; Massucci, M. A. *J. Catal.* **1987**, *103*, 346.
(172) Clearfield, A.; Thakur, D. S. *Appl. Catal.* **1986**, *26*, 1.
(173) Dines, M. B.; Digiacomo, P. *Inorg. Chem.* **1981**, *20*, 92.
(174) Dines, M. B.; Griffith, P. C. *J. Phys. Chem.* **1982**, *86*, 571.
(175) Clearfield, A. *Comments Inorg. Chem.* **1990**, *10*, 89.
(176) Segawa, K.; Sugiyama, A.; Kurusu, Y. *Stud. Surf. Sci. Catal.* **1991**, *60*, 73.
(177) King, D. L.; Cooper, M. D.; Sanderson, W. A.; Schramm, C. M.; Fellmann, J. D. *Stud. Surf. Sci. Catal.* **1991**, *63*, 247.
(178) Derouane, E. G.; Jullien-Lardot, V. *Surf. Sci. Catal.* **1994**, *83*, 11.
(179) Castillo, M. L.; Guil, A.; Grange, P. *Catal. Lett.* **1996**, *36*, 237.
(180) Yang, R. T.; Chen, J. P.; Kikkinides, E. S.; Cheng, L. S.; Ciechanowicz, J. E. *Ind. Eng. Chem. Res.* **1992**, *31*, 1440.
(181) Chen, J. P.; Hansladen, M. C.; Yang, R. T. *J. Catal.* **1995**, *151*, 135.
(182) Chen, J. P.; Yang, R. T. *J. Catal.* **1990**, *125*, 411.
(183) Rajadhyaksha, R. A.; Knozinger, H. *Appl. Catal.* **1989**, *51*, 81.
(184) Lamesch, A.; Del Castillo M.; Vanderwegen, P. ; Daza, L.; Jannes, G.; Grange, P. *Stud. Surf. Sci. Catal.* **1993**, *78*, 299.
(185) Choudary, B. M.; Shobha Rani, S.; Narender, N. *Catal. Lett.* **1993**, *19*, 299.
(186) Takahama.K; Sako, F.; Yokoyama, M.; Hirao, S. *Nippon Kagaku Kaishi* **1994**, *613*, 7.
(187) Volzone, C. *Clays Clay Miner.* **1995**, *43*, 377.
(188) Tzou, M. S.; Pinnavaia, T. J. *Catal. Today* **1988**, *2*, 243.
(189) Sychev, M.; de Beer, V. H. J., Van Santen, R. A.; Prihoko, R.; Goncharuk, V. *Stud. Surf. Sci. Catal.* **1994**, *84*, 267.
(190) Kiyozumi, Y.; Suzuki, K.; Shin, S.; Owaga, K.; Saito, K.; Yamanaka, S. *Jpn. Kokai Tokyo Koho* **1984**, *59-2166*, 31.
(191) Bergaya, F.; Hassoun, N.; Gatineau, L.; Barrault, J. *Stud. Surf. Sci. Catal.* **1991**, *63*, 329.
(192) Mari, D.; Barrault, J.; Zivkov, C.; Van Damme, H.; Hassoun, N. FR Patent 2,167,739, 1989.
(193) Landau, S. D.; Hinnenkamp, J. A. U.S. Patent 4,963,518, 1990.
(194) Kleinfeld, E. R.; Ferguson, G. S. *Science* **1994**, *265*, 370.
(195) Cao, G.; Hong, H. G.; Mallouk, T. E. *Acc. Chem. Res.* **1992**, *25*, 420.
(196) Miredami, B. K.; Morrison, S. R. *J. Appl. Phys.* **1990**, *67*, 1515.
(197) Smith, R. L.; Rohrer, G. S. *Advances in Porous Materials*; Komarneni, S., Smith, D. M., Beck, J. S., Eds.; Materials Research Society: Pittsburgh, PA, 1995; Vol. 371, p 187.
(198) Foley, H. C.; Kane, M. S.; Goellner, J. F. *Access in Nanoporous Materials*; Pinnavaia, T. J., Thorpe, M. F., Eds.; Plenum: New York, 1995; p 39.
(199) Mann, S.; Ozin, G. A. *Nature* **1996**, *382*, 313.
(200) Tanev, P. T.; Pinnavaia, T. J. *Science* **1996**, *271*, 1267.
(201) Landis, M. E.; Aufdembrink, B. A.; Chu, P.; Johnson, I. D.; Kirker, G. W.; Rubin, M. K. *J. Am. Chem. Soc.* **1991**, *113*, 3189.
(202) Hou, W.; Yan, Q.; Peng, B.; Fu, X. *J. Mater. Chem.* **1995**, *5*, 109.
(203) Iler, R. K. *J. Colloid Sci.* **1964**, *139*, 648.
(204) Borbely, G.; Beyer, H. K.; Karge, H. G.; Schwieger, W.; Brandt, A.; Bergk, K.H. *Clays Clay Miner.* **1991**, *39*, 490.
(205) Lagaly, G.; Beneke, K. *Colloid Polym. Sci.* **1991**, *269*, 1198.
(206) Rojo, J. M.; Ruiz-Hitzky, E.; Sanz, J.; Sarratosa, J. M. *Rev. Chim. Miner.* **1983**, *20*, 807.
(207) Dailey, J. S.; Pinnavaia, T. J. *Chem. Mater.* **1992**, *4*, 855.
(208) Kosuge, K.; Tsunashima, A. *J. Chem. Soc., Chem. Commun.* **1995**, 2427.
(209) Schreyeck, L.; Caullet, P.; Mougend, T. C.; Guth, J. L.; Marler, B. *J. Chem. Soc., Chem. Commun.* **1995**, 2187.
(210) Mitchell, T. O.; Whitehurst, D. D. U.S. Patent 4,003,825, 1977.
(211) Magee, J. S.; Daugherty, R. P. U.S. Patent 3,912,619, 1975.
(212) Vaughan, D. E. W.; Maher, P. K.; Albers, E. W. U.S. Patent 3,838,037, 1974.
(213) Manton, M. R. S.; Davidtz, J. C. *J. Catal.* **1979**, *60*, 156.
(214) Corma, A.; Pérez-Pariente, J.; Fornés, V.; Rey, F.; Rawlence, D. *Appl. Catal.* **1990**, *63*, 145.
(215) Samoson, A.; Lippmaa, E.; Engelhardt, G.; Lohse, D.; Jerschwitz, H. G. *Chem. Phys. Lett.* **1987**, *134*, 589.
(216) Bellusi, G.; Perego, C.; Carati, A.; Peratello, S.; Previde Massara, E.; Perego, G. *Stud. Surf. Sci. Catal.* **1994**, *84*, 85.
(217) Corma, A.; Martínez, A.; Pergher, S.; Peratello, S.; Perego, C.; Bellusi, G. *Appl. Catal. A* **1997**, 3687.
(218) Corma, A.; Martínez, A.; Pergher, S.; Peratello, S.; Perego, C.; Bellusi, G. Manuscript to be published.
(219) Kresge, C. T.; Leonowicz, M. E.; Roth, W. J.; Vartulli, J. C. U.S. Patent 5,098,684, 1992.
(220) Kresge, C. T.; Leonowicz, M. E.; Roth, W. J.; Vartulli, J. C.; Beck, J. S. *Nature* **1992**, *359*, 710.
(221) Beck, J. S.; Chu, C. T.; Johnson, I. D.; Kresge, C. T.; Leonowicz, M. E.; Roth, W. J.; Vartulli, J. C. U.S. Patent 5,108,725, 1992.
(222) Beck, J. S.; Calabro, D. C.; McCullen, S. B.; Pelrine, B. P.; Schmitt, K. D.; Vartulli, J. C. U.S. Patent 5,145,816, 1992.
(223) Beck, J. S.; Kresge, C. T.; Leonowicz, M. E.; Roth, W. J.; Vartulli, J. C. U.S. Patent 5,264,203, 1993.
(224) Beck, J. S.; Smith, K. D.; Vartulli, J. C. U.S. Patent 5,334,368, 1994. Beck, J. S.; Kresge, C. T.; McCullen, S. B.; Roth, W. J.; Vartulli, J. C. U.S. Patent 5,370,785, 1994.
(225) Beck, J. S.; Vartulli, J. C.; Roth, W. J.; Leonowicz, M. E.; Kresge, C. T.; Schmitt, K. D.; Chu, C. T.-W.; Olson, D. H.; Sheppard, E. W.; McCullen, S. B.; Higgins, J. B.; Schlenker, J. L. *J. Am. Chem. Soc.* **1992**, *114*, 10834.
(226) Vartulli, J. C.; Kresge, C. T.; Leonowicz, M. E.; Chu, A. S.; McCullen, S. B.; Johnson, I. D.; Sheppard, E. W. *Chem. Mater.* **1994**, *6*, 2070.
(227) Beck, J. S.; Vartulli, J. C.; Kennedy, G. J.; Kresge, C. T.; Roth, W. J.; Schramm, S. E. *Chem. Mater.* **1994**, *6*, 1816.
(228) Vartulli, J. C.; Schmitt, K. D.; Kresge, C. T.; Roth, W. J.; Leonowicz, M. E.; McCullen, S. B.; Hellring, S. D.; Beck, J. S.; Schlenker, J. L.; Olson, D. H.; Sheppard, E. W. *Stud. Surf. Sci. Catal.* **1994**, *84*, 53.
(229) Winsor, P. A. *Chem. Rev.* **1968**, *68*, 1.
(230) Ekwall, P. In *Advances in Liquid Crystals*; Brown, G. H., Ed.; Academic Press Inc.: New York, 1971; p 1.
(231) Chen, C. Y.; Burkett, S. L.; Li, H. X; Davis, M. E. *Microporous Mater.* **1993**, *2*, 27.
(232) Monnier, A.; Schüth, F.; Huo, Q.; Kumar, D.; Margolese, D.; Maxwell, R. S.; Stucky, G. D.; Krishnamurty, M.; Petroff, P.; Firouzi, A.; Janicke, M.; Chmelka, B. F. *Science* **1993**, *261*, 1299.
(233) Huo, Q.; Margolese, D. I.; Ciesla, U.; Feng, P.; Sieger, P.; Leon, R.; Petroff, P.; Schüth, F.; Stucky, G. D. *Nature* **1994**, *368*, 317.
(234) Stucky, G. D.; Monnier, A.; Schüth, F.; Huo, Q.; Margolese, D. I.; Kumar, D.; Krishnamurty, M.; Petroff, P.; Firouzi, A.; Janicke, M.; Chmelka, B. F. *Mol. Cryst. Liq. Cryst.* **1994**, *240*, 187.
(235) Ciesla, U.; Demuth, D.; León, R.; Petroff, P.; Stucky, G.; Unger, K.; Schüth, F. *J. Chem. Soc., Chem. Commun.* **1994**, 1387.
(236) Bull, L. M.; Kumar, D.; Millar, S. P.; Besier, T.; Janicke, M.; Stucky, G. D.; Chmelka, B. F. *Stud. Surf. Sci. Catal.* **1994**, *84*, 429.
(237) Firouzi, A.; Kumar, D.; Bull, L. M.; Besier, T.; Sieger, P.; Huo, Q.; Walker, S. A.; Zasadzinski, J. A.; Glinka, C.; Nicol, J.; Margolesse, D.; Stucky, G. D.; Chmelka, B. F. *Science* **1995**, *267*, 1138.
(238) Huo, Q.; León, R.; Petroff, P. M.; Stucky, G. D. *Science* **1995**, *268*, 1324.
(239) Stucky, G. D.; Huo, Q.; Firouzi, A.; Chmelka, B. F.; Schacht, S.; Voigt-Martin, I. G.; Schüth, F. *Stud. Surf. Sci. Catal.* **1997**, *105*, 3.
(240) Glinka, C. J.; Nicol, J. M.; Stucky, G. D.; Ramli, E.; Margolese, D. I.; Huo, Q. *Advances in Porous Materials; Mater. Res. Proc.* Komarneni, S., Smith, D. M., Beck, J. S., Eds.; Materials Research Society: Pittsburgh, PA, 1995, Vol. 371, p 47.
(241) Calabro, D. C.; Valyocsik, E. W.; Ryan, F. X. *Microporous Mater.* **1996**, *7*, 243.
(242) Tanev, P. T.; Pinnavaia, T. J. *Science* **1995**, *267*, 865.
(243) Bagshaw, S. A.; Prouzet, S. A.; Pinnavaia, T. J. *Science* **1995**, *269*, 1242.
(244) Attard, G. S.; Glyde, J. C.; Goltner, C. G. *Nature* **1995**, *378*, 366.
(245) Behrens, P. *Angew. Chem., Int. Ed. Engl.* **1996**, *35*, 515.
(246) Corma, A.; Khan, Q.; Rey, F. Manuscript to be published.
(247) Tanev, P. T.; Chibwe, M.; Pinnavaia, T. J. *Nature* **1994**, *368*, 321.
(248) Elder, K. J.; White, J. W. *J. Chem. Soc., Chem. Commun.* **1995**, 155.
(249) Chu, P.; Dwyer, F. G.; Vartuli, J. C. U.S. Patent 4,778,666, 1988.
(250) Lohse, U.; Bertram, R.; Jancke, K.; Kurzawski, I.; Parlitz, B.; Loeffler, E.; Schreier, E. *J. Chem. Soc., Faraday Trans.* **1995**, *91*, 1163.
(251) Girnus, I.; Jancke, R.; Vetter, R.; Richter-Mendau, J.; Caro, J. *Zeolites* **1995**, *15*, 33.
(252) Meng, X.; Xu, W.; Tang, S.; Pang, W. *Chin. Chem. Lett.* **1992**, *3*, 69.
(253) Arafat, A.; Janson, J. C.; Ebaid, A. R.; van Bekkum, H. *Zeolites* **1993**, *13*, 162.
(254) Wu, Ch.G.; Bein, Th. *J. Chem. Soc., Chem. Commun.* **1995**, 925.
(255) Ryoo, R.; Kim, J. M.; Ko, C. H.; Shin, C. H. *J. Phys. Chem.* **1996**, *100*, 17718.
(256) Ryoo, R.; Kim, J. M. *J. Chem. Soc., Chem. Commun.* **1995**, 711.
(257) Ko, Ch.H.; Ryoo, R. *J. Chem. Soc., Chem. Commun.* **1996**, 2467.
(258) Ulagappan, N.; Rao, C. N. R. *J. Chem. Soc., Chem. Commun.* **1996**, 2759.
(259) Beck, J. S. U.S. Patent 5,057,296, 1991.
(260) Khushalani, D.; Kuperman, A.; Ozin, G. A.; Tanaka, K.; Garcés, J.; Olken, M.M.; Kuperman, A. *Adv. Mater.* **1996**, *7*, 842. Corma, A.; Kan, Q.; Navarro, M. T.; Pérez-Pariente, J.; Rey, F. Manuscript to be published.
(261) Yanagisawa, T.; Shimizu, T.; Kuroda, K.; Kato, C. *Bull. Chem. Soc. Jpn.* **1990**, 63.
(262) Inagaki, S.; Fukushima, Y.; Kada, A. O.; Kuranchi, T.; Kuroda, K.; Kato, C. *9th Inter. Zeol. Conf.* Von Ballmos, et al., Ed.), Butterworth-Heinemann: Boston, 1993; p 305.
(263) Inagaki, S.; Fukushima, Y.; Kuroda, K. *Stud. Surf. Sci. Catal.* **1994**, 84, 125.
(264) Yanagisawa, T.; Shimizu, T.; Kuroda, K.; Kato, C. *Bull. Chem. Soc. Jpn.* **1990**, *63*, 1535.
(265) Ishikawa, T.; Matsuda, M.; Yasukawa, A.; Kandori, K.; Inagaki, S.; Fukushima, Y.; Kondo, S. *J. Chem. Soc. Faraday Trans.* **1996**, *92*, 1985.

(266) Chen, C. Y.; Xiao, S. Q.; Davis, M. E. *Microporous Mater.* **1995**, *4*, 1.
(267) O'Brien, S.; Francis, R. J.; Price, S. J.; O'Hare, D.; Clarck, S. M.; Okazaki, N.; Korada, K. *J. Chem. Soc., Chem. Commun.* **1995**, 2423.
(268) Kolodziejski, W; Coma, A.; Navarro, M. T.; Pérez-Pariente, J. *Solid State Nucl. Magn. Reson.* **1993**, *2*, 253.
(269) Corma, A.; Fornés, V.; Navarro, M. T.; Pérez-Pariente, J. *J. Catal.* **1994**, *148*, 569.
(270) Schmidt, R.; Junggreen, H.; Stocker, M. *J. Chem. Soc., Chem. Commun.* **1996**, 875.
(271) Schmidt, R.; Akporiaye, D.; Stöcker, M.; Ellestad, O. H. *J. Chem. Soc. Chem. Commun.* **1994**, 1493.
(272) Luan, Z.; Cheng, Ch. F.; Zhou, W.; Klinowski, J. *J. Phys Chem.* **1995**, *99*, 1018.
(273) Janicke, M.; Kumar, D.; Stucky, G. D.; Chmelka, B. F. *Stud. Surf. Sci. Catal.* **1994**, *84*, 243.
(274) Schmidt, R.; Akporiaye, D.; Stocker, M.; Ellestad, O. H. *Stud. Surf. Sci. Catal.* **1994**, *84*, 61.
(275) Borade, R. B.; Clearfield, A. *Catal. Lett.* **1995**, *31*, 267.
(276) Busio, M.; Jänchen, J.; Van Hooff, J. H. C. *Microporous Mater.* **1995**, *5*, 211.
(277) Luan, Z.; Cheng, Ch.F.; He, H.; Klinowski, J. *J. Phys Chem.* **1995**, *99*, 10590.
(278) Beck, J. S.; Vartuli, J. C. *Curr. Opinions Solid State Mater. Sci.* **1996**, *1*, 76.
(279) Perego, G.; Bellusi, G.; Corno, C.; Taramasso, M.; Buonomo, F.; Exposito, A. *Stud. Surf. Sci. Catal.* **1986**, *28*, 129.
(280) Camblor, M. A.; Corma, A.; Pérez-Pariente, J. *J. Chem. Soc., Chem. Commun.* **1993**, 557.
(281) Corma, A.; Camblor, M. A.; Esteve, P.; Martínez, A.; Pérez-Pariente, J. *J. Catal.* **1994**, *145*, 151.
(282) Corma, A.; Navarro, M. T.; Pérez-Pariente, J. *J. Chem. Soc., Chem. Commun.* **1994**, 147.
(283) Tanev, P. T.; Chibwe, M.; Pinnavaia , T. J. *Nature* **1994**, *368*, 321.
(284) T. J.; Bagshaw, S. A.; Renzo, F.; Fajula, F. *J. Chem. Soc., Chem. Commun.* **1996**, 2209.
(285) Blasco, T.; Corma, A.; Navarro, M. T.; Pérez-Pariente, J. *J. Catal.* **1995**, *156*, 65.
(286) Zhang, W.; Fröba, M.; Wang, J. ; Tanev. P. T.; Wong, J.; Pinnavaia, T. J. *J. Am. Chem. Soc.* **1996**, *118*, 9164.
(287) Zhang W.; Pinnavaia, T. J. *Catal. Lett.* **1996**, *38*, 261.
(288) Morey, M.; Davidson, A.; Stucky, G. *Microporous Mater.* **1996**, *6*, 99.
(289) Reddy, K. M.; Mondrakovski, I.; Sayari, A. *J. Chem. Soc., Chem. Commun.* **1994**, 1059.
(290) Chapus, T.; A. Tuel, A.; Ben Taarit, Y.; Naccache, C. *Zeolites* **1994**, *14*, 349.
(291) Zhao, D.; Goldfarb, D. *J. Chem. Soc., Chem. Commun.* **1995**, 875.
(292) Zhao, D.; Goldfarb, D. In *Zeolites: A refined tool for Designing Catalytic Sites*; Bonneviot, L., Kaliaguine, S., Eds.; Elsevier B.V.: Amsterdam, 1995; p 185.
(293) Marti, P. E.; Maciejewski, M.; Baixer, A. *J. Catal.* **1993**, *139*, 494.
(294) Batamack, P.; Bucsi, I.; Molnar, A.; Olah, G. A. *Catal. Lett.* **1994**, *25*, 11.
(295) Cheung, T. K.; d'Itri, J. L., Gates, B. C. *J. Catal.* **1995**, *151*, 464.
(296) Iglesia, E.; Soled, S. L.; Kramer, G. M. *J. Catal.* **1993**, *144*, 238.
(297) Hino, M.; Arata, K. *Catal. Lett.* **1995**, *30*, 25.
(298) Ciesla, U.; Demuth, D.; Leon, R.; Petroff, P.; Stucky, G.; Unger, K.; Schüth, F. *J. Chem. Soc., Chem. Commun* **1994**, 1387.
(299) Yada, M.; Machida, M.; Kijima, T. *J. Chem. Soc., Chem. Commun.* **1996**, 769.
(300) Bagshaw, S. A.; Pinnavaia, T. J. *Angew. Chem., Int. Ed. Engl.* **1996**, *35*, 1102.
(301) Vandry, F.; Khodabandeh, S.; Davis, M. E. *Chem. Mater* **1996**, *8*, 1451.
(302) Schüth, F.; Ciesla, H.; Schacht, S. *Angew. Chem.* **1996**, *35*, 541.
(303) Hudson, M. J.; Knowles, J. A. *J. Mater. Chem.* **1996**, *6*, 89.
(304) Larsen, G.; Lotero, E.; Nabity, M.; Petrovic, L. M.; Shobe, D. S. *J. Catal.* **1996**, *164*, 246.
(305) Kim, A.; Bruinsma, P.; Chen, Y.; Wang, L. Q.; Liu, J. *J. Chem. Soc., Chem. Commun.* **1997**, 161.
(306) Ulagappan, N.; Battaram, N.; Raju, U. N. Rao, C. N. R. *J. Chem. Soc., Chem. Commun.* **1996**, 2243.
(307) Antonelli, D. M.; Ying, J. Y. *Angew. Chem., Int. Ed. Engl.* **1995**, *34*, 2014.
(308) Ulagappan, N.; Rao, C. N. R. *J. Chem. Soc., Chem. Commun* **1996**, 1685.
(309) Sayari, A.; Moudrakovski, I.; Reddy, J. S. *Chem. Mater.* **1996**, *8*, 2080.
(310) Soghomoniam, V.; Chen, Q.; Haushalter, R. C.; Zubieta, J. *Angew. Chem., Int. Ed. Engl.* **1993**, *32*, 610.
(311) Matsubayashi, G.; Otha, S. *Chem. Lett.* **1990**, 787.
(312) Matsubayashi, G.; Kakajima, H. *Chem. Lett.* **1993**, 31.
(313) Doi, T.; Miyake, T. *J. Chem. Soc., Chem. Commun.* **1996**, 1635.
(314) Alfredsson, V.; Anderson, M. W. *Chem. Mater.* **1996**, *8*, 1141.
(315) Schmidt, R.; Stöcker, M.; Ellestad, O. H. *A Refined Tool for Designing Catalytic Sites*; Bonneviot, L., Kaliaguine, S., Eds.; Elsevier Science B.V.: Amsterdam, 1995; p 149.
(316) Schmidt, R.; Stöcker, M.; Akporiaye, D.; Heggelund Törstad, E.; Olsen, A. *Microporous Mater.* **1995**, *5*, 1.
(317) Ortlam, A.; Rathousky, J.; Schulz-Ekloff, G.; Zukal, A. *Microporous Mater.* **1996**, *6*, 171.
(318) Cheng, Ch. F.; He, H.; Zhou, W.; Klinowski, J. *Chem. Phys. Lett.* **1995**, *244*, 117.
(319) Feuston, B. P.; Higgings, J. B. *J. Phys. Chem.* **1994**, *98*, 4459.
(320) Zhao, X. S.; Lu, G. Q.; Millar, G. J. *Ind. Eng. Chem. Res.* **1996**, *35*, 2075.
(321) Behrens, G.; Stucky, G. D. *Angew. Chem., Int. Ed. Engl.* **1993**, *32*, 696.
(322) Chenite, A.; Le Page, Y.; Sayari, A. *Chem. Mater.* **1995**, *7*, 1015.
(323) Garcés, J. M. *Adv. Mater.* **1996**, *8*, 434.
(324) Branton, P. J.; Hall, P. G.; Sing, K. S. W. *J. Chem. Soc., Chem. Commun.* **1993**, 1257.
(325) Branton, P. J.; Hall, P. G.; Sing, K. S. W.; Reichert, H.; Schüth, F.; Unger, K. K. *J. Chem. Soc., Faraday Trans.* **1994**, *90*, 2965.
(326) Ravikovitch, P. I.; Domhnaill, S. C. O.; Neimark, A. V.; Schüth, F.; Unger, K. K. *Langmuir* **1995**, *11*, 4765.
(327) Franke, O.; Schulz-Ekloff, G.; Rathousky, J.; Starck, J.; Zukal, A. *J. Chem. Soc., Chem. Commun.* **1993**, 724.
(328) Komarneni, S.; Menon, V. C.; Pidugu, R. *J. Porous Mater.* **1996**, *3*, 115.
(329) Llewellyn, P. L.; Grillet, Y.; Schüth, F.; Reichert, H.; Unger, K. K. *Microporous Mater.* **1994**, *3*, 345.
(330) Schmidt, R.; Stöcker, M.; Hansen, E.; Akporiaye, D.; Ellestad, O. H. *Microporous Mater.* **1995**, *3*, 443.
(331) Rathousky, J.; Zukal, A.; Franke, O.; Schulz-Ekloff, G. *J. Chem. Soc., Faraday Trans.* **1995**, *91*, 937.
(332) Maddox, M. W.; Gubbins, K. E. *Proc. Int. Conf. 5th Levan*; Douglas, M., Ed.; Kluwer: Boston, 1995; p 563.
(333) Llewellyn, P. L.; Schüth, F.; Grillet, Y.; Rouquerol, F.; Unger, K. K. *Langmuir* **1995**, *11*, 574.
(334) Baker, F. S.; Sing, K. S. W. *J. Colloid Interface Sci.* **1976**, *55*, 605.
(335) Chen, C. Y.; Li, H. X.; Davis, M. E. *Microporous Mater.* **1993**, *2*, 17.
(336) Glaser, R.; Roesky, R.; Boger, T.; Eigenberger, G.; Ernst, S.; Weitkamp, J. *Stud. Surf. Sci. Catal.* **1997**, 105.
(337) Link, J.; Kaufmann, J.; Schenker, K. *Magn. Reson. Imag.* **1994**, *12*, 203.
(338) Kleinberg, R. L. *Nature* **1994**, *351*, 467.
(339) Patriba, N. S.; Schwartz, L. M.; Partha, P. M. *Magn. Reson. Imag.* **1995**, *12*, 227.
(340) Schmidt, R.; Hansen, E. W.; Stöcker, M.; Akporiaye, D.; Ellestad, O. H. *J. Am. Chem. Soc.* **1995**, *117*, 4049.
(341) Hansen, E. W.; Schmidt, R.; Stöcker, M.; Akporiaye, D. *Microporous Mater.* **1995**, *5*, 143.
(342) Meiboons, S.; Gill, D. *Rev. Sci. Instrum.* **1958**, *29*, 688.
(343) Le Doussal, P.; Sen, P. N. *Phys. Rev. B* **1992**, *46*, 3465.
(344) Leherte, L.; Andre, J. M.; Derouane, E. G.; Vercauteren, P. *Catal. Today* **1991**, *10*, 177.
(345) Sayari, A.; Moudrakovski, I.; Danumah, Ch.; Ratcliffe, Ch. I.; Ripmeester, J. A.; Preston, K. F. *J. Phys. Chem.* **1995**, *99*, 16373.
(346) Millini, R.; Perego, G. *Gazz. Chim. Ital.* **1996**, *126*, 133.
(347) Blasco, T.; Camblor, M. A.; Corma, A.; Pérez-Pariente, J. *J. Am. Chem. Soc.* **1993**, *115*, 11806.
(348) Boccuti, M. R.; Rao, K. M.; Zecchina, A.; Leofanti, G.; Petrini, G. *Structure and Reactivity of Surface*; Morterra, C., Zecchina, A., Costa, G., Eds.; Elsevier: Amsterdam, 1989; p 133.
(349) Geobaldo, E.; Bordiga, S.; Zecchina, A.; Giamelo, E.; Leofanti, G.; Petrini, G. *Catal. Lett.* **1992**, *16*, 109.
(350) Petrini, G.; Cesana, A.; De Alberti, G.; Genoni, F.; Leofanti, G.; Padovan, M.; Paparatto, G.; Rofia, P. *Stud. Surf. Sci. Catal.* **1991**, *68*, 761.
(351) Pei, S.; Zajac, G. W.; Kaduk, J. A.; Faber, J.; Boyanov, B. I.; Duck, D.; Fazzini, D.; Morrison, T. I.; Yang, D. S. *Catal. Lett.* **1993**, *21*, 333.
(352) Bordiga, S.; Boscherini, F.; Coluccia, S.; Genoni, F.; Lamberti, C.; Leofanti, G.; Marchese, L.; Petrini, G.; Vlaic, G.; Zecchina, A. *Catal. Lett.* **1994**, *26*, 195.
(353) Rao, P. R. H. P.; Kumar, R.; Ramaswamy, A. V.; Ratnasamy, P. *Zeolites* **1993**, *13*, 663.
(354) Tuel, A.; Ben Taarit, Y. *Zeolites* **1994**, *14*, 18. Sayari, A. *Mater. Res. Soc. Symp. Proc.* **1995**, *371*, 871.
(355) Reddy, S. J.; Ping, L.; Sayari, A. *Appl. Catal. A* **1996**, *148*, 7.
(356) Sayari, A. *Chem. Mater.* **1996**, *8*, 1840.
(357) Aufdembrink, B. A.; Chester, A. W.; Herbst, J. A.; Kresge, C. T. U.S. Pantent 5,258,114, 1993.
(358) Aguado, J.; Serrano, D. P.; Romero, M. D.; Escola, J. M. *J. Chem. Soc., Chem. Commun* **1996**, 725.
(359) Corma, A.; Grande, M. S.; Gonzalez-Alfaro, V.; Orchilles, A. V. *J. Catal.* **1996**, 159, 375.
(360) Wachter, W. A. U.S. Patent 5,221,648, 1993.
(361) Shipper, P. H.; Owen, H.; Herbst, J. A.; Kirker, G. W.; Huss, A., Jr.; Chu, P.; U.S. Patent 5,179,054, 1993.
(362) Roos, K.; Liepold, A.; Roschetilowski, W.; Schmidt, R.; Karlsson, A.; Stöcker, M. *Stud. Surf. Sci. Catal.* **1994**, *84*, 389.
(363) Liepold, A.; Roos, K.; Reschetilowski, W. *Chem. Eng. Sci.* **1996**, *51*, 3007.

(364) Liepold, A.; Roos, K.; Reschetilowski, W.; Esculcas, A. P.; Rocha, J.; Philippou, A.; Anderson, M. W. *J. Chem. Soc., Faraday Trans.* **1996**, *92*, 4623.
(365) Corma, A.; Rey, F. Manuscript to be published.
(366) Le, Q. N.; Thomson, R. T. U.S. Patent 5,232,580, 1993.
(367) Feng, X.; Lee, J. S.; Lee, J. W.; Lee, J. Y.; Wei, D.; Haller, G. L. *Chem. Eng. J.* **1996**, *64*, 255.
(368) Ryoo, R.; Jun, S. *J. Phys. Chem. B* **1997**, *101*, 317.
(369) Mc Cullen, S. B.; Vartuli, J. C. U.S. Patent 5,156,829, 1992.
(370) Constel, N.; Di Renzo, F.; Fajula F. *J. Chem. Soc., Chem. Commun.* **1994**, 967.
(371) Chen, C. Y.; Xiao, S. Q.; Dahmen, U. *Book of abstract*; 11th Int. Zeolite Conf. Seul RP63, 1996. Ryoo, R.; Jun, S. *J. Phys. Chem. B* **1997**, *101*, 317.
(372) Kresge, Ch. T.; Leonowicz, M. E.; Roth, W. J.; Vartuli, J. C.; Keville, K. M.; Shih, S. S.; Degnan, T. F.; Dwyer, F. G.; Landis, M. E. U.S. Patent 5,183,561, 1993.
(373) Shih, S. S. U.S. Patent 5,344,553, 1994.
(374) Ward, J. W. *Fuel Process. Technol.* **1993**, *35*, 55.
(375) Maxwell, I. E. *Catal. Today* **1987**, *1*, 385.
(376) Nat, P. J.; Wogt, E. T. C. WO 94/26847, 1994.
(377) Corma, A.; Martínez, A.; Martínez-Soria, V.; Monton, J. B. *J. Catal.* **1995**, *153*, 25.
(378) Degnan, T. F., Jr.; Keville, K. M.; Landis, M. E.; Marler, D. O.; Mazzone, D. N. U.S. Patent 5,183,557, 1993.
(379) Degnan, T. F., Jr.; Keville, K. M.; Landis, M. E.; Marler, D. O.; Mazzone, D. N. U.S. Patent 5,290,744, 1994.
(380) Reddy, K. M.; Song, C. S. *Catal. Today* **1996**, *31*, 137.
(381) Apelian, M. R.; Degnan, T. F., Jr.; Marler, D. O.; Mazzone, D. N. U.S. Patent 5,227,353, 1993.
(382) Del Rossi, K. J.; Hatzikos, G. H.; Huss, A., Jr. U.S. Patent 5,256,277, 1993.
(383) Girgis, M. J.; Tsao, Y. P. *Ind. Eng. Chem. Res.* **1996**, *35*, 386.
(384) Marler, D. O.; Mazzone, D. N. U.S. Patent 5,288,395, 1994.
(385) Le, Q. N.; Thomson, R. T.; Yokomizo, G. H. U.S. Patent 5,134,241, 1992.
(386) Pelrine, B. P.; Schmidt, K. D.; Vartuli, J. C. U.S. Patent 5,105,051, 1992.
(387) Pelrine, B. P.; Schmidt, K. D.; Vartuli, J. C. U.S. Patent 5,270,273, 1993.
(388) Kim, J. B.; Imui, T.; *Catal. Lett.* **1996**, *36*, 255.
(389) Hartmann, M.; Pöppl, A.; Kevan, L. *Stud. Surf. Sci. Catal.* **1996**, *101*, 801.
(390) Bellusi, G.; Perego, C.; Caratti, A.; Peretello, S.; Massara, P. E.; Perego, E. *Stud. Surf. Sci. Catal.* **1994**, *85*, 84.
(391) Imui, T. *Stud. Surf. Sci. Catal.* **1989**, *44*, 189.
(392) Armengol, E.; Cano, M. L.; Corma, A.; García, H.; Navarro, M. T. *J. Chem. Soc., Chem. Commun.* **1995**, 519.
(393) Armengol, E.; Corma, A.; García, H.; Primo, J. *Appl. Catal. A* **1995**, *126*, 391.
(394) Armengol, E.; Corma, A.; García, H.; Primo, J. *Appl. Catal. A* **1997**, *149*, 411.
(395) Le, Q. N. U.S. Patent 5,191,134, 1993.
(396) Gunnewegh, E. A.; Gopie, S. S.; Van Bekkum, H. *J. Mol. Catal. A: Chem.* **1996**, *106*, 151.
(397) Van Bekkum, H.; Hoefnagel, A. J.; Van Koten, M. A.; Gunnewegh, E. A.; Vogt, A.H. G.; Kouwenhoven, H. W. *Stud. Surf. Sci. Catal.* **1994**, *83*, 379.
(398) Kloestra, K. R.; Van Bekkum, H. *J. Chem. Res. (S)* **1995**, *1*, 26.
(399) Tashiro, M. *Synthesis* **1979**, 921.
(400) Wojciechowski, B. W.; Corma, A. *Catalytic Cracking: Catalysis, Chemistry and kinetics*; Marcel Dekker: New York, 1986.
(401) Venuto, P. B. *Microporous Mater.* **1994**, *2*, 297.
(402) Spagnol, M.; Gilbert, L.; Alby, D. *The Roots of organic Development*; Desmurs, J. R., Ratton, S., Eds.; Elsevier: New York, 1996; p 29.
(403) Climent, M. J.; Corma, A.; Iborra, S.; Navarro, M. C.; Primo, J. *J. Catal.* **1996**, *161*, 786.
(404) Dai, L. X.; Hayasaka, R.; Iwaki, Y.; Tatsumi, T. *Sogo Shikensho Nenpo (Tokyo Daigaku, Kogakubu)* **1996**, *55*, 159.
(405) De Goede, A. Th. J. W.; Van der Leij, I. G.; Van der Heijden, A. M.; Van Rantwijk, F. Van; Van Bekkum, H. EP 95, 201,325, 1995.
(406) Corma, A.; Guil, R.; Iborra, S.; Primo, J. Manuscript to be published.
(407) Godefroi, E. F.; Meers, J. U.S. Patent 3,575,999, 1971.
(408) Walker, K. A. M. U.S. Patent 4,150,153, 1979.
(409) Bauer, K.; Garbe, D.; Surburg, H. *Common fragances and flavors Materials*, 2nd ed.; VCH: Weinheim, 1990.
(410) Aucejo, A.; Burguet, M. C.; Corma, A.; Fornés, V. *Appl. Catal.* **1986**, *22*, 187.
(411) Curtin, T.; Hodnett, B. K. *Stud. Surf. Sci. Catal.* **1993**, *78*, 535.
(412) Sato, H.; Hirose, K. *Chem. Lett.* **1993**, 1765.
(413) Singh, P. S.; Bandyopadhyay, R.; Hegole, S. G.; Rao, B. S. *Appl. Catal. A* **1996**, *136*, 249.
(414) Katada, N.; Tsubouchi, T.; Niwa, M.; Murakami, Y. *Appl. Catat. A* **1995**, *124*, 1.
(415) Corma, A.; Fornés, V.; Martín, R. M.; Garcia, H.; Primo, J. *Appl. Catal.* **1990**, *59*, 237.
(416) Barthomeuf, D. *Catal. Rev. Sci. Eng.* **1996**, *38*, 521.
(417) Kloetstra, K. R.; Van Bekkum, H. *J. Chem. Soc., Chem. Commun.* **1995**, 1005.
(418) Clerici, M. C. *Appl. Catal.* **1991**, *68*, 249.
(419) Bellusi, G.; Carati, A.; Clerici, M. G.; Meddinelli, G.; Millini, R. *J. Catal.* **1992**, *133*, 220.
(420) Huybrechts, D. R. D.; De Bruycher, L.; Jacobs, P. A. *Nature* **1990**, *345*, 240.
(421) Camblor, M. A.; Corma, A.; Martínez, A.; Pérez-Pariente, J. *J. Chem. Soc., Chem. Commun.* **1992**, 8.
(422) Corma, A.; Esteve, P.; Martínez, A.; Valencia, S. *J. Catal.* **1995**, *152*, 18.
(423) Blasco, T.; Camblor, M. A.; Corma, A.; Esteve, P.; Martínez, A.; Prieto, C.; Valencia, S. *J. Chem. Soc., Chem. Commun.* **1996**, 2367.
(424) Corma, A.; Navarro, M. T.; Pérez-Pariente, J.; Sánchez, F. *Stud. Surf. Sci. Catal.* **1994**, *84*, 69.
(425) Zhang, W.; Wang, J.; Taner, P. T.; Pinnavaia, T. J. *J. Chem. Soc., Chem. Commun.* **1996**, 979.
(426) Sayari, A.; Karra, V. R.; Reddy, J. S.; Moudrakovski *Mater. Res. Soc. Symp. Proc.* **1995**, *371*, 81.
(427) Kulawik, K.; Schulz-Ekkof, G.; Rathousky, J.; Zukal, A. *Collect. Czech. Chem. Commun.* **1995**, *60*, 451.
(428) Gontier, S.; Tuel, A. *Stud. Surf. Sci. Catal.* **1995**, *97*, 157.
(429) Reddy, J. S.; Sayari, A. *Appl. Catal. A* **1995**, *128*, 231.
(430) Gontier, S.; Tuel A. *J. Catal.* **1995**, *157*, 124.
(431) Tonti, S.; Roffia, P.; Cesana, A.; Mategazza, M.; Padovan, M. Eur. Patent 314,147, 1988.
(432) Sakane, S.; Tsubakino, T.; Nishiyama, Y.; Ishii, Y. *J. Org. Chem.* **1993**, *58*, 3633.
(433) Corma, A.; Iglesias, M.; Sanchez, F. *Catal. Lett.* **1996**, *39*, 153.
(434) Morey, M.; Davidson, A.; Stucky, G. *Microporous Mater.* **1996**, *6*, 9.
(435) Corma, A.; Iglesias, M.; Sanchez, F. *J. Chem. Soc., Chem. Commun.* **1995**, 1635.
(436) *Jpn. Kokai Tokkio Koho* 59,225,176, 1984.
(437) Dutoit, D. C. M.; Schneider, M.; Baiker, A. *J. Catal.* **1995**, *153*, 165.
(438) Hutter, R.; Mallat, T.; Baiker, A. *J. Catal.* **1995**, *153*, 177.
(439) Hutler, R.; Dutoit, D. C. M.; Mallat, T.; Schneider, M.; Baiker, A. *J. Chem. Soc., Chem. Commun.* **1995**, 163.
(440) Klein, S.; Thorimbert, S.; Maier, W. F. *J. Catal.* **1996**, *163*, 476.
(441) Liu, Z.; Crumbaugh, G. M.; Davis, R. J. *J. Catal.* **1996**, *159*, 83.
(442) Klein, S.; Martens, J. A.; Parton, R.; Vercruyse, K.; Jacobs, P. A.; Maier, W. F. *Catal. Lett.* **1996**, *38*, 209.
(443) Hutler, R.; Mallat, T.; Dutoit, D.; Baiker, A. *Top. Catal.* **1996**, *3*, 421.
(444) Rey, F.; Sankar, G.; Maschmeyer, T.; Thomas, J. M.; Bell, R. G.; Greaves, G. N. *Top. Catal.* **1996**, *3*, 121.
(445) Reddy, J. S.; Sayari, A. *J. Chem. Soc., Chem. Commun.* **1995**, 2231.
(446) Das, T. K.; Chandary, K.; Chandwadkar, A. J.; Sivasanker, S. *J. Chem. Soc., Chem. Commun.* **1995**, 2495.
(447) Abdel-Fattah, T. M.; Pinnavaia, T. J. *J. Chem. Soc., Chem. Commun.* **1996**, 665.
(448) Wang, G. R.; Wang, X. Q.; Wang, X. S.; Yu, S. X. *Stud. Surf. Sci. Catal.* **1993**, *83*, 67.
(449) Dongare, M. K.; Sringh, P.; Moghe, P. P.; Ratnasamy, P. *Zeolites* **1991**, *11*, 690.
(450) Tuel, A.; Gontier, S. *J. Chem. Soc., Chem. Commun* **1996**, 651.
(451) Gontier, S.; Tuel, A. *Appl. Catal. A* **1996**, *143*, 125.
(452) Kresge, Ch.T. ; Marler, D. O.; Rav, G. S.; Rose, B. H. U.S. Patent 5,366,945, 1994.
(453) Kozheunikov, I. V.; Sinnema, A.; Jansen, R. J. J.; Pamin, K.; Van Bekkum, H. *Catal. Lett.* **1995**, *30*, 241.
(454) Kozhevnikov, I. V.; Kloetstra, K. R.; Sinnema, A.; Zandbergen, H. W.; Van Bekkum, H. *J. Mol. Catal. A* **1996**, *114*, 287.
(455) Corma, A.; Jorda, J. L.; Martínez, A.; Rey, F. Manuscript to be published.
(456) Brunel, D.; Canvel, A.; Fajula, F.; Di Renzo, F. *Stud. Surf. Sci. Catal.* **1995**, *97*, 173.
(457) Cauvel, A.; Brunel, D.; DiRenzo, F.; Fajula, F. *Organic Coatings*; Proceedings of 53rd International Meeting of Physical Chemistry; American Institute of Physics: New York, NY, 1996, Vol. 354, p 477.
(458) Cauvel, A.; Renard, G.; Brunel, D. *J. Org. Chem.* **1997**, in press.
(459) Junges, U.; Jacobs, W.; Voigt-Martín, I.; Krutzsch, B.; Schuth, F. *J. Chem. Soc., Chem. Commun.* **1995**, 2283.
(460) Ryoo. R.; Ko, Ch. H.; Kim, J. M.; Howe, R. *Catal. Lett.* **1996**, *37*, 29.
(461) Armor, J. N. *Appl. Catal. A* **1994**, *112*, N21.
(462) Reddy, K. M.; Song, Ch. *Catal. Today* **1996**, *31*, 137.
(463) Inui, T.; Kim, J. B.; Seno, M. *Catal. Lett.* **1994**, *29*, 271.
(464) Corma, A.; Martínez, A.; Martínez-Soria, V. *J. Catal.* **1997**, in press.
(465) Stanislaus, A.; Cooper, B. H. *Catal. Rev. Sci. Eng.* **1994**, *36*, 75.
(466) Cooper, B. H.; Donnis, B. B. L. *Appl. Catal. A.* **1996**, *137*, 203.
(467) Schnider, M.; Wildberger, M.; Maciejeswski, M.; Duff, D. G.; Mallat, T.; Baiker, A. *J. Catal.* **1994**, *148*, 625.
(468) Bhore, N. A.; Johnson, I. D.; Keville, K. M.; Le, Q. N.; Yokomizo, G. H. U.S. Patent 5,260,501, 1993.

(469) Hartmann, M.; Pöppl, A.; Kevan, L. *Stud. Surf. Sci. Catal.* **1996**, *101*, 801.
(470) Hartmann, M.; Pöppl, A.; Kevan, L. *J. Phys. Chem.* **1996**, *100*, 9906.
(471) Beck, J. S.; Socha, R. F.; Shihabi, D. S.; Vartuli, J. C. U.S. Patent 5,143,707, 1992.
(472) Maschmeyer, T.; Rey, F.; Sankar, G.; Thomas, J. M. *Nature* **1995**, *378*, 159.
(473) Burch, R.; Cruise, N.; Gleeson, D.; Tsang, S. Ch. *J. Chem. Soc., Chem. Commun.* **1996**, 951.
(474) Morey, M.; Davidson, A.; Eckert, H.; Stucky, G. *Chem. Mater.* **1996**, *8*, 486.
(475) Diaz, J. F.; Bedioni, F.; Briot, E.; Devynck, J.; Balkus, K. J., Jr. *Mater. Res. Soc. Symp. Proc.* **1996**, *431*, 89.
(476) Diaz, J. F.; Balkus, K. J., Jr.; Bedioni, F.; Kurshev, V.; Kevan, L. *Chem. Mater.* **1997**, *9*, 61.
(477) Huber, C.; Moller, K.; Bein, T. *J. Chem. Soc., Chem. Commun.* **1994**, 2619.
(478) Jorgensen, K. A. *Chem. Rev.* **1989**, *89*, 431.
(479) Zhang, W.; Jacobsen, E. N. *J. Org. Chem.* **1991**, *56*, 2296.
(480) Sutra, P.; Brunel, D. *J. Chem. Soc., Chem. Commun.* **1996**, 2485.
(481) Corma, A.; Iglesias, M.; del Pino, C.; Sanchez, F. *J. Chem. Soc., Chem. Commun.* **1991**, 1253.
(482) Sabater, M. J.; García, H.; Corma, A. *J. Chem. Soc., Chem. Commun.* **1997**, in press.
(483) Chibwe, M.; Barodawalla, A.; Pinnavaia, T. J. *14th North American Catalysis Meeting of the Catalysis Society* Snowbird, UT, June 1995 paper PB107.
(484) Balkus, K. J.; Diaz, J. F. *Abstracts of papers of the American Chemical Society*, 212th National Meeting of the American Chemical Society, Boston, MA, Fall 1996; American Chemical Society: Washington, DC, 1996; p 231.

CR960406N